UNIVERSITAT POLITÈCNICA DE CATALUNYA
PONTIFICIA UNIVERSIDAD CATÓLICA DEL PERÚ
CENTRE TECNOLÒGIC DE TELECOMUNICACIONS DE CATALUNYA

Projecte Fi de Carrera
Enginyeria de Telecomunicació

DESIGN OF A CIRCULARLY POLARIZED PATCH ANTENNA FOR SATELLITE MOBILE COMMUNICATIONS IN L-BAND

by
Gustavo Adolfo Sotelo Bazán

A thesis submitted in partial fulfillment for the degree of Engineer in the
Escola Tècnica Superior d'Enginyeria de Telecomunicacions de Barcelona Departament de Teoria del Senyal i Comunicacions

December 2010

Name **:** Gustavo Adolfo Sotelo Bazán.

Thesis Title **:** Desing of a Circularly Polarized Patch Antenna for Satellite Communications in L-Band

Department of Signal Theory and Communications

Polytechnic University of Cataluña.

Thesis Advisor **:** Apostolos Georgiadis.

Academic Year **:** 2010

Abstract

This project provides a detailed study of the Design of a Circularly Polarized Patch Antenna for Satellite Communications in L-band for it use on communication-navigation services such as INMARSA'T and GNSS systems.

The designs were done with simulating software Advance Design System-ADS, which provides fairly reliable simulations and useful data in designing these kinds of antennas. For the construction of the antennas it has been used microstrip antenna technology, because it has been demonstrated that it is suitable for these applications due to their many advantages such as low profile and weight, easy integration with printed circuits. The antennas are etched on a RT/Duroid with dielectric substrate of 3.38 with the height of 20mil.

Simulated and experimental results of several designs of the antenna are presented.

Agradecimientos

A mi padre Gustavo y a mi madre Judith, quienes me enseñaron el valor de la educación; a mis hermanas Yudy e Sofía, por su comprensión y alegría y que a pesar de la distancia siempre estuvieron presentes. Gracias a ellos por sus oraciones, palabras de aliento, continuo apoyo y su inquebrantable fe en mí, estoy profundamente en deuda con ellos.

A mi asesor, Apóstolos Georgiadis, por darme la oportunidad de realizar este proyecto de fin de carrera, así como también por sus sugerencias oportunas, orientación y estímulo; sin su apoyo constante ésta tesis no habría sido posible de realizar. Gracias Doc!

A Selva Via y Ana Collado, por su gran ayuda, paciencia e incondicional apoyo en el desarrollo de los aspectos técnicos del proyecto.

A los amigos ganados a lo largo de la carrera por sus valiosas sugerencias, palabras de aliento y ayuda durante esta etapa universitaria; pero sobre todo, a aquellos amigos con los que hemos compartido los “ires y venires” en el transcurso de esta enriquecedora estancia en Barcelona, con los cuales he compartido casa, viajes, cumpleaños e incontables horas de estudio.

Por último, a todos y cada uno que estuvo directa o indirectamente implicado en la finalización con éxito de este proyecto.

A todos ellos Muchas Gracias!

Gustavo Adolfo Sotelo Bazán
Diciembre 2010

Contents

List of Figures

List of Tables

1 INTRODUCTION

This project involves the development of an antenna for use in L-band commonly used in the receiving antennas of BGAN systems and GNSS systems. For the build of the antenna, it has been used microstrip antenna technology because it has been demonstrated that it is suitable for these applications due to their many advantages such as low profile and weight, easy integration with printed circuits [1-7].

This chapter explains some features about BGAN and GNSS systems, we are going to set the objectives of the project and describe the specifications of the antenna design.

1.1 Motivation

L-band satellite communications systems have been object of a considerable interest in the last years and a growing number of communication-navigation services are already working or are planning to work in this band. After the successful launch and acquisition of the third Inmarsat-4 satellite on August 18, 2008, a new broadband satellite communication system called BGAN (developed by IMMARSAT) can complete the global coverage at the L-band [1-8]. On the other side, Global Navigation Satellite Systems (GNSS) allow a wide range of new applications that make them particularly attractive today, these applications can be : navigation, location, disaster management; these systems are an increasingly present reality and its deployment is a global infrastructure, some of them are GPS, GALILEO, GLONASS, COMPAS.

1.1.1 GNSS

GNSS is the standard generic term for Global Navigation Satellite Systems, which provide autonomous geo-spatial positioning with global coverage.
GNSS allows the user, who has a small electronic receiver, determine their location (longitude, latitude and altitude) using time signals transmitted from a constellation of satellites with some accuracy (because it has some meters of difference) [1-1]

At the present time there are two such operative systems: the American GPS (Global Positioning System) and the Russian GLONASS (GLObal'naya NAvigasionnay Sputnikovaya Sistema). Galileo is the European contribution to the future GNSS and is in initial deployment phase, scheduled to be operational in 2014. A Chinese system called COMPASS is the evolution of Beidou navigation system. India too is developing IRNSS.

In the current GNSS systems, the receiver calculates its position on the earth surface, based in two basic parameters; these parameters are the satellite position and clock it. The satellites use an atomic clock to maintain synchronization with the

satellites of the constellation, since the precision of the calculation of the position depends on the accuracy of the information in time. The satellite sent this information to the receiver, and the process of calculating the position begins [1-2]:

1. The situation of the satellites is known by the receiver through a set of orbital parameters that indicates the position of the satellite; these parameters are transmitted by the satellites themselves.

2. The GNSS receiver measures its distance from the satellites, and uses that information to calculate its position. This distance is measured by calculating the time the signal takes to reach the receiver. Known that time and based on the fact that the signal travels at the speed of light (except for some corrections that apply), we can calculate the distance between receiver and satellite.

3. Each satellite indicates that the receiver is at a point on the surface of the sphere that is centered on the satellite and where the radius is the total distance to the receiver.

4. At least we need four satellites to obtain position, with three satellites are able to calculate the position in three dimensions, while the fourth satellite allows us to calculate the altitude of the receiver and eliminate errors of synchronization

For our study we will focus on the frequency bands of work of some GNSS, specially: GPS, GLONASS, GALILEO and COMPASS, so we are going to explain some features about these systems.

1.1.1.1 NAVSTAR-GPS

The system NAVSTAR-GPS (Navigation System and Ranging - Global Positioning System), more commonly known as GPS is an all-weather, space-based navigation system developed in the 1970 and managed by the Department of Defense from the U.S.

The space segment of GPS was primarily designed with 24 satellites distributed equally in six orbital circular planes, with an inclination of 55 degrees above the horizon line and an altitude of about 20200 km. This guaranteed that a minimum of five satellites (usually six) will be available anywhere in the world; however other satellites have been added to improve the performance of GPS service, so there are currently a total of 30 satellites in the GPS space segment, they are not uniformly distributed and ensure a better performance of the system.

There are several generations of satellites that have been used during the long life of the GPS system; they use CDMA technology (Code Division Multiple Access) for the issuance of all GPS signals. These satellite generations have been named and classified by blocks [1-3]:

Blocks of satellite I / II / IIA / IIR have transmitted GPS signals at two carrier frequencies, referred as Link 1 (L1) at 1575.42 MHz and Link 2 (L2) at 1227.6 MHz
The satellites of Block IIR-M introduced two new signals, one military (known as M-code) and a new civil signal called L2C, both in L1 and L2 carrier frequencies.
Block IIF satellites introduced a new civil navigation signal in a new carrier frequency at 1176.45 MHz; both are known as Link 5 (L5).
The last block of satellites, the Block III, it will add another civil navigation signal (L1C), in this case in the L1 carrier frequency.
For point positioning and timing, GPS provides two levels of service: the standard position service (SPS) which is used for civilian access; and the precise positioning service (PPS) for access for authorized users (military use).

The SPS is freely available to all kinds of users in a continuous and world-wide basis.

The PPS is the military service with high precision, speed and temporary service, its use is restricted to US armed forces, US federal agencies, and some selected allied armed forces and governments.

1.1.1.2 GLONASS

GLONASS is a satellite navigation system operated by the Russian Federation. The first GLONASS satellite was launched in October 1982. The GLONASS constellation nominally consists of 24 satellites in three orbital planes, with an inclination angle of 64.8 degrees and an altitude of 19 100 km [1-3].

Currently, the system only has 13 satellites fully operational due to lack of resources, but the GLONASS program has been reinvigorated, because Russia, since 2001, is following a plan to restore full operation of the system.

A frequency-division multiple access (FDMA) design for the signals are utilized. The current GLONASS satellites broadcast navigation signals in two sub bands of L-band referred to as L1 and L2.

The L1 carrier frequencies are given by

$$f_{K1} = f_{01} + K.\Delta f_1$$

and the L2 carrier frequencies by

$$f_{K2} = f_{02} + K.\Delta f_2$$

Where f_{01}=1602 MHz, f_{02}=1246 MHz, Δf_1=0.5625 MHz, Δf_2=0.4375 MHz, and K is the channel number.

The currently operational satellites used the channels from -2 to +6; but when the system will be fully operational, the plans are to use a broader channel range of -7 to +9.

In GLONASS there was 3 generations of satellites. The first generation of satellites, it is known as GLONASS satellites, emitted two direct DSSS navigation signals with rectangular symbols. One signal is the standard accuracy designated for civilian use, and the other was the signal of high accuracy, which is designed for military use.

GLONASS satellites emit the standard accuracy signal on L1, while the high accuracy signal was broadcast only in the L2 band [1-3].

The GLONASS-M satellites broadcast both signals (the high and standard accuracy) in the L2 carriers, satellites also have an improved design that allows them to reach more years of life

The GLONASS-K satellites are the next generation and they are currently in development. They will broadcast navigation signals on L1, L2 and in an additional sub-band, the L3 sub band (1198-1213 MHz). In these new satellites are plans to introduce CDMA in addition to previously used FDMA.

1.1.1.3 Galileo

Galileo is the European satellite navigation system. Galileo is still being implemented, it is specifically designed for civil and commercial purposes and it will be interoperable with the other radio-navigation systems. This will be beneficial to all users as they will be able to use more satellites for redundancy and higher accuracy.

Galileo will offer four distinct navigation services and one service to support search and rescue. These services are:

- The Open Service (OS): Is the result of a combination of open signals. This service will provide position and time with similar characteristics to other GNSS systems.

- The Safety of Life Service (SoL): It improves the open service performance, since when cannot guarantee certain accuracy limits are given timely warnings to users.

- The Commercial Service (CS): It provides access to two additional signals, this feature allows a throughput rate higher and improve accuracy in the location of the users.

- Public Regulated Service (PRS Public Regulated Service): It provides the location and time to specific users requiring a high continuity of service.

The Galileo system consists of 27 operational satellites in three Medium Earth Orbit (MEO) orbital planes, at about 23 000km altitude and inclined at 56 ° to the equatorial plane. It has three spare satellites (one in each orbital plane) where each satellite is able to cover for any failed satellite in that plane [1-3].

The Galileo navigation signals are transmitted in four frequency bands, these are referred as: E5a (1164-1191 MHz), E5b (1191-1215 MHz), E6 (1215-1300 MHz) y E1 (1559-1591 MHz). CDMA is used within each frequency band and as we can note, the frequency bands are overlapping or contiguous to frequency bands used by others GNSS constellations. This will allow the combined use of several constellations (GPS, COMPASS and GLONASS) to increase performance and robustness of the navigation services.

1.1.1.4 COMPASS

The Compass/BeiDou Navigation Satellite System (CNSS), better known as COMPASS, is a satellite navigation system developed by China. The space segment of CNSS will consist of 30 MEO satellites at an altitude of 21 490 km and five geostationary satellites.

It will offer two services, the Open Service that will provide accuracies of 10m positioning, 0.2m/s in velocity, and 50 ns in time dissemination; and the Authorized Service, which is only intended for entities authorized by the Chinese government [1-3].

CNSS is a CDMA-based system with DSSS signals planned on four carrier frequencies, these frequencies are: 1207.14 MHz (shared with GALILEO E5b), 1268.52 MHz (shared with GALILEO E6), 1561.098 MHz (E2), and 1589.742 MHz (E1).

.

GNSS	POLARIZATION		Carriers	Band (MHz)	
				Fmin	Fmax
GPS	RHCP	L1	1575.42	1563	1587
		L2	1227.6	1215	1237
		L5	1176.45	1164	1191
GLONASS	RHCP	G1	1602	1593	1612
		G2	1246	1238	1255
		G3	1204.704	1198	1213
GALILEO	RHCP	E1	1575.42	1559	1591
		E6	1278.75	1260	1300
		E5 E5a	1176.45	1164	1191
		E5b	1207.14	1191	1214
COMPASS	RHCP	E1	1589.742	1587.69	1591.79
		E2	1561.098	1559.05	1563.15
		E6	1268.52	1256.52	1280.52
		E5b	1207.14	1195.14	1219.14

Table 1-1 Shows the frequency bands of GNSS systems

1.1.2 BGAN

The Broadband Global Area Network (BGAN) is a mobile communication system, developed by IMMARSAT, which consists of a constellation of geostationary satellites working in conjunction with portable, lightweight, surface-based terminals about the size of a laptop or so. It was created to transmit broadband wireless voice (make telephone calls), video and data communications) almost anywhere on the surface of the earth.[1-4]

We can see in Figure 1.1, the coverage map where it shows the footprints of the BGAN system; but does not represent a guarantee of service.[1-5]

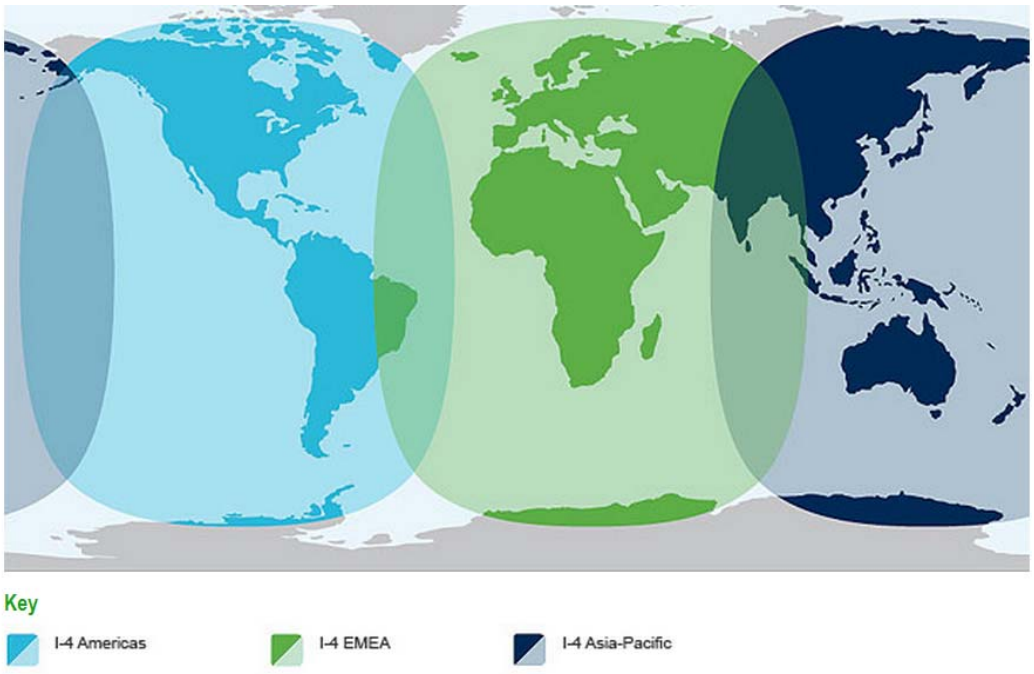

Figure 1.1 Shows Inmarsat's expectations of coverage.

As we already mentioned it, some services supported by BGAN are: It allows us to access to internet using a Packet Switched connection. With this connection we can access to e-mail, transfer files and sent or receive data; we can have video conferences anytime and anywhere. We also can make telephone calls; due a Circuit switched service having an optimum voice quality. BGAN system also provides a Short Messaging Service (SMS) for sending and receiving messages. Some other supplementary services are call hold, call waiting, call forwarding, voice mail, call barring and calling line identification. In Figure 1.2 we can see and overview of the BGAN system, which can explain the basic operation of the system (EXPLORER 300 is the receiver equipment developed by INMARSAT).

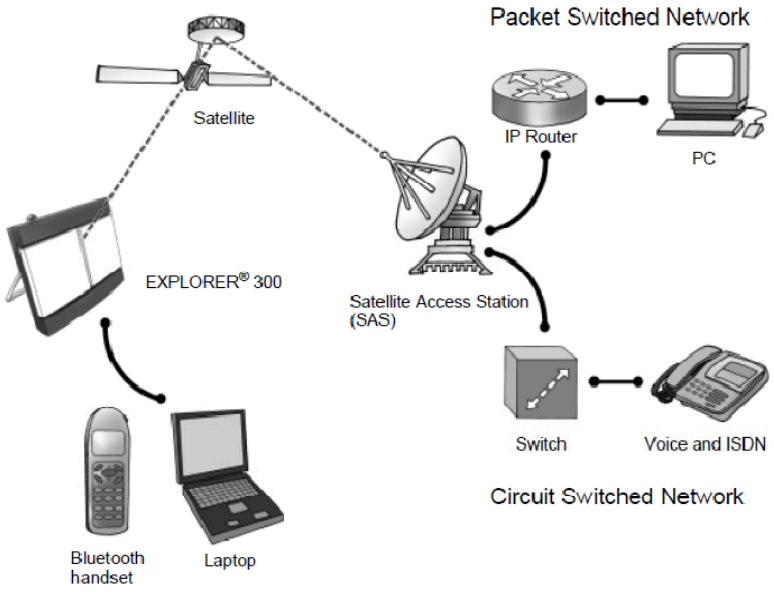

Figure 1.2 Shows a diagram of a complete BGAN system**.**

Now we are going to see the specifications of the antenna for the receiver equipment. The Table 1.2 will show them.[1-5]

Item		Specification
Polarization		Right Hand Circular Polarization (RHCP)
Frequencies Inmarsat		
	Transmit	1626.5 to 1660.5 MHz
	Receive	1525.0 to 1559.0 MHz
	Bearer bandwidth	200 KHz
GPS		1575.42 MHz
Bluetooth		2400 to 2483.5 MHz

Table 1-2 Specifications of the antenna for the receiver equipment.[1-5]

1.2 Objectives

In this project we are going to build a broadband antenna, which main objective is to cover the frequency bands from 1.520-1.56 GHz and 1.62 to 1.660 GHz; we also can build a broadband antenna to cover the frequency band from 1.52 to 1.66 GHz, which is a relative bandwidth of about 8.8% centered at 1.59 GHz, according to equation 2.11.

From Table 1.1 we can see that using this frequency band, allows us to work with all the GNSS systems described before. For GPS we cover the L1 band, for GLONASS the G1 band, for GALILEO the E1 band and for COMPASS the E1 and E2 band, so we can receive signal from all these GNSS systems.
From Table 1.2 we can see that we can cover the entire frequency band for BGAN system, 1.525–1.560 GHz (downlink) and 1.625–1.660 GHz (uplink).

So, in summary, Table 1.3 displays the specifications of the antenna.

FREQUENCY BAND	1525-1660 (MHz)
AXIAL RATIO	< 3dB in all the bandwidth
POLARIZATION	RHCP
INPUT IMPEDANCE	50 Ω
GAIN	> 10dBi [1-6]

Table 1-3 Shows the antenna's specifications**.**

1.3 Organization of the Thesis

The completed project report is divided into 6 chapters; in the following lines we show a summary for each one:

Chapter 1. Introduction
It is the present chapter, which provides a brief introduction, motivation and overall project objectives.

Chapter 2. Parameters of Antennas
This chapter explains the basic concepts used throughout the project for the design of the antenna

Chapter 3. Microstrip Theory
This chapter explains the concepts of microstrip technology used for the design of the antenna

Chapter 4. Microstrip Patch Antenna Design and Results
This chapter details the design process, including the construction and measurements of the antennas.

Chapter 5. Conclusions and Guidelines for Future Work
This section presents the conclusions of the project. It also proposes future lines to enhance the behavior of the antenna.

Chapter 6. Appendix
This section presents some additional information related to the project.

1.4 References

[1-1] Hofmann-Wellenhof, B., Lichtenegger, H. and Wasle, E, "GNSS-Global Navigation SatelliteSystems, GPS, GLONASS, Galileo &more", SpringerWienNewYork, 2008

[1-2] D. A. García, "Sistema GNSS", Memory of the Final Project, UAM, January 2008

[1-3] C. J. Hegarty, E. Chatre, "Evolution of the Global Navigation Satellite System (GNSS)", Proc. IEEE, vol. 96, No. 12, December 2008.

[1-4] D.C. Morse and K.Griep, Next generation FANS Over inmarsat broadband global area network (BGAN), 23rd DASC Conference, 2004, 11.B., p. 4–1–13.

[1-5] INMARSAT,"Explorer 300- User Manual", Thrane & Thrane A/S. June 2007

[1-6] K. Fujimoto and J.R. James, Mobile Antenna Systems Handbook, Boston : Artech House Inc. 1994

[1-7] S. Koulouridis and J.L. Volakis, "L-band Circularly Polarized Small Aperture Thin Textured Patch Antenna," IEEE Antennas and Wireless Propagat. Letters, Vol. 7, 2008, pp. 225-228.

[1-8] S.Q.Fu, S.J. Fang, Z. B. Wang, and X. M. Li. "A Wideband Circular Polarization Antenna for Portable Inmarsat BGAN Terminal Applications" School of Information Science and Technology, Dalian Maritime University, Dalian, China; January 2009

2 ANTENNA'S PARAMETERS AND DEFINITIONS

2.1 Introduction

An antenna is a part of a transmitting or receiving system, designed specifically to radiate or receive electromagnetic waves [2-1].The antenna is a passive linear reciprocal device that can convert electromagnetic radiation into electric current and vice-versa, so it is a transitional structure between the free space and a guiding device. [2-2]

In this chapter we are going to give definitions of some antenna's parameters, which are going to be useful along the project development to describe the performance of the antenna.

2.2 Radiation Pattern

The radiation pattern is the spatial distribution of a quantity that characterizes the electromagnetic field generated by an antenna. This distribution can be expressed as a mathematical function or as graphical representation [2-1].

Most of the time, the radiation pattern, is determinated in the far-field region and is usually represented with the spherical coordinate system [2-3].

Figure 2.1 Illustrates an antenna and its three dimensional radiation pattern.

When we are going to describe an antenna, there are two most important measurements: The E-plane and H-plane patterns.
If we are working with an antenna that is linearly polarized, the E-plane is formed by the maximum radiation direction and the plane that contains the electric field in that direction. The H-plane is the plane that is formed by the maximum radiation direction and the magnetic field in that direction. Finally the H-plane is perpendicular to the E-plane, and the intersection of this fields form the direction of maximum antenna radiation

The radiation pattern can be displayed with a 3D representation; but is common to show it in sections that follow the meridians (constant φ) or parallels (constant θ). These sections can be represented in polar diagram that provides clearer information about the distribution of power in different spatial directions, or cartesian coordinates that allow us to see important details in antennas with high values of directivity.

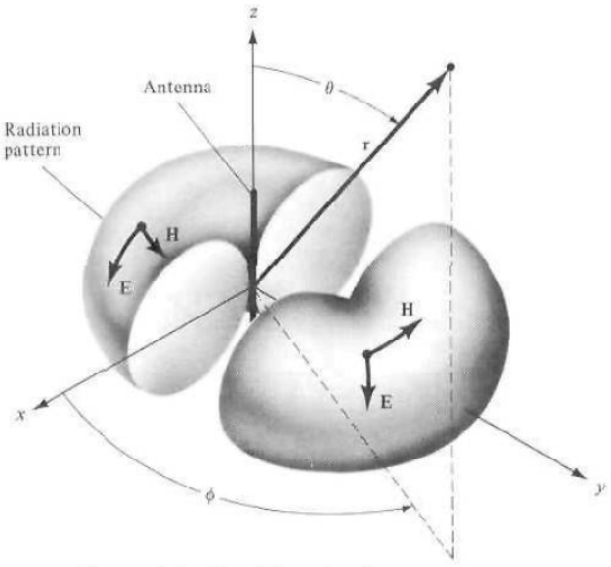

Figure 2.1 Omnidirectional antenna pattern [2-4]

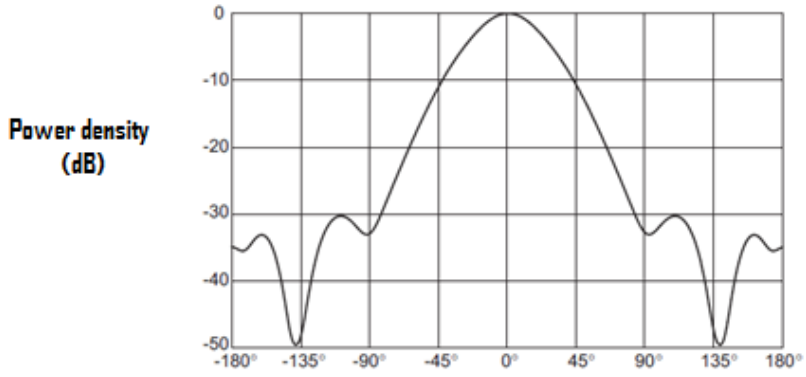

Figure 2.2 **I**llustrates the radiation pattern in cartesian coordinates (dB vs degrees) [2-2]

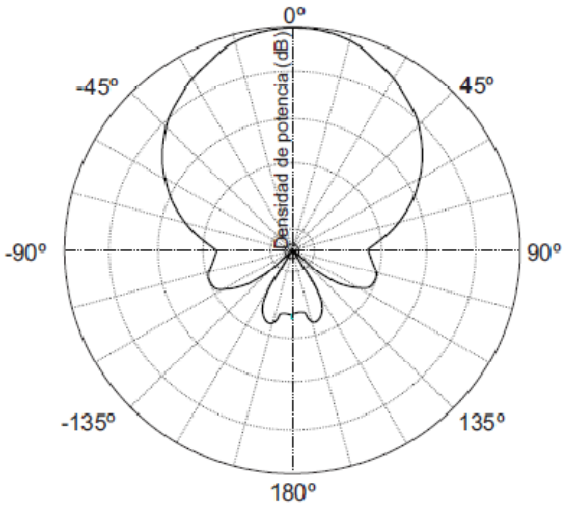

Figure 2.3 Illustrates the radiation pattern in polar coordinates [2-2]

2.3 Parameters of the radiation pattern

There are parameters associated with the radiation pattern, we refer to them as 'lobes', and a radiation lobe is defined as the portion of the diagram bounded by regions of low radiation (nulls). The lobes that are usually defined:

2.3.1 **Major lobe or main beam.**

It is the radiation lobe containing the direction of maximum radiation.

2.3.2 **Minor lobe.**

It is any lobe, except a major lobe. They represent radiation in undesired directions, so it is wasted energy for transmitting antennas and potential noise sources for receiving antennas that is why they should be minimized.

2.3.3 Side lobe.

It is a radiation lobe in any direction other than the intended lobe. It is adjacent to the main lobe and occupies the hemisphere in the direction of the main beam.

2.3.4 Back lobe.

It is the lobe which is in the opposite direction to the main lobe.

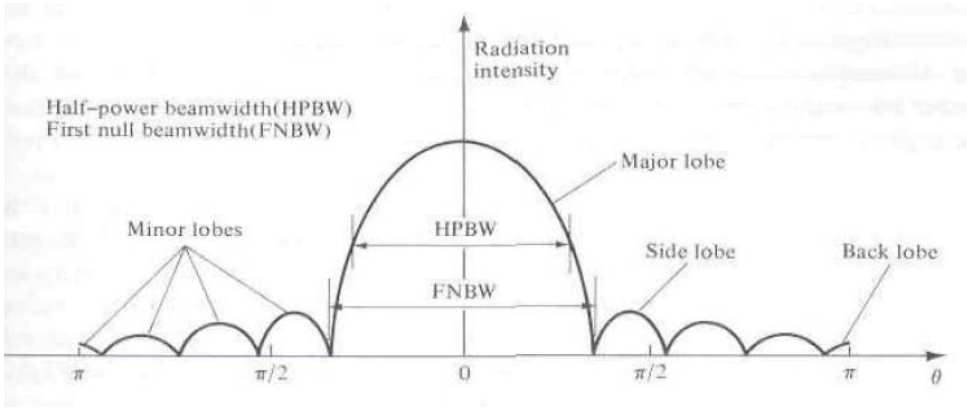

Figure 2.4 Shows the linear plot of power pattern and its associated lobes and beamwidths [2-4].

The parameters HPBW and FNBW, shown in Figure 2.4, are going to be explained later.

The quantities that are most common to characterize the radiation pattern of an antenna are radiation power density, radiation intensity, directivity, phase, polarization, and gain, so we are going to explain them all.

2.4 Radiation Power Density

The radiation power density is defined as the power per unit area in a certain direction. The units are watts per square meter. It can be calculated from the RMS values (Root Mean Square) of the fields E and H.

$$\vec{\rho}(\theta,\phi) = Re\left(\vec{E}\ x\ \vec{H}^{*}\right)\ \text{W/m}^2 \tag{2.1}$$

We can get the radiated power density as a function of the transversals components of the electric field:

$$\rho(\theta,\phi) = \frac{|E_\theta|^2 + |E_\phi|^2}{\eta} \tag{2.2}$$

If we calculate the integral of power density on a spherical surface that enclosing the antenna, we can get the total radiated power:

$$P_r = \iint_s \vec{\rho}(\theta, \phi).d\vec{s}$$

(2.3)

2.5 Radiation Intensity

It is defined as the power radiated from an antenna per unit solid angle [2-2]. Its units are watts per steradian. This parameter, in large distances, has the property of being independent of the distance that the antenna is. It is related to the radiated power density as follows:

$$K(\theta, \phi) = \rho(\theta, \phi).r^2$$

(2.4)

We can also obtain the total radiated power by calculating the integral of the radiation intensity in all directions in space.

$$P_r = \iint_{4\pi} K(\theta, \phi)\, d\Omega$$

(2.5)

Where:

$d\Omega$= solid angle differential in spherical coordinates

$$d\Omega = \frac{ds}{r^2} = (sen\theta)d\theta d\phi$$

(2.6)

2.6 Beamwidth

The beamwidth is a parameter that is related with the pattern of an antenna, and is the angular separation between two identical points on opposite sides of the pattern maximum. It is very important because is used like a trade-off between it and the side lobe level, so if the beamwidth decreases then the side lobe increases and vice versa.

One of the most used beamwidth is the “half-power beamwidth” (HPBW), and is the angle at which the main lobe has half of its power.

We have also the “first-null beamwidth” (FNBW) and it is the angular separation between the first nulls of the pattern.

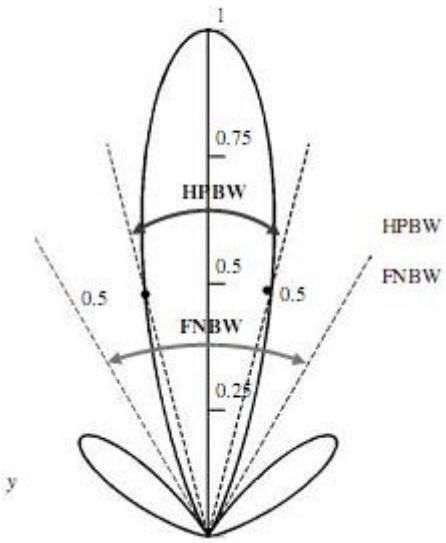

Figure 2.5 Illustrates the HPBW and FNBW for a pattern in linear scale [2-4].

2.7 Directivity

According to the definition that has been given by IEEE [2-1], the directivity of an antenna is defined as “the ratio of the radiation intensity in a given direction from the antenna to the radiation intensity averaged over all directions. The average radiation intensity is equal to the total power radiated by the antenna divided by 4π. If the direction it is not specified, the direction of maximum radiation intensity is implied”.

$$D(\theta,\phi) = \frac{K(\theta,\phi)}{K_{AV}} \tag{2.7}$$

$$D(\theta,\phi) = \frac{\rho(\theta,\phi)}{\frac{Pr}{4\pi r^2}} \tag{2.8}$$

Where:

- $K(\theta,\phi)$: Radiation Intensity.
- K_{AV} : Radiation Intensity Average.

- Pr : Total radiated power
- $\rho(\theta,\phi)$: Radiation Power Density

2.8 Antenna Efficiency

The total antenna efficiency takes into account the ohmic losses of the antenna through the dielectric material, the reflective losses at the input terminals and losses within the structure of the antenna.

$$e_o = e_r e_c e_d \tag{2.9}$$

Where:
e_0: Total antenna efficiency (dimensionless)
e_r: Reflection efficiency = $(1-|\Gamma|^2)$ (dimensionless)
e_c :Conduction efficiency (dimensionless)
e_d: Dielectric efficiency(dimensionless)

2.9 Gain

Gain is a useful measure that helps to describe the performance of an antenna. It is defined by IEEE [2-1] as "the ratio of the intensity, in a given direction, to the radiation intensity that would be obtained if the power accepted by the antenna were radiated isotropically. The radiation intensity corresponding to the isotropically radiated power is equal to the power accepted (input) by the antenna divided by 4π".

$$(\theta,\phi) = \frac{\rho(\theta,\phi)}{\frac{P_{delivered}}{4\pi r^2}} = \frac{P_{radiated}}{P_{delivered}} \cdot \frac{\rho(\theta,\phi)}{\frac{P_{radiated}}{4\pi r^2}} = \eta_i D(\theta,\phi) \tag{2.10}$$

From the equation (2.10) we can see that the gain it is linearly related with the directivity measurement through the antenna radiation efficiency (*"n"* paragraph 2.12).

2.10 Bandwidth

We cannot build an infinite antenna, so due to it finite geometry, the antenna is limited to operate successfully in a band or frequency range and this frequency range is known as bandwidth.

For narrowband antennas, the bandwidth can be specified as the ratio of the frequency range in which the specifications are met and the center frequency; mathematically is:

$$BW = \frac{f_{max} - f_{min}}{f_o} .100 \tag{2.11}$$

For broadband antennas the bandwidth is usually expressed as:

$$BW = \frac{f_{max}}{f_{min}} : 1 \tag{2.12}$$

Where:
- *fmax* : Maximum frequency.
- *fmin* : Minimum frequency range.
- f_0 : Center frequency.

2.11 Polarization

The polarization of an antenna in a given direction indicates the polarization of the radiated wave of the antenna in that direction. If the direction is not stated, the polarization is taken to be the polarization in the direction of maximum gain.

The polarization of a radiated wave is the property of an electromagnetic wave describing the time varying direction and relative magnitude of the electric-field vector at a fixed location in space, and the sense in which it is traced, as observed along the direction of propagation [2-1].

The polarization is indicated by the vector that describes the electric field at a point in space as a function of time. We have three classifications of antenna polarization: linear, circular and elliptical. The circular and linear polarizations are special cases of elliptical polarization.

The sense of rotation of the electric field, in both circularly polarized waves as elliptical, is said to be a right-hand polarization if the field is traced in a clockwise

(CW), and if it is in the opposite way (counterclockwise) then is said to be a left-hand polarization.

The polarization is an important concept in satellite communications and radio systems, because the receiving antenna is only able to capture the power contained in the field polarization that coincides with their own.

Now we are going to explain about the general characteristics and the necessary conditions that the wave must have in order to possess linear, circular, or elliptical polarization.

2.11.1 Linear Polarization

If the electric-field vector at a given point in the space is always oriented along the same straight line at every instant of time, we can say that the time-harmonic wave is linearly polarized at that point.

This is accomplished if the electric field vector possesses the following characteristics:

1. Only one component, or
2. Two orthogonal linear components that are in time phase or 180◦ (or multiples of 180◦) out-of-phase.

2.11.2 Circular Polarization

If the electric-field vector at a given point in space, traces a circle as a function of time, we are talking about that the time-harmonic wave is circularly polarized.

The conditions to accomplish this are if the electric field vector possesses all of the following:

1. The field must have two orthogonal linear components.
2. The two components must have the same magnitude.
3. The two components must have a time-phase difference of odd multiples of 90^0.

These three characteristics must be met at all times.

2.11.3 Elliptical Polarization

If the tip of the electric-field vector traces an elliptical locus in space, then the time-harmonic wave is elliptically polarized.

A wave is elliptically polarized if it is not linearly or circularly polarized, and in the real world there is no perfect linear or circular polarized antenna, but they are more or less elliptical.

The necessary and sufficient conditions to accomplish this are if the electric field vector possesses all of the following:

1. The field must have two orthogonal linear components, and
2. The two components can be of the same or different magnitude.
3.

(a) If the two components are not of the same magnitude, then the time-phase difference between the two components must not be 0◦ or multiples of 180◦, because then it will be a lineal polarization.

(b) If the two components are of the same magnitude, then the time-phase difference between the two components must not be odd multiples of 90◦, because it will then be a circular polarization.

2.11.3.1 Axial Ratio

The axial ratio is a very important parameter that helps to quantify the polarization of an antenna. The axial ratio of a wave elliptically polarized, is the relationship between major and minor axes of the ellipse, and it can take values among one and infinity.

For an antenna that has a purely linear polarization, the axial ratio tends to infinity because one of the components of electric field is zero.
For antennas that have perfect circular polarization, the axial ratio is 1 (or 0 dB), because you have electric field components of the same magnitude, if it is an antenna with elliptical polarization, the axial ratio is greater than 1.

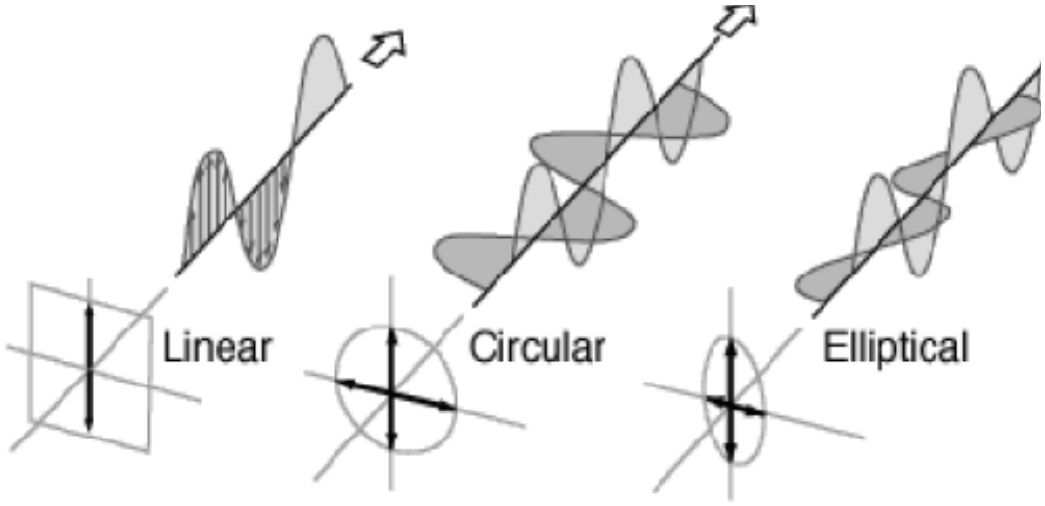

Figure 2.6 Illustrates the three types of polarization [2-5].

2.12 Input Impedance

The input impedance of the antenna (Z_A) is the relationship between voltage and current at the input terminals of the antenna, with no load attached.

We can represent it as:

$$Z_A = R_A + jX_A \tag{2.13}$$

Where:
Z_A = Antenna impedance at terminals (ohms)
R_A = Antenna resistance at terminals (ohms)
X_A = Antenna reactance at terminals (ohms)

The input impedance of an antenna is generally a function of frequency, so the relationship between voltage-current at the input of the antenna depends on the frequency, and Z_A, R_A, and X_A depend also on the frequency.

If at a given frequency, the reactance of the input impedance antenna is equal to zero, it is said that the antenna is resonant at that frequency.

The resistive part R_A, consists of two components:

$$R_A = R_r + R_L \tag{2.14}$$

Where:
R_r = radiation resistance of the antenna
R_L = loss resistance of the antenna

The radiation resistance is the ohmic resistance and it is used to represent the power delivered to the antenna for radiation. The loss resistance, models the ohmic resistance that would dissipate the same power that is lost in the antenna. Then we can define the radiated power and power loss as:

$$P_{radiated} = |I|^2 . R_r$$

$$P_{loss} = |I|^2 . R_\Omega \quad (2.15)$$

(2.16)

Where I is the intensity supplied by a generator connected to the hypothetical antenna.

And because the antenna radiates some power, and another is lost in the antenna we can define the power delivered to the antenna as the sum of these two:

$$P_{delivered} = P_{radiated} + P_{loss} = |I|^2 R_r + |I|^2 R_\Omega$$

Due to the existence of the power loss, not all the radiated power is delivered, so we can define the antenna radiation efficiency (η) as the ratio between the radiated power and the power delivered to the antenna, or equivalently between the input resistance of this antenna, if it were ideal (no losses), and the input resistance that really has.

$$\eta = \frac{\text{Pradiated}}{\text{Pdelivered}} = \frac{\text{R}_\text{r}}{\text{R}_\text{r} + R_\Omega} \text{ (Dimensionless)}$$

(2.17)

2.13 Matching

In transmission and reception, the antenna usually connects to a transmission line or directly to the transmitter or receiver.

It is important that the transmission line or the load connected to the antenna and the antenna have impedance values (Z_L and Z_A, respectively) that allow maximum power transfer.

We can take as an example working with the antenna as receiving antenna; figure 2.7 shows an equivalent circuit for the antenna.

.

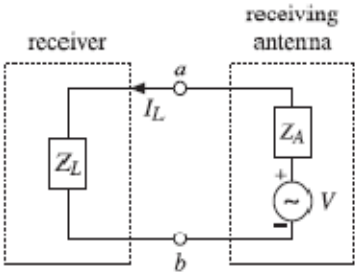

Figure 2.7 Equivalent circuit for a receiving antenna.

.

Where:

$$Z_A = R_A + jX_A$$

$$Z_L = R_L + jX_L$$

So if we want to have maximum power transfer, Z_L and Z_A must be complex conjugate, then it should be satisfy:

$$Z_L = Z_A^*.$$

In this case the power transferred to the load is equal to:

$$P_{Lmax} = \frac{|V_{ca}|^2}{4R_a} \tag{2.18}$$

Where:
-V_{ca}: Is the open circuit voltage at the antenna terminals [2-3].

In general, if there is no adaptation, then the power delivered to the load is:

$$P_L = P_{Lmax}(1 - |\rho|^2) \tag{2.19}$$

Where “ρ” is the reflection coefficient, calculated as:

$$\rho = \frac{Z_L - Z_A}{Z_L + Z_A} \tag{2.20}$$

2.14 References

[2-1] IEEE Standards Board, “IEEE Standard Definitions of Terms for Antennas”, IEEE Std 145-1993, Mayo 1993.

[2-2] C. A. Balanis, “Antena Theory, analisis and design”, 2nd Ed, Wiley., 1998.

[2-3] A.Cardama, L. Jofre et. Al., “Antenas”, Ediciones UPC, Septiembre 2002.

[2-4] C. A. Balanis, “Modern Antenna Handbook”, Wiley, 2002.

[2-5] Rosu, Julian,“Small Antennas for High Frequencies”, Yo3dac - Va3iul. Consulted October 2010 <” http://www.qsl.net/va3iul/”>

3 MICROSTRIP ANTENNA

3.1 Introduction

The microstrip antenna concept was first proposed by Deschamps in 1953. However this concept was undeveloped until 1970 when the revolution in electronic circuit miniaturization and large-scale integration helped to build practical antennas. The antennas developed by Munson were used as low-profile flush-mounted antennas on rockets and missiles, this work showed that microstrip antenna was a practical concept for use in many systems problems. [3-1]

The microstrip antennas have many unique and attractive advantages, such as its low profile, light weight, small volume, and ease of fabrication using printed-circuit technology that led to the design of several configurations for various applications. Nowadays with increasing requirements for personal and mobile communications, the demand for smaller and low-profile antennas has brought the microstrip antennas to the forefront, because they are being use not only in military applications but also in commercial areas such as mobile satellite communications, terrestrial cellular communications, direct broadcast satellite (DBS) system, global positioning system (GPS), remote sensing, and hyperthermia. [3-1, 3-2, 3-3]

In this chapter, we are going to discuss some of the microstrip antenna's technical features, its advantages and disadvantages, considerations of the substrate material , feeding techniques, polarization behaviors and bandwidth characteristics.

3.2 Features of the Microstrip Antenna

A microstrip antenna, in its simplest form, consists of a radiating patch on one side of a dielectric substrate and a ground plane on the other side.

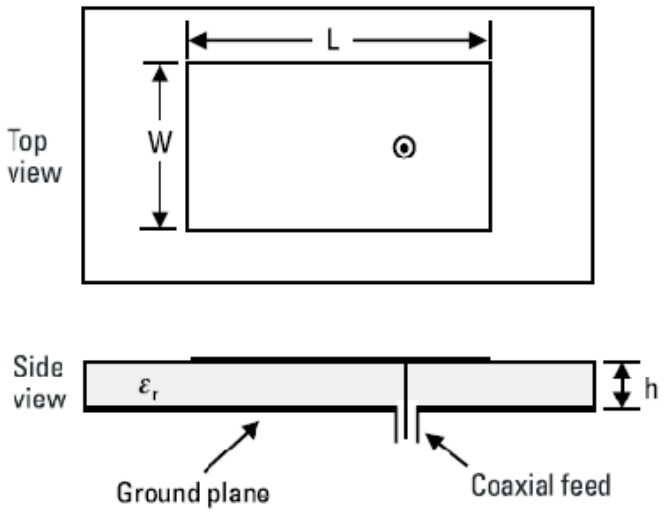

Figure 3.1 Shows the top and side views of a rectangular microstrip antenna [3-3].

The radiating patch can be designed with a variety of shapes such as: square, circular, triangular, semicircular, sectoral, and annular ring shapes; but rectangular and circular configurations are the most commonly used configuration because of ease of analysis and fabrication.

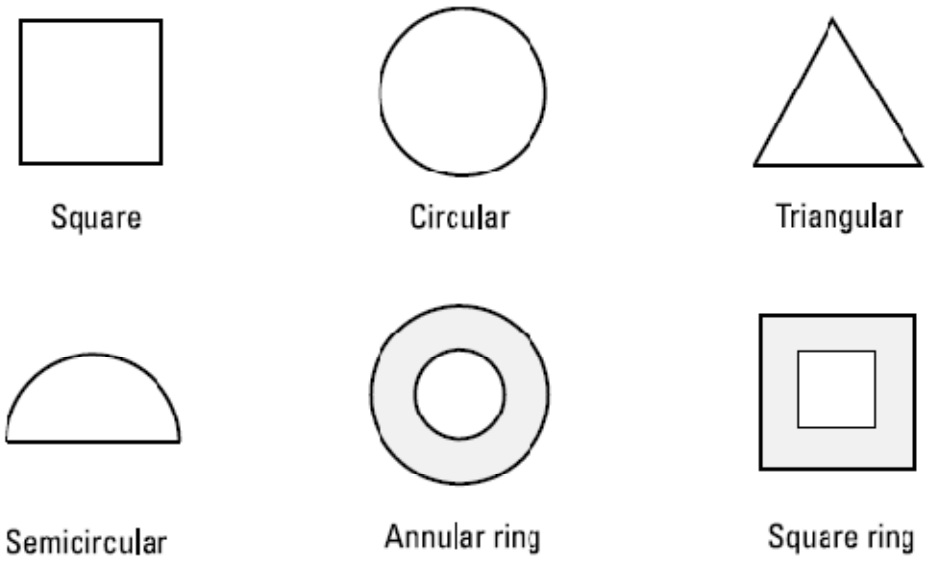

Figure 3.2 Shows other shapes of microstrip antennas [3-3].

The radiating patch is normally made of a thin copper foil, or is copper-foil plated with gold or nickel because they are corrosion resistive metals.

The substrate panel is used to maintain the required precision spacing between the patch and its ground, to give mechanical support for the radiating patch, and it has a thickness in the range of 0.01–0.05 free-space wavelength (λ_0). It is also often used with high dielectric-constant material to load the patch and reduce its size.
For large array application, the substrate material should be low in insertion loss with a loss tangent of less than 0.005.

We can separate the substrate materials into three categories, in accordance with their dielectric constant:

1. Having a relative dielectric constant ε_r:

$$1.0<\varepsilon_r<2.0$$

This type of material can be polystyrene foam, air.

2. Having a relative dielectric constant ε_r :

$$2.0<\varepsilon_r<4.0$$

Material consisting mostly of fiberglass reinforced Teflon.

3. Having a relative dielectric constant ε_r :

$$4.0<\varepsilon_r< 10.0$$

The material can consist of ceramic, quartz, or alumina.

We can also find materials with a much larger ε_r than 10, but a high dielectric constant can lead to a significant reduction in the radiation efficiency of the antenna.

For good performance of the antenna (typically for broadband applications), it is best to use a thicker substrate, whose dielectric constant is in the lower range and have small losses, but the thicker substrate will provide a low efficiency and lower dielectric constant will have an impact on a larger antenna. So compensation should be made between the dimensions of the antenna and the antenna performance.

3.3 Advantages and Disadvantages

The microstrip antenna has proved to be an excellent radiator for many applications because of its several advantages, but it also has some disadvantages; however some of them can be overcome using new techniques of feeding, configuration of the patch, etc.

3.3.1 Advantages

- They are light in weight and take up little volume because their low profile.

- They can be made conformal to the host surface.
- Low fabrication cost, hence can be manufactured in large quantities.
- They are easier to integrate with other microstrip circuits on the same substrate.
- They support both, linear as well as circular polarization.
- They can be made compact for use in personal mobile communication and hand held devices.
- They allow multiple-frequency operation, because you can use stacked patches.
- Mechanically robust when mounted on rigid surfaces.

3.3.2 Disadvantages

- Narrow bandwidth.
- Lower power gain.
- Lower power handling capability.
- Polarization impurity.
- Surface wave excitation.
- Extraneous radiation from feeds and junctions.
- Poor end fire radiator except tapered slot antennas.

3.4 Methods of Analysis

The analytic models for microstrip antenna allow the designer to predict the antenna characteristics, such as input impedance, resonant frequency, bandwidth, radiation patterns and efficiency. We can divide these methods into two groups [3-3].

In the first group, we have:

- The transmission line model;
- The cavity model;
- The multiport network model (MNM)

These methods are based on equivalent magnetic current distribution around the patch edges. The transmission line model is the simplest of all; the cavity model is more accurate and complex. All methods provide a good physical insight of the basic antenna performance.

In the second group, we have:

- The method of moments (MoM);
- The finite-element method (FEM);

- The spectral domain technique (SDT);
- The finite-difference time domain (FDTD) method.

These methods are based on the electric current distribution on the patch conductor and the ground plane. These models provide more accurate results, but they are also more complicated to analyze.

The simulating software used in this study is "Advanced Design System"; it is based in the method of moments, so we are going to give a brief review into the method of moments.

The method of moments uses the surface currents to model the microstrip patch; and the volume polarization currents in the dielectric piece are used to model the fields in the dielectric piece. An integral equation is formulated for each of the unknown currents on the microstrip patch, the feed lines and their images in the ground plane. Integral equations are then transformed into algebraic equations that can be easily solved using a computer.

The moment method, is considered very accurate because takes into account the fringing fields outside the physical boundary of the two-dimensional patch and includes the effects of mutual coupling between two surface current elements as well as the surface wave effect in the dielectric, thus providing a more exact solution [3-3].

3.5 Excitation Techniques of Microstrip Antennas

The feeding method or excitation technique is an important design parameter because it influences to the input impedance, the polarization characteristic and the antenna efficiency. As the feeding method influences to the input impedance, is often used for purposes of impedance matching.

We can excite or feed a microstrip antenna directly or indirectly. A microstrip antenna is fed directly using a connecting element such as the use of a coaxial probe or by a microstrip line, when it is excited indirectly, there is no direct metallic contact between the feed line and radiating patch, and it could be using proximity coupling or by aperture coupling [3-3].

3.5.1 Coaxial or Probe Feed

As shown in Figure 3.3, the center conductor of the coaxial connector extends through the substrate and then is soldered to the radiating patch, while the outer conductor is connected to the ground plane.

The main advantage of this type of feeding scheme is that the feed can be placed at any desired location inside the patch in order to match with its input impedance (to achieve impedance matching). This feed method is easy to fabricate and has low spurious radiation.

The main disadvantage of a coaxial feed antenna is the requirement of drilling a hole in the substrate to reach the bottom part of the patch. Other disadvantages are that the connector protrudes outside the bottom ground planet, so that it is not completely planar and include narrow bandwidth.

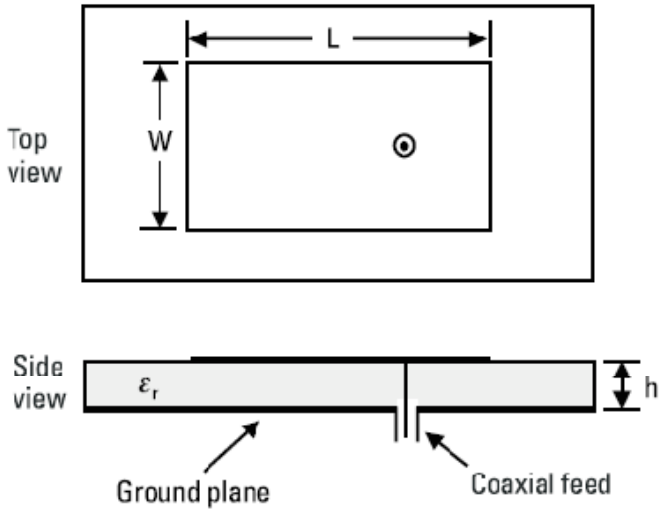

Figure 3.3 Coaxial or Probe Feed [3-3]

3.5.2 Microstrip line feed

A microstrip patch excited by microstrip transmission line feed is shown in Figure 3.4, as we can see the microstrip line is connected directly to the edge of the microstrip patch; the edge impedance should be matched with the impedance of the feed line for maximum power transfer. A method of impedance matching between the feed line and radiating patch is achieved by introducing a single or multi-section quarter-wavelength transformers.

This feed arrangement has the advantage that the feed can be etched on the same substrate to provide a planar structure, so they are easy to fabricate.

The conducting strip is smaller in width as compared to the patch; however in the millimeter-wave range, the size of the feed line is comparable to the patch size, leading to increased undesired radiation

The disadvantage is the radiation from the feed line, which leads to an increase in the cross-polar level.

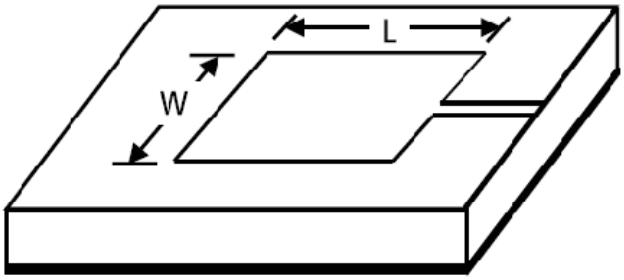

Figure 3.4 Microstrip line feed [3-3]

3.5.3 Proximity Coupling

This method uses electromagnetic coupling between the feed line and the radiating patch, which are printed on the same or separate substrates.

The feed line can be placed underneath the patch, or can also be placed in parallel and very close to the edge of a patch but always avoiding any soldering connection. Figure 3.5 shows a proximity coupled rectangular patch antenna.

The advantage of this coupling is that it yields the largest bandwidth compared to other coupling methods due to overall increase in the thickness of the microstrip patch antenna; it is easy to model and has a low spurious radiation. The disadvantage is that it is more difficult to fabricate.

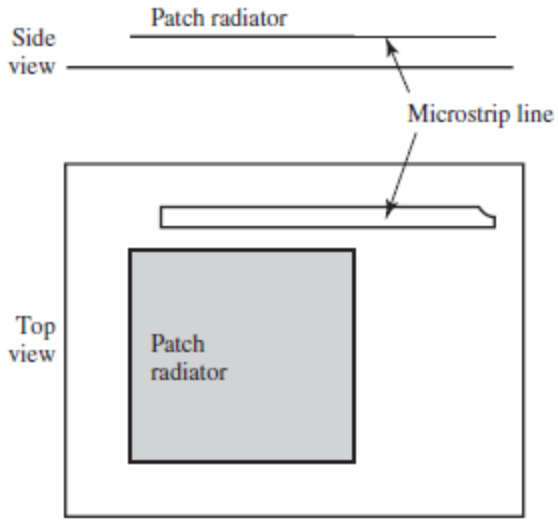

Figure 3.5 Proximity coupling for underneath the patch [3-2]

3.5.4 Aperture Coupled Feed

This is an indirect method of feeding the patch. In this type of feeding technique, the ground plane separates the radiating patch and the microstrip feed line. The coupling between the radiation patch and the feed line is made through an opening slot or an aperture in the ground plane. Figure 3-6 illustrates an aperture coupled microstrip rectangular antenna.

The coupling aperture is usually centered under the patch, leading to lower cross polarization due to symmetry of the configuration. The amount of coupling from the feed line to the patch is determined by the shape, size and location of the aperture. The slot aperture can be either resonant or nonresonant. The resonant slot provides another resonance in addition to the patch resonance thereby increasing the bandwidth, but at the expense of back radiation.

An advantage of this feeding technique is that the radiator is shielded from the feed structure by the ground plane; another advantage is the freedom of selecting two different substrates to get an optimum antenna performance (one for the feed line and another for the radiating patch).

The use of a thick substrate or stacked parasitic patches allows the patch to achieve wide bandwidth. [3-2]

In this study we are going to use this fed technique for all the antennas that we are going to simulate and build, because it can provide low cross-polarization levels, more freedom in impedance-matching design and it does not have

direct contact between the feed circuit and the radiating elements, hence it allows an independent optimization of these parts of the antenna.

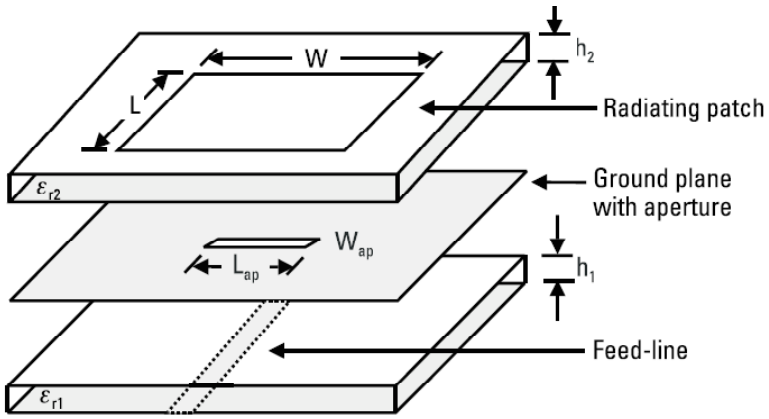

Figure 3.6 Aperture coupled microstrip rectangular antenna [3-3].

3.6 Circularly Polarized Microstrip Antennas

In our study we are going to build a microstrip antenna that it's going to work with circular polarization, this kind of antennas is widely used as efficient radiators in satellite communications because of the advantages that can provide us.

The most important of these advantages is that the orientation of the transmitting antenna and receiving antenna orientation need not necessarily be the same, so this allows the designer to have more freedom to design the transmission and reception system. With the use of circular polarized antennas, the system can tolerate changes in the polarization of the signal, these changes may be caused by the reflectivity, absorption, multipath, inclement weather and line of sight problems; conditions that (most of the time) can affect the polarization of a transmitted wave.
Hence, circular polarized antennas give us a higher probability of a successful link because they can transmit and receive signals on all planes.

In an antenna, circular polarization can be achieved through a single feed or using two feeds in the same patch. In an antenna array, we can generate circular polarization by the sequential rotation of the feeders. In next lines we are going to explain and describe these methods.

3.6.1 Dual-orthogonal feed circularly polarized microstrip antennas.

The most common and direct way to generate a circular polarization is through the use of a dual-feed technique. The two orthogonal modes required for the generation of circular polarization can be simultaneously excited using two feeds at orthogonal positions that are fed by $1\angle 0°$ and $1\angle 90°$ as shown in Figure 3.7

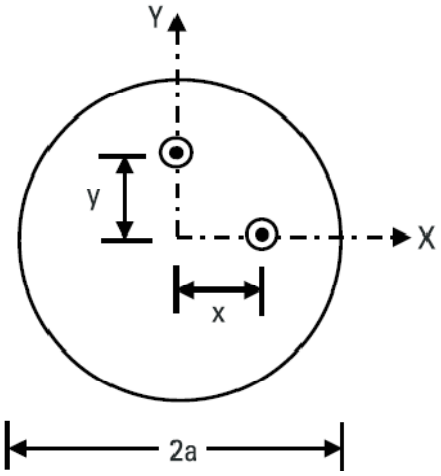

Figure 3.7 Dual feed in a circular microstrip antenna [3-3].

When we are designing a microstrip antenna, first we have to match it to the feed lines, this process can be achieved by an appropriately electing of the feed locations or through the use of impedance transformers.
Another technique is using a power divider circuit, which provides the required amplitude and phase excitations. Some of them, which have been successfully employed in a feed network of a circular polarization patch, are:

- The 180-Degree Hybrid
- The Wilkinson Power Divider
- The T-Junction Power Divider
- The Quadrature Hybrid

In this study we are going to use the “Quadrature Hybrid”, so we are going to give some theory about it.

3.6.1.1 The Quadrature (90 º) Hybrid

It is also known as Branch-line hybrid. The quadrature hybrids are 3dB directional couplers with 90° phase difference in the outputs through and coupled arms.
Its basic operation is: The input signal at port 1 is equally split in amplitude at the output ports 2 and 3 with a 90 degrees shift phase between these outputs. Because of this shift phase, any reflections from the patch tend to cancel at the output port 1 so that the match remains accepted [3-1].

The port 4, it is the isolated port because no power is coupled to that port. However, the combined mismatch at port 4 should be absorbed by a matched load to prevent potential power division degradation of the hybrid which, otherwise, can affect axial ratio performance.
The type of 3dB coupler that it has been designed for this project is as shown in Figure 3.8

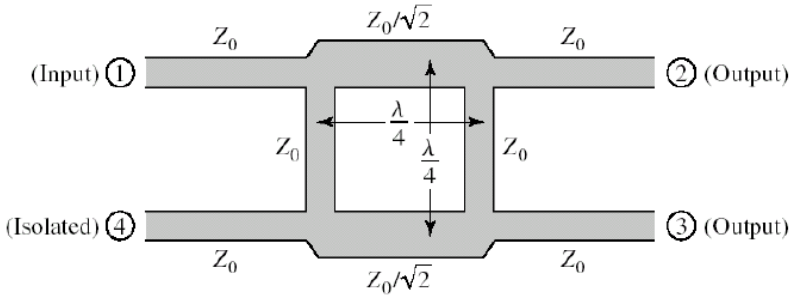

Figure 3.8 Geometry of a Branch-Line Coupler. [3-5]

The Table 3.1 shows some features about the Power Divider Networks, and it can explain why we decide to use the Quadrature Hybrid for our case of study.

	90° Phase Shift	Output Port Isolation	Input Match	Change of CP
T-junction divider	No*	No	Yes†	No
Wilkinson divider	No*	Yes	Yes†	No
Quadrature hybrid	Yes	Yes	Yes	Yes, by switching input and isolate ports
Ring hybrid	No*	Yes	Yes†	Yes,† by switching input and isolate ports

*Requires a quarter-wavelength of line extension in one output arm to generate phase shift.
†With a quarter-wavelength of line extension in one output arm in place.

Table 3-1 General characteristics of Power Divider Networks. [3-6]

We can mention that the main features are that we do not need to add any other device to get the 90 phase shift and neither for the input match; besides it give us an easy way to change the sense of circular polarization. These features led us to use less material and build a smaller and lighter antenna.

3.6.2 Singly Fed Circularly Polarized Microstrip Antennas

A singly – fed circular polarization may be regarded as one of the simplest radiators for exciting circular polarization and is very helpful in situations where the space do not allow to accommodate dual-orthogonal feeds with a power divider network.
This technique generally radiates linear polarization; but in our study case we want to achieve a circular polarization, so we are going to talk of some techniques used to achieve this goal.

Circular polarization can be accomplished by inserting a pair of symmetric perturbation elements at the boundary of a square or circular patch, in this case (as we can see at Figure 3.9.) a pair of truncated corners [3-1].

In our study, for the design and development of one of the antennas, we are going to employ this technique to enhance the axial ratio bandwidth of the antenna.

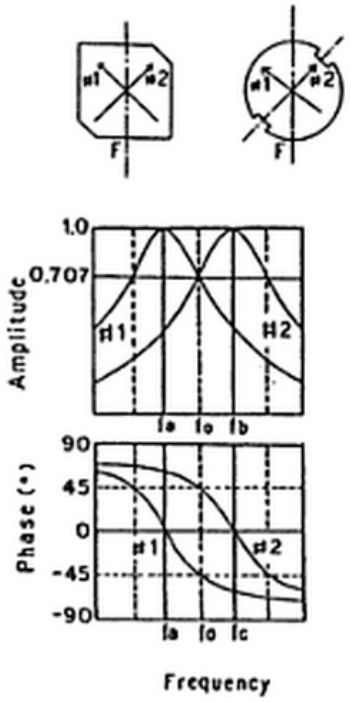

Figure 3.9 Aperture and phase of orthogonal modes in single point feed circularly polarized microstrip patch [3-1]

Other simple and common techniques to generate circular polarization are cutting a diagonal slot in the square or circular patch, or using a nearly square patch (also can be a nearly circle) on the diagonal, this produces two resonance modes corresponding to lengths W and L (where W/L= [1.01 - 1.10] in the case of a square patch), this two modes are spatially orthogonal, have equal magnitude and are in phase quadrature. The circular polarization is obtained at a frequency that is between the resonance frequencies of these two modes. [3-3]

3.6.2.1 Sequential Rotation Feeding Technique

One disadvantage we have with a single – feed microstrip antenna is that it give us a narrow impedance and axial ratio bandwidths; but we can increased them by using a sequentially rotated array configuration. [3-1, 3-3, 3-7, 3-8].

To get a circular polarized wave, the antenna elements are physically rotated relative to each other and the feed phase is individually adjusted to each element to compensate for the rotation.
It has been mathematically demonstrated in reference [3-1], that the sequential array radiates perfect circular polarized wave independently of

the polarization of the elements, I mean that the elements could be circularly or linearly polarized [3-3,3-7]; but we will have better results using circularly polarized elements.

Another feature of the sequential array is that can greatly reduce the cross polarization, even at off-center frequency, hence we can get a wideband circularly polarized microstrip array.

Figure 3.10 shows two 8-element arrays. One is a conventional (Figure 3.10a) and the other is sequential array (Figure 3.10b)

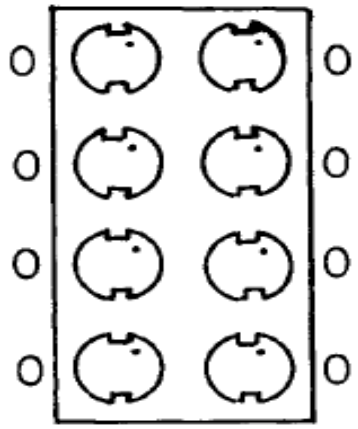

a)Conventional array

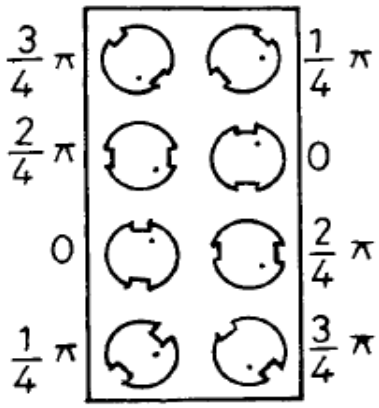

(b) Sequential array

Figure 3.10 Arrangement of elements for two test arrays [3-1]

We can see from the graphs that in the conventional array, there is no rotation of the CP elements and all elements are fed with equal amplitude

and 0 degrees phase difference; but in the sequential array the elements are rotated and fed with equal amplitude but with a phase difference equal to the angle of rotation.

Figure 3.10 and Figure 3.11 show the axial ratio and VSWR of these arrays.

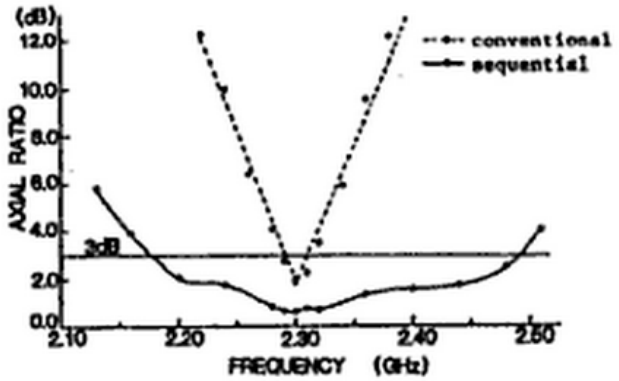

Figure 3.11 Measured axial ratio vs Frequency [3-1]

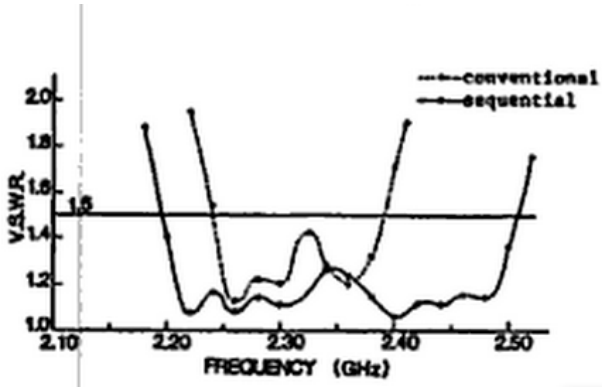

Figure 3.12 Measured V.S.W.R vs Frequency [3-1]

From figure 3.9 and 3.10, we can see that the sequential array has more wideband characteristics of polarization and impedance than the conventional array.

3.7 References

[3-1] D. M. Pozar and D. H. Schaubert, “Microstrip Antennas: The analysis and design of microstrip antennas and arrays”, IEEE Press, New York, 1995.

[3-2] C. A. Balanis, “ Modern Antenna Handbook”, Wiley, 2002.

[3-3] G. Kumar, K. P. Ray: “Broadband microstrip antennas”. Artech House, 2003. [3-4] Newman, E. H., and P. Tulyathan, ‘‘Analysis of Microstrip Antennas Using Method of Moments’’, *IEEE Trans. Antennas Propagation,* Vol. AP-29, January 1981, pp. 47–53.

[3-5] D. M. Pozar “Microwave Engineering”, 2nd Ed, Wiley, 1998.

[3-6] *Ramesh Garg*, Prakash Bhartia, Inder Bahl, Apisak Ittipiboon “*Microstrip Antenna Design Handbook*”, Artech House Inc Boston.London, 2001

[3-7] John J. Huang, “A technique for an array to generate circular polarization with linearly polarized elements,” *IEEE Trans. Antennas Propagat.*, vol. AP-34, pp. 1113–1124, Sept. 1986.

[3-8] Raul R. Ramirez*,* F. Flaviis, and N.G. Alexopoulos*,”* Single-Feed Circularly Polarized Microstrip Ring Antenna and Arrays” *IEEE Trans. Antennas Propagat.*, vol. 48, NO. 7, July 2000.

[3-9] S.D. Targonski, D.M. Pozar, "Design of wideband circularly polarized aperture-coupled microstrip antennas," *IEEE Transactions on Antennas and Propagation,* , vol.41, no.2, pp.214-220, Feb 1993

4 MICROSTRIP PATCH ANTENNA DESIGN AND RESULTS

4.1 Introduction

This chapter explains the procedure for designing a microstrip patch antenna, with a frequency band from 1520 MHz to 1660MHz. We have tried with four different configurations and each one is going to be explained.

In the design process, for all the configurations and as we already mentioned it in Chapter 3, we have used a simulating software; this software is the Advanced Design System.
Finally, for each design, we will show the results obtained from the simulations which will be compared with the measurements.

4.2 Design Specifications

In Chapter 1, Table 1-3 summarizes the antenna's specifications.

Another important issue in the design of the antenna, is the choice of materials to be used, because is necessary to set it them into the simulating software. In Table 4-1 we find a list of materials that are going to be used and their respective parameters. All these materials were provided by Centre Tecnològic de Telecomunicacions de Catalunya (CTTC).

		MATERIALS	
		Arlon 25N (A25N)	Rohacell51
PARAMETERS	Permittivity (Er)	3.38	1.05
	Loss Tagent (TanD)	0.0025	0.0008
	Substrate Thickness (H)	0.508 mm	3 mm (width)
	Conductivity (cupper)	5.813·107	-

Table 4-1 Shows materials used and their parameters**.**

4.3 Designs of Antennas.

We have developed four antenna designs, which have been separated according to the number of feeds they have. For this project we have used designs with one or two feedings.

4.3.1 Design of antennas with one feed.

4.3.1.1 Desing I

For this design we are going to use a design proposed by Wang and Chang [4-1].
The antenna of this design consists of three layers including a feed structure, foam and a radiation patch. The side and top view of the antenna are shown in Fig. 4.1 and Fig. 4.2 respectively.

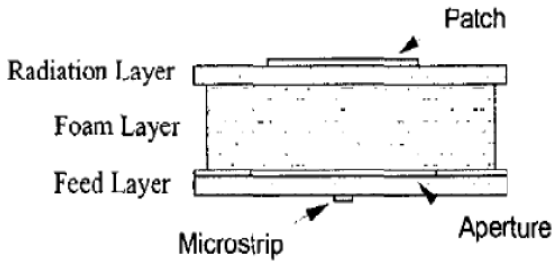

Figure 4.1 Side view of the antenna.[4-1]

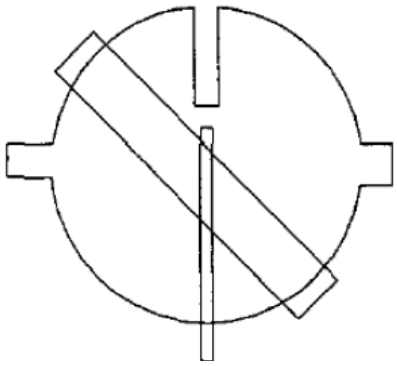

Figure 4.2 Top view of the antenna. [4-1]

The bottom substrate is a feed circuit which is conformed by an aperture and the microstrip feed line. The aperture is etched on the metal layer between the feed and foam layer with a 45 degrees orientation relative to the microstrip feed line.
The length of the slot helps us to adjust the matching between the feed network and the radiation patch

The middle layer is a foam layer which is employed to fix the distance between the feed circuit and radiation patch.

The top layer is a circular radiation patch, perturbed by a slot and two stubs to get the circular polarization and for the matching of the antenna.

Following these features, our objective is to design an antenna with an axial ratio bandwidth from 1.52 to 1.66 GHz.
As we already mentioned, we have to set the parameters, on the simulating software, of the substrate and we have to define the layers that are going to be part of the antenna.

Now we need to select the dimensions of every part of the antenna; we have to mention that we follow a trial and error method to get the best results for our antenna.
Figure 4.3 shows the tags that identify one by one the parts of the antenna.

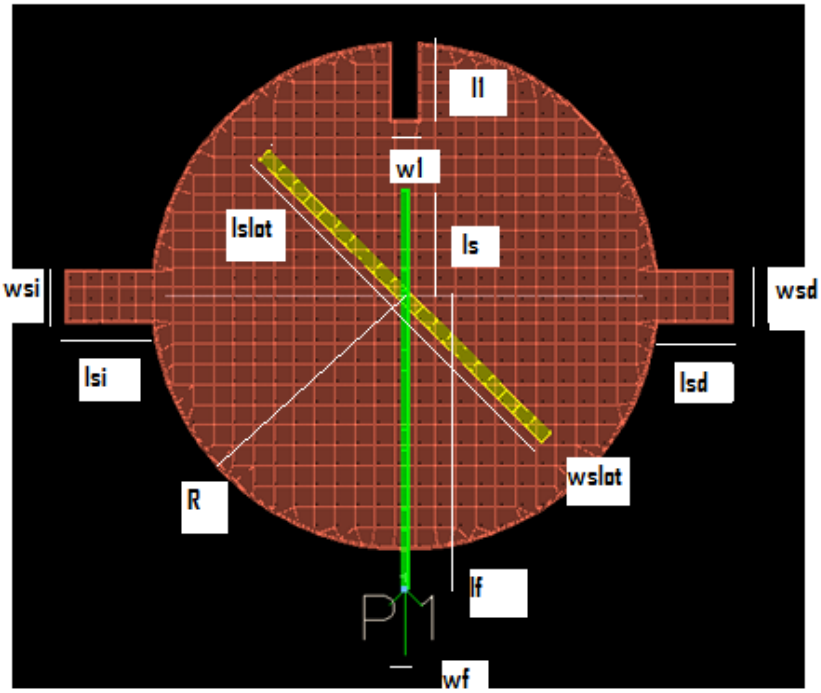

Figure 4.3 Shows the tags that identify one by one the parts of the antenna.

We have to mention that the parameters Feed Length (lf) and Feed Width (wf) belong to the line feed.
They were obtained using Line Calc tool; but we have to do an observation here, the value of the parameter E_Eff (that we have to set it inside Line Calc tool) affects to the length of the line feed; but not to the width. Besides we have changed the value of the length of the line feed (Feed Length) that was provided it by Line Calc to obtain a good value for the best performance of the antenna.

After using the Line Calc tool, we obtain:

Lf: 57.67 (using E_Eff of 180 degrees)
Wf: 1.169

After having made several simulations, this design allows us to reach a maximum axial radio bandwidth of 3.65%, that is why we decided to build an antenna for each one of the bands of 1.52-1.56 GHz and 1.62 -1.66

GHz; and thereby ensure the reception and transmission for BGAN systems.

4.3.1.1.1 Design I-1

After several tests and trials we obtained the dimensions of every part of the antenna for its best performance for the band from 1.62 – 1.66 GHz. Table 4.2 shows these values.

Part of the antenna	Tag	Dimensions(mm)
Opening length	l1	11.49
Opening width	w1	4
line length	ls	16
Slot length	lslot	59.96
Slot width	wslot	2
Feed length	lf	44
Feed width	wf	1.1
Radius	R	38.05
Right Stub length	lsd	11.4
Right Stub widht	wsd	8
Left Stub length	lsi	13.24
Left Stub widht	wsi	8
foam	-	12

Table 4-2 Shows the values of the parts of the antenna.

The simulated return loss of the antenna it is shown at Figure 4.4 and it is extended from 1.48 GHz to 1.76 GHz (17.28% with central frequency 1.62 GHz). The Smith chart plot it is shown at Figure 4.5 and shows the resonance of the antenna at the frequency of 1.56 GHz. At 1.7 GHz we can see that there is a loop, indicating two resonances very near in frequency, which is characteristic of a circular polarization.

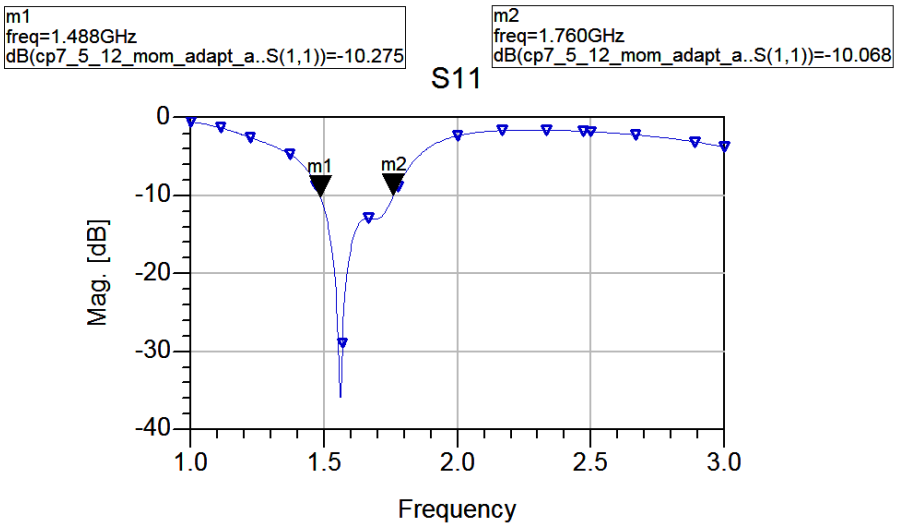

Figure 4.4 Simulated return loss for antenna design I-1**.**

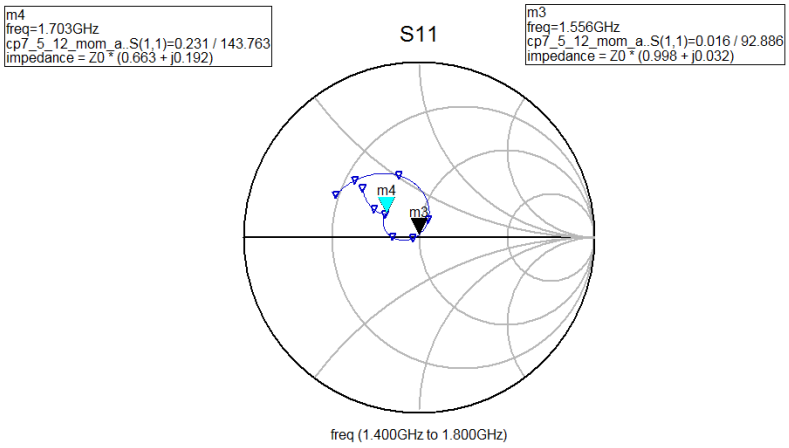

Figure 4.5 Simulated Smith Chart plot for this antenna design I-1.

Now we have to find the axial ratio bandwidth. Table 4.3 shows the axial ratio for this antenna design. The frequencies that are painted in green are those which meet the requirement of be minor than 3dB, these frequencies correspond to the axial ratio bandwidth which it is extended from 1.61 GHz to 1.67 GHz (60 MHz, 3.65 % with central frequency 1.64).In Figure 4.6 we can see a plot of these frequencies in all the impedance bandwidth.

Frequency(GHz)	Axial Ratio (dB)
1.48	14.95
1.5	13.174
1.52	11.356
1.54	9.505
1.56	7.632
1.58	5.753
1.6	3.89
1.61	2.992
1.62	2.067
1.64	0.439
1.66	1.513
1.67	2.308
1.68	3.129
1.7	4.67
1.72	6.122
1.74	7.48
1.76	8.746

Table 4-3 Shows the axial ratio for each frequency inside the impedance bandwidth.

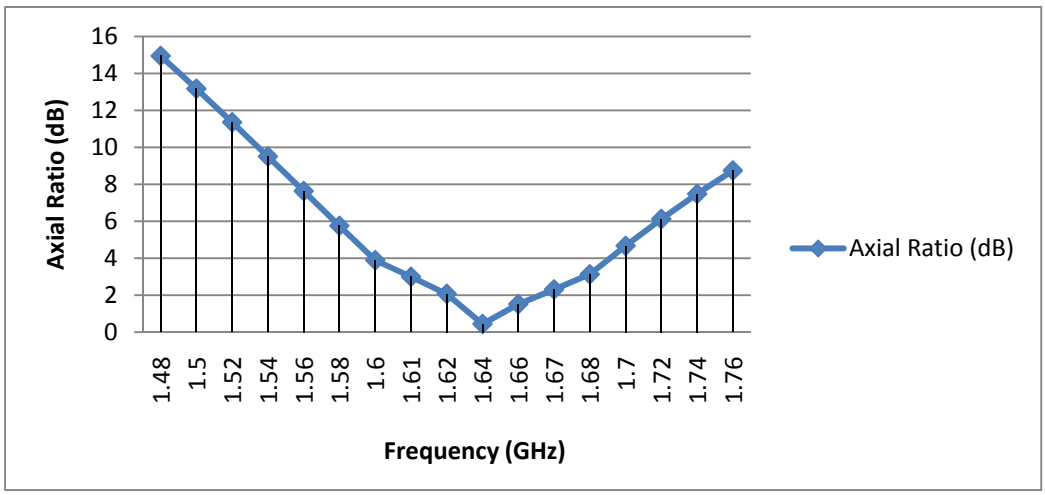

Figure 4.6 Shows the Axial Ratio for each frequency inside the impedance bandwidth.

As we can see from Figure 4.6, this antenna can be useful to cover only one band of the frequency objectives that we have proposed (1626.5 to 1660.5 MHz).

4.3.1.1.2 Design I-2

Again, after several tests and trials we obtained the dimensions of every part of the antenna to cover the other frequency band of 1.525 to 1.559 GHz.
Table 4.4 shows these values.

Part of the antenna	Tag	dimensions(mm)
Opening length	l1	18.52
Opening width	w1	4
line length	ls	13.61
Slot length	lslot	59.96
Slot width	wslot	2
Feed length	lf	53.81
Feed width	wf	1.1
Radius	R	41.31
Right Stub length	lsd	12.07
Right Stub widht	wsd	8
Left Stub length	lsi	8.3
Left Stub widht	wsi	8
foam	-	12

Table 4-4 Shows the values of the parts of the antenna**.**

Figure 4.7 shows the simulated return loss of the antenna, which is extended from 1.42 GHz to 1.68 GHz (16.77% with central frequency 1.55 GHz). The Smith chart plot it is shown at Figure 4.8 and it shows a loop indicating two resonances very near in frequency at 1.55 GHz.

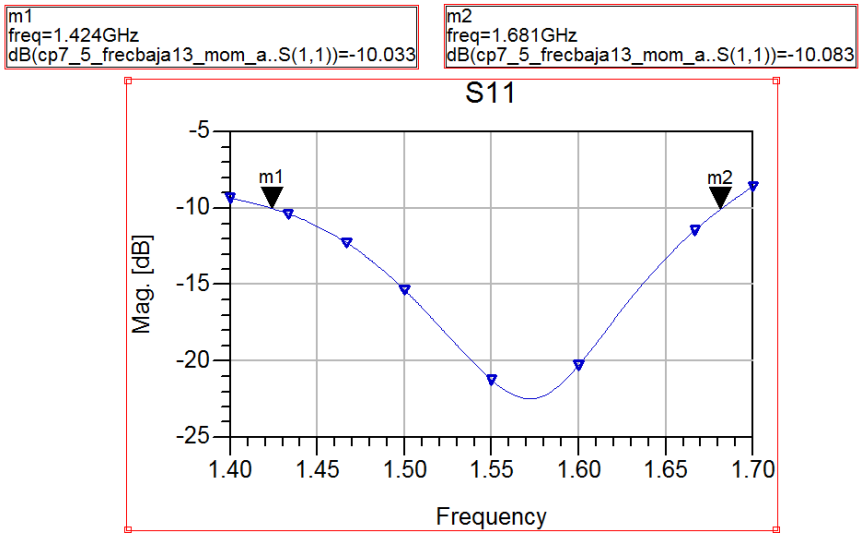

Figure 4.7 Simulated return loss for antenna design I-2.

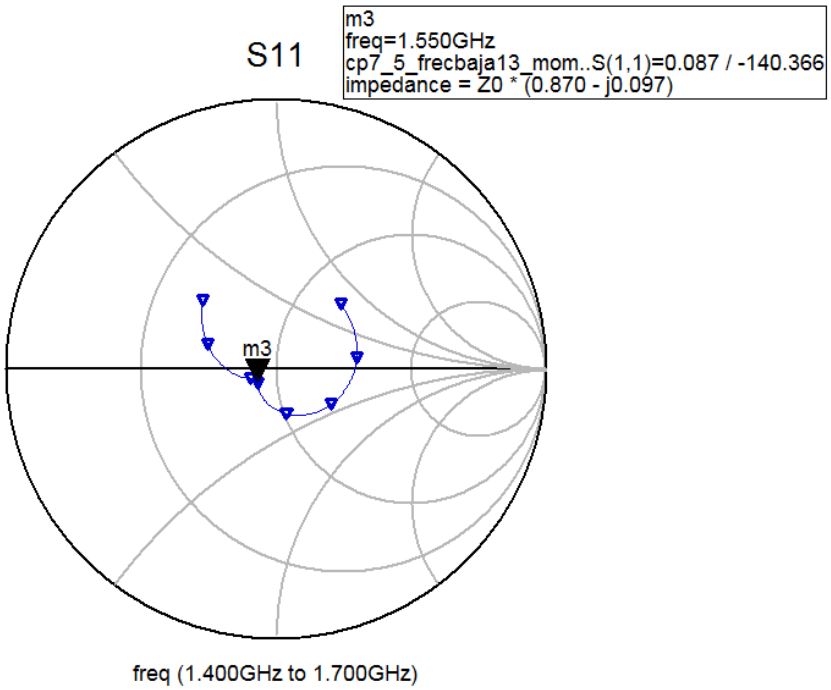

Figure 4.8 Simulated Smith Chart plot for antenna design I-2

Table 4.5 shows the axial ratio for this antenna design. Again, the frequencies that are painted in green are those which meet the requirement of be minor than 3dB, these frequencies correspond to the axial ratio bandwidth which it is extended from 1.52 GHz to 1.57 GHz (50MHz, 3.23 % with central frequency 1.545 GHz).

In Figure 4.9 we can see a plot of these frequencies in all the impedance bandwidth.

Frequency(GHz)	Axial Ratio (dB)
1.42	13.38
1.44	11.22
1.46	9.05
1.48	6.787
1.5	4.567
1.51	3.471
1.52	2.391
1.53	1.339
1.54	0.398
1.55	0.82
1.56	1.781
1.57	2.735
1.58	3.662
1.6	5.42
1.62	7.045
1.64	8.537
1.66	9.903
1.68	11.15
1.7	12.289

Table 4-5 Shows the axial ratio for each frequency inside the impedance bandwidth**.**

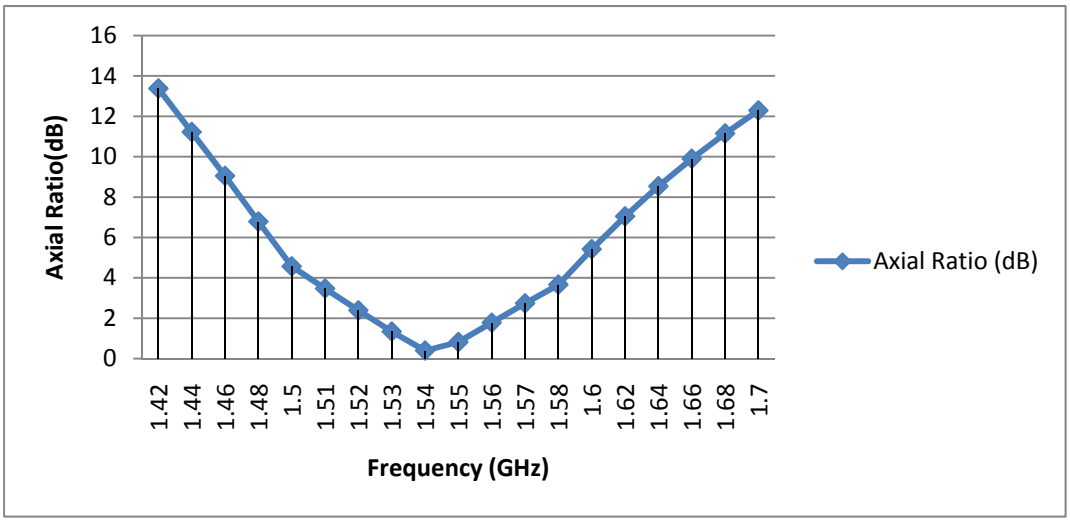

Figure 4.9 Shows the Axial Ratio for each frequency inside the impedance bandwidth.

Finally, Table 4.6 gives us a summary of both designs, it compares impedance bandwidth, axial ratio bandwidth and frequency band of use.

	Design I-1		Design I-2	
Impedance Bandwidth	1.48 -1.76 (GHz)	17.28%	1.42- 1.68 (GHz)	16.77%
Axial Ratio Bandwidth	1.61 - 1.67 (GHz)	3.65%	1.52- 1.57 GHz	3.23%
Frequency band of use	1.625–1.660 (GHz)	-	1.525–1.560 (GHz)	-

Table 4-6 Summary and comparison of both designs.

From the results of the simulations we can see that the bandwidth of the antennas is limited by the axial ratio bandwidth.
In this case, the major axial ratio bandwidth achieved is 60MHz (3.65%, Design I-1), but it is far from our objective of 140 MHz (8.8%).

Although in the paper referred previously it has a 7.2% measured of axial ratio bandwidth, we have to remember that they have used a substrate with a lower dielectric constant (they have used 2.33 and we have used 3.38), this feature can affect drastically the performance of the antenna.

4.3.1.2 Design II

Now, we are going to work with the design proposed by Jeen-Sheen Row [4-2]. The structure of the antenna is shown at Figure 4.10.

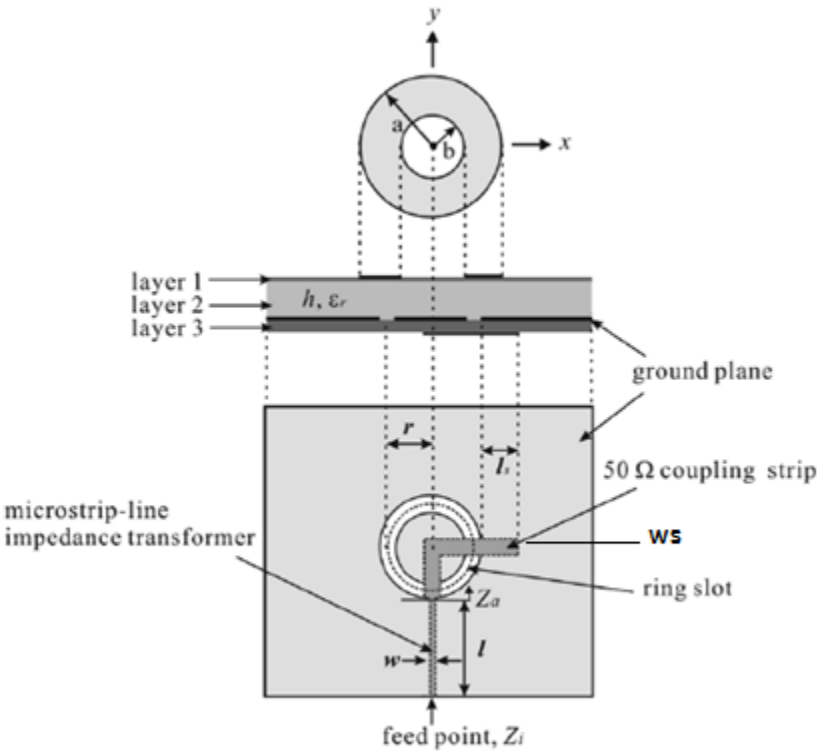

Figure 4.10 Shows the structure of the antenna. [4-2]

As we can see, also consist of three layers.

The top substrate (layer 1) it is an annular-ring patch with outer radius and inner radius.

The middle substrate (layer 2) it is a dielectric material of thickness "h" and relative permittivity "Er" and it is used it for easily adjusting the substrate thickness of antenna.

The bottom substrate (layer 3), it is composed by the microstrip feed line and the ring slot. They are respectively fabricated on the two faces of this substrate.
The microstrip feed line is composed of a 50 Ω coupling strip and a microstrip-line impedance transformer, which is used to transfer the slot impedance, seen at the edge of the ring slot, to the required input impedance at the feed point.

From Figure 4.10, we can see that:
-*"a"* and *"b"* are the outer and inner radius respectively.
- The mean radius of the ring slot centered below the annular-ring patch is *"r".*
- The impedance transformer has dimensions of *"l"* for its length and *"w"* for its width.
- And *"ls"* is the length of the stub.

The input impedance $Z_{i,}$ it is related to *r,l* and *w*, while the circular polarization is mainly controlled by the stub length *"ls" .*

In the simulating software, we have set the parameters of the substrate and we have defined the layers that are going to be part of the antenna. This antenna has the same structure of layers than the "Design I".

Now following the trial and error method, we need to select the dimensions of every part of the antenna to get its best performance.

We have to find the width of the 50Ω coupling strip, for that we are going to use, again, the Line Calc tool. As we already mentioned the value of E_Eff affects to the length of the coupling strip; in this case does not matter, because we will have change the length of the coupling strip (varying "ls" or "r").

After using the Line Calc tool, we obtain:

Lf: 57.67 (using E_Eff of 180 degrees)
Wf: 1.169

Again, after having made several simulations, this design allows us to reach a maximum axial radio bandwidth of 4.28% which is higher than 3.65% (Design I).
We decided to build an antenna for each one of the bands of 1.52-1.56 GHz and 1.62 -1.66 GHz.

4.3.1.2.1 Design II-1

Again, after several tests and trials we obtained the dimensions of every part of the antenna to operate in the frequency band of 1.62-1.66 GHz.

Table 4.7 shows these values.

Part of the antenna	Tag	dimensions(mm)
Outer radius	a	36
Inner radius	b	8
Mean radius of the ring slot	r	20.2
Stub width	ws	1.17
Stub length	ls	11
Impedance transformer length	l	32
Impedance transformer width	w	0.34
foam(h)	-	9
Permitivity(Er)	-	3.38

Table 4-7 Shows the dimensions of the antenna.

Before explaining the simulation results, we are going explain how we got the values of the microstrip-line impedance transformer.

After a lot of trials we obtained an acceptable impedance bandwidth, however we can enhance this bandwidth by improving the impedance matching; for that reason we have moved the reference of the port, from the end point to the start point of the impedance transformer. Figure 4.11 shows the tool used to transfer the reference of the port.

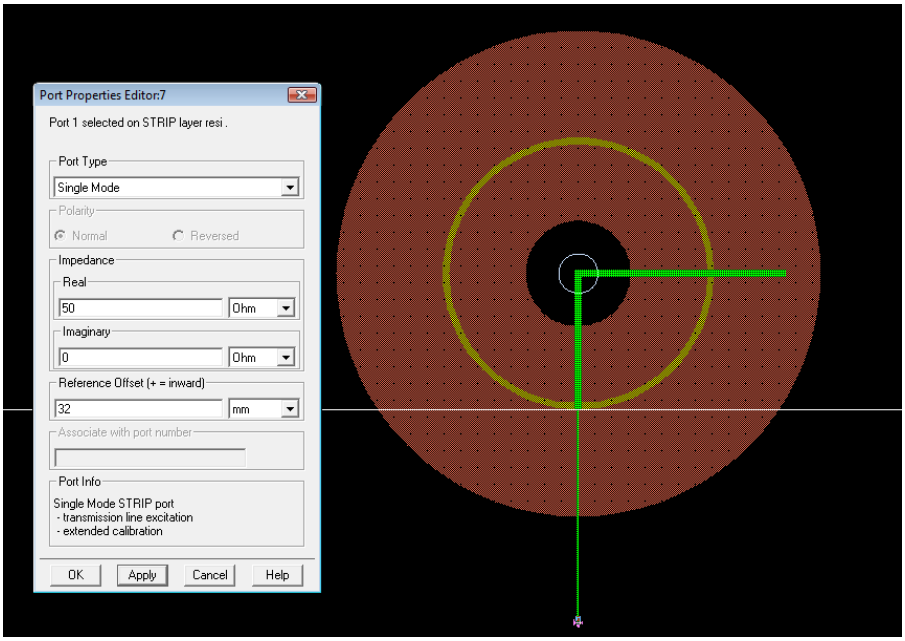

Figure 4.11 Shows the tool used to transfer the reference of the port.

Now we have to simulate our design; and from the results we will be able to extract impedance information. This information will allow us to know the impedance that we need to use to get the right impedance matching. Figure 4.12 has the results of this simulation.

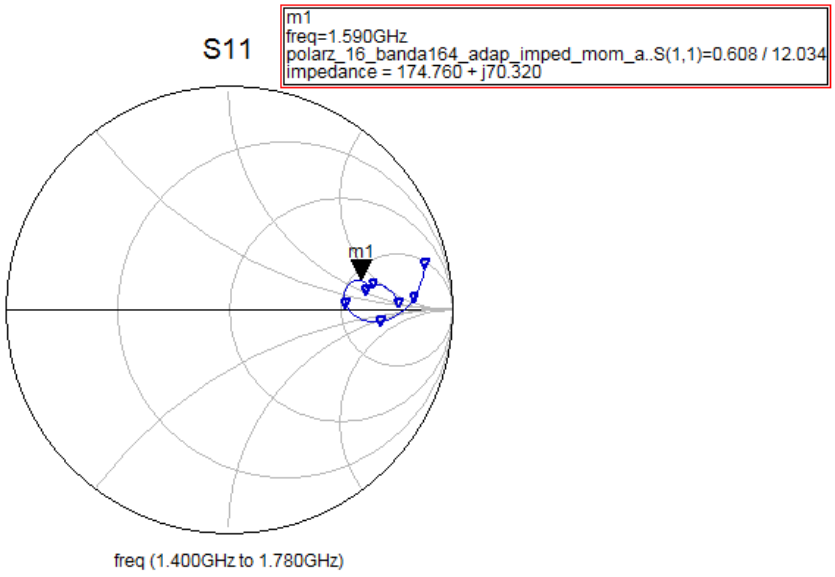

Figure 4.12 Shows the simulation results for the case when the reference of the port has been moved.

We can see from Figure 4.12 that at 1.59 GHz (we selected this frequency because is in the center of the bandwidth required), we have an impedance of 174.76 + j70.320 (we are going to work just with the real part). Then using:

$$Z_0 = \sqrt{Z_1 * Z_2}$$

Eq(4.1)

Where:

- Z_0 : Desired impedance
- Z_1 : Z_{in} = 174.76Ω.
- Z_2 : Z_a = 50Ω

Then, replacing values we have:

$$Z_0 = 93.47\Omega$$

With this impedance value we have to go to Line Calc tool to calculate the width of the impedance transformer. From the results of the Line Calc we have that the width of the impedance transformer should be 0.34 mm, so that by replacing this value in the antenna design we will have a good impedance matching.

Now we are going to see the simulation results for this design of antenna, Figure 4.13 shows the simulated return lossof the antenna, which is extended from 1.47 GHz to 1.75 GHz (17.37% with central frequency 1.61 GHz). The Smith chart plot it is shown at Figure 4.14 and it shows a loop indicating two resonances very near in frequency at 1.66 GHz. As we can see it is really good matched.

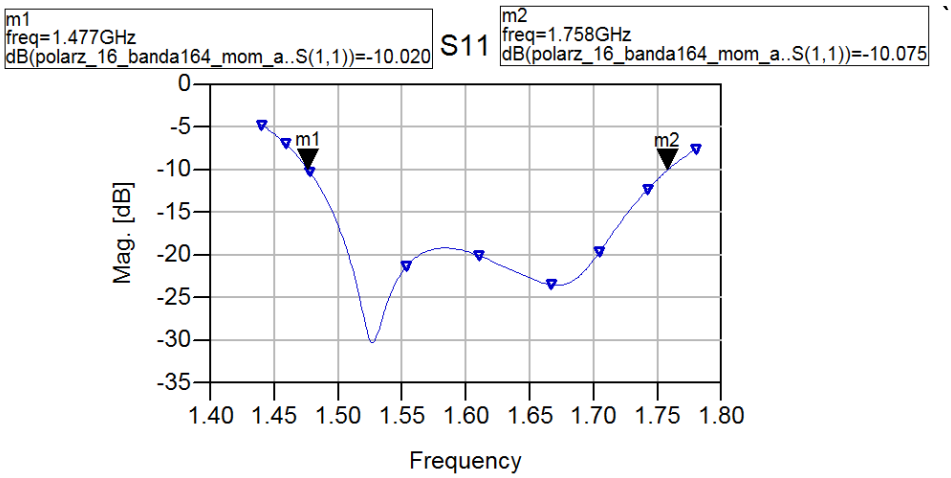

Figure 4.13 Simulated return loss for antenna design II-1.

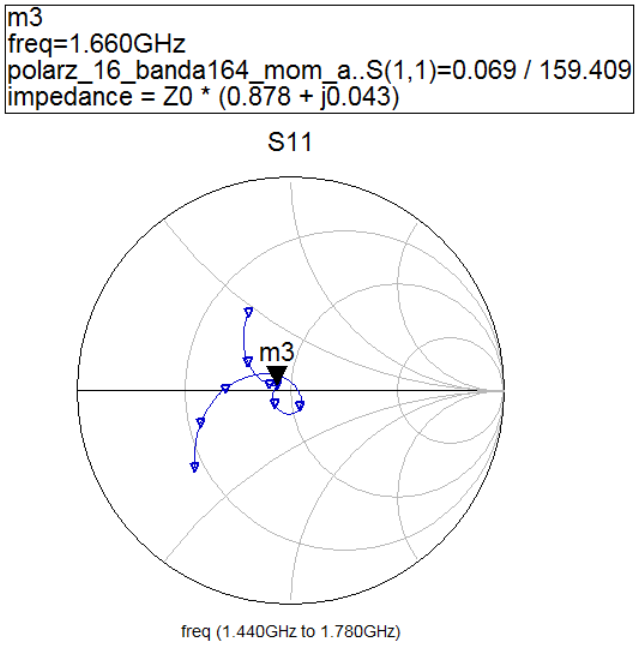

Figure 4.14 Simulated Smith Chart plot for antenna design II-1.

Table 4.8 shows the axial ratio for this antenna design. Frequencies on green are those which meet the requirement of be minor than 3dB, these frequencies correspond to the axial ratio bandwidth which it is extended from 1.6 GHz to 1.67 GHz (70MHz, 4.28 % with central frequency 1.645GHz).

In Figure 4.15 we can see a plot of these frequencies in all the impedance bandwidth

Frequency(GHz)	Axial Ratio (dB)
1.47	12.992
1.49	11.197
1.51	9.471
1.53	7.825
1.55	6.27
1.57	4.813
1.59	3.468
1.6	2.85
1.61	2.289
1.62	1.818
1.63	1.51
1.64	0.956
1.65	1.676
1.66	2.078
1.67	2.579
1.68	3.132
1.69	3.715
1.71	4.933
1.73	6.196
1.75	7.488
1.77	8.799

Table 4-8 Shows the axial ratio for each frequency inside the impedance bandwidth

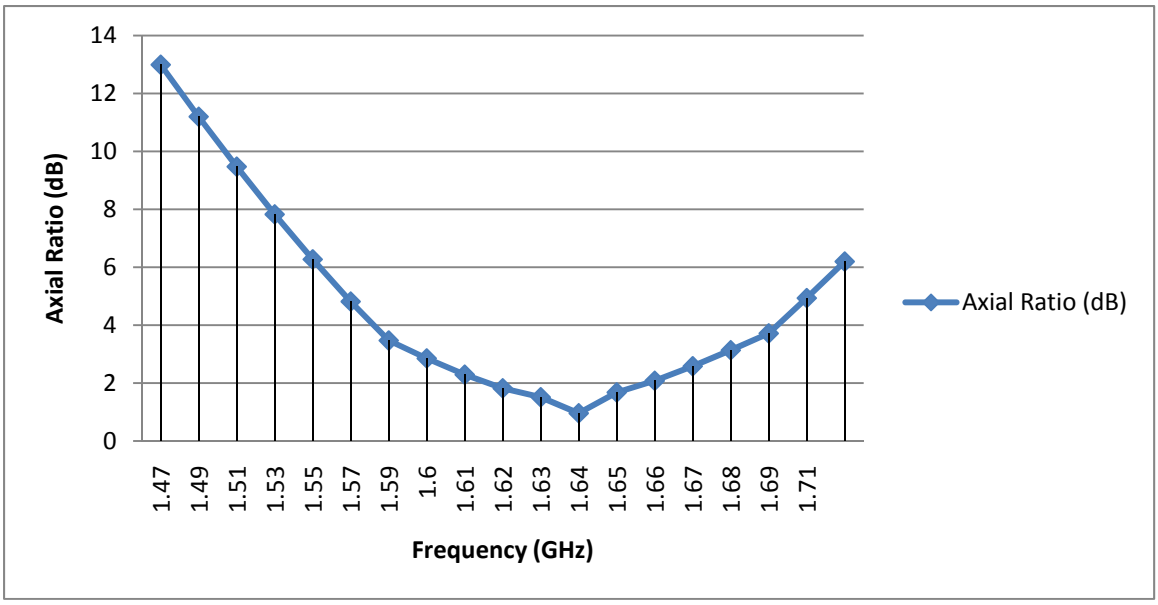

Figure 4.15 Shows the Axial Ratio for each frequency inside the impedance bandwidth

4.3.1.2.2 Design II-2

Now we are going to find the dimensions of the antenna to operate in the frequency band of 1.52- 1.56 GHz.

Table 4.9 shows these values.

Part of the antenna	Tag	dimensions(mm)
Outer radius	a	39.5
Inner radius	b	8
Mean radius of the ring slot	r	20.2
Stub width	ws	1.17
Stub length	ls	9.84
Impedance transformer length	l	35.94
Impedance transformer width	w	0.35
foam(h)	-	9
Permitivity(Er)	-	3.38

Table 4-9 Shows the dimensions of the antenna.

The values of the microstrip-line impedance transformer were obtained following the procedure described before (in Design II-1).

We found that at 1.54 GHz (we selected this frequency because is in the center of the bandwidth we are looking for), we have an impedance of 171.778 + j69.240 (we are going to work just with the real part). Then using Equation 4.1, we obtain:

$$Z_0 = 93.67\Omega$$

With this impedance value, we have to go to Line Calc tool, to calculate the width of the impedance transformer, and we obtained the value of 0.35 mm, so that by replacing this value in the antenna design we will have a good impedance matching.

Now we are going to see the simulation results for this antenna design, Figure 4.16 shows the simulated return lossof the antenna, which is extended from 1.45 GHz to 1.66 GHz (13.5% with central frequency 1.55 GHz). The Smith chart plot it is shown at Figure 4.17.

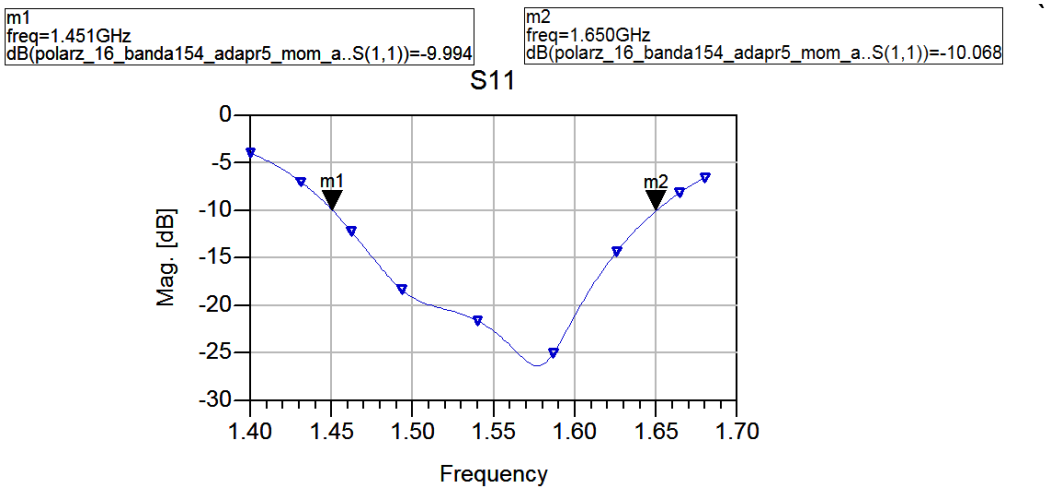

Figure 4.16 Simulated return loss for the antenna design II-2**.**

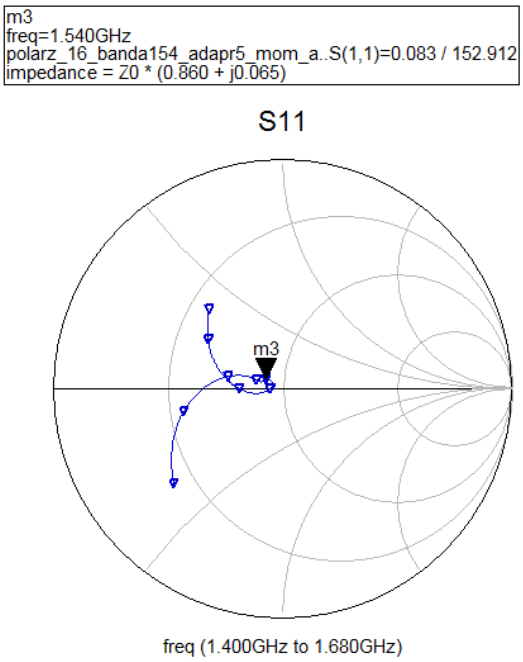

Figure 4.17 Simulated Smith Chart plot for the antenna design II-2.

Table 4.10 shows the axial ratio for this antenna design. Frequencies on green are those which meet the requirement of be minor than 3dB, these frequencies correspond to the axial ratio bandwidth which it is extended from 1.51 GHz to 1.55 GHz (40MHz, 2.61 % with central frequency 1.645GHz). Figure 4.18 shows a plot where are related the axial ratio and the each frequency inside the frequency range.

In Figure 4.22 we can see a plot of these frequencies in all the impedance bandwidth

Frequency(GHz)	Axial Ratio (dB)
1.45	9.601
1.47	6.969
1.49	4.469
1.5	3.28
1.51	2.212
1.52	1.287
1.53	0.906
1.54	1.463
1.55	2.318
1.56	3.208
1.57	4.084
1.59	5.752
1.61	7.302
1.63	8.744
1.66	10.738

Table 4-10 Shows the axial ratio for each frequency inside the impedance bandwidth

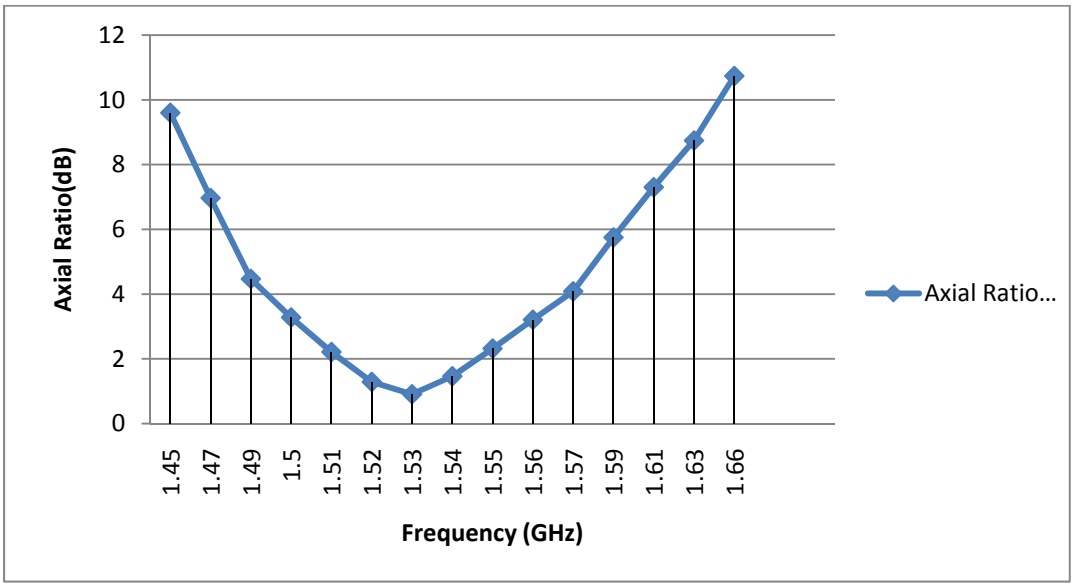

Figure 4.18 Shows the Axial Ratio for each frequency inside the impedance bandwidth

Finally, Table 4.11 gives us a summary of both designs, it compares impedance bandwidth, axial ratio bandwidth and frequency band of use.

	Design II-1		Design II-2	
Impedance Bandwidth	1.47 -1.75 (GHz)	17.37%	1.45 - 1.66 (GHz)	13.50%
Axial Ratio Bandwidth	1.60 - 1.67 (GHz)	4.28%	1.51- 1.55 (GHz)	2.61%
Frequency band of use	1.625–1.660 (GHz)	-	1.525–1.560 (GHz)	-

Table 4-11 Summary and comparison of both designs.

Again, the major axial ratio bandwidth achieved is 70MHz (4.28%,Design II-1), but it is far from our objective of 140 MHz (8.8%).

4.3.1.3 Design III

This design is a mixture of the two previous designs; we took some of their features to improve the axial radio bandwidth. From the first design, we have taken the perturbation elements at the boundary of the circular patch; and from the second design we have taken the annular shape for the radiating patch, the ring slot and the microstrip feed line. We can see the top view of the antenna at Figure 4.19.

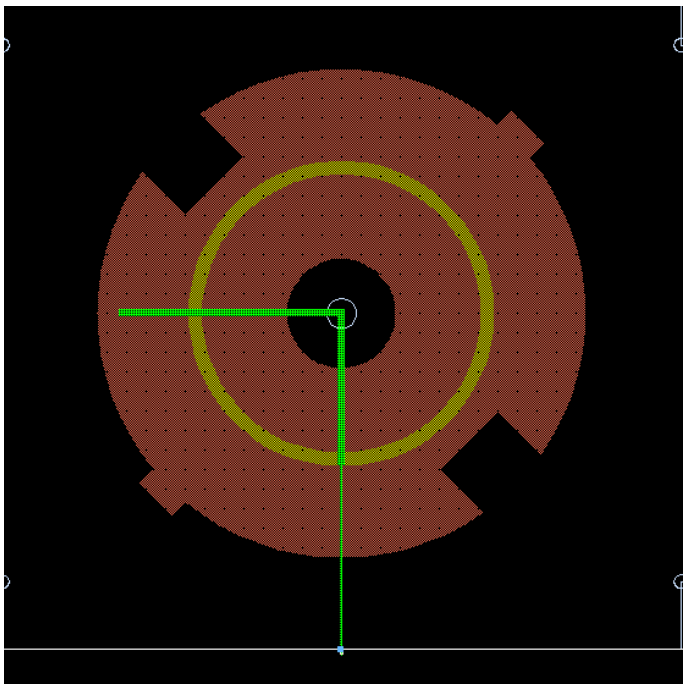

Figure 4.19 Shows the top view of the antenna.

The top substrate (in red color) it is an annular-ring patch, but we have added perturbation elements at its boundary.

The middle substrate (foam layer) it is a dielectric material of thickness (h) and relative permittivity (Er) and it is used it for easily adjusting the substrate thickness of antenna.

The bottom substrate it is composed by the microstrip feed line (in green color), and the ring slot (in yellow color). They are respectively fabricated on the two faces of this substrate.

The microstrip feed line has the same features as in Design II, except that it is rotated; we did that to achieve RHCP (result of simulations).

Following these features, our objective is to design an antenna with an axial ratio bandwidth from 1.52 to 1.66 GHz.

Parametric analysis.

To make the parametric analysis, the Figure 4.20 shows the labels of every part of the antenna that will be employed. (For more information see appendix 6.1 about the behavior of these parts.)

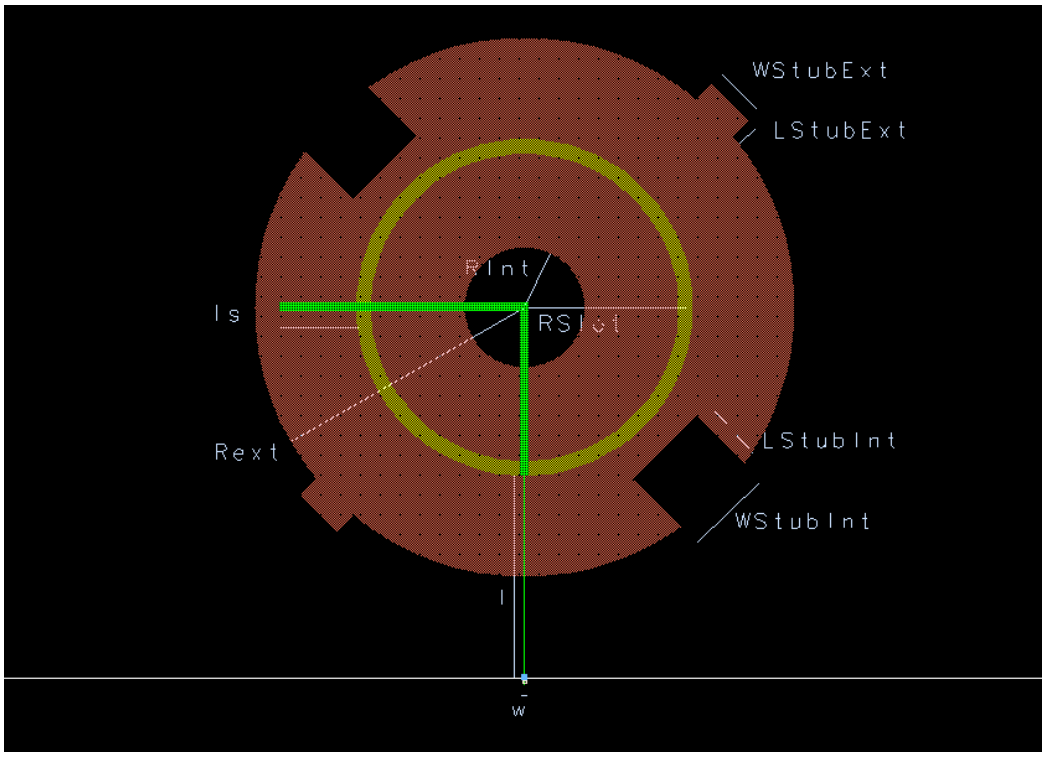

Figure 4.20 Shows the labels of the parts art of the antenna.

- **Adjusting the Length of the impedance transformer (l)**

It affects to the input impedance, but not to axial ratio.

- **Adjusting the Width of the impedance transformer (w)**

The effect in axial ratio is not very large; but for the input impedance it is an important parameter, because even little the variations in “w” affect to the input impedance.

- **Adjusting the Outer Radius (Rext)**

It affects the axial ratio; and also affects the input impedance

- **Adjusting the Inner Radius (Rint)**

It affects the axial ratio; but not to the impedance matching.

- **Adjusting the Length Stub (ls)**

It affects the axial ratio and the input impedance.

- **Adjusting the Inner Stub**

For the inner stub, we have studied the behavior of its width and its length.

Its width affects the axial ratio and the input impedance.

Its length affects the axial ratio and the input impedance.

- **Adjusting the Outer Stub**

For the outer stub, we also have studied the behavior of its width and its length.

Its width affects the axial ratio; and the input impedance but not in large scale

Its length affects the axial ratio; and the input impedance.

- **Adjusting the ring slot**

The mean radius of the slot and its width affects the input impedance.

Having an approximate knowledge of the parameters of the antenna and after having made several simulations, we obtained the dimensions of every part of the antenna to operate in the frequency band of 1.52-1.66 GHz. Table 4.12 shows these values

Part of the antenna	Tag	dimensions(mm)
Outer radius	Rext	36
Inner radius	Rint	8
Mean radius of the ring slot	Rslot	21.6
Width of the ring slot	Wslot	2
Stub width	ws	1.17
Stub length	ls	10.2
Impedance transformer length	l	27
Impedance transformer width	w	0.2
Length of the inner stub	LStubInt	9
Width of the inner stub	WStubInt	12
Length of the outer stub	LStubExt	3
Width of the outer stub	WStubExt	7
foam	h	18
Permitivity	Er	3.38

Table 4-12 Shows the dimensions of the antenna.

4.3.1.3.1 Simulation results

Now we are going to see the simulation results for this design of antenna, Figure 4.21 shows the simulated return lossof the antenna, which is extended from 1.49 GHz to 1.69 GHz (12.57% with central frequency 1.59 GHz). The Smith chart plot it is shown at Figure 4.22.

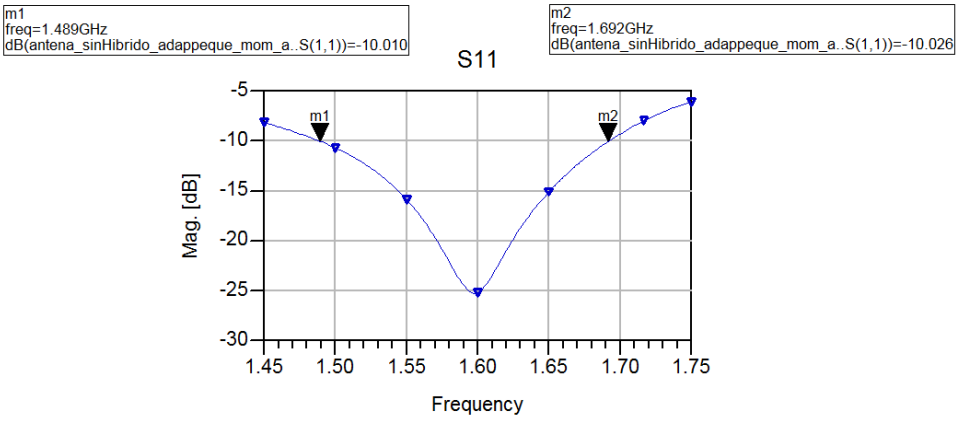

Figure 4.21 Simulated return loss for antenna design III.

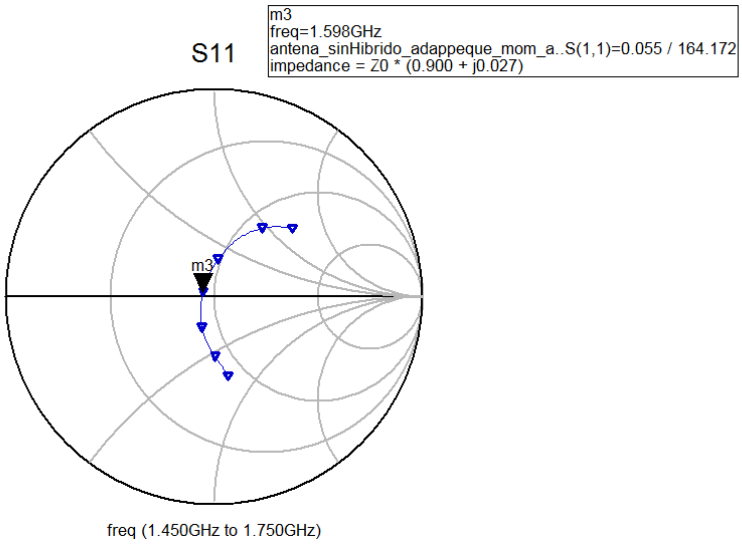

Figure 4.22 Simulated Smith Chart plot for antenna design III.

Table 4.13 shows the axial ratio for this antenna design. Frequencies on green are those which meet the requirement of be minor than 3dB, these frequencies correspond to the axial ratio bandwidth which is extended from 1.5 GHz to 1.66 GHz (160MHz, 10.12 % with central frequency 1.58GHz).
Figure 4.23 shows the plot of the axial ratio vs. frequency.
.

Frequency(GHz)	Axial Ratio (dB)
1.49	3.2
1.5	2.711
1.52	2.167
1.54	1.684
1.56	1.231
1.58	0.81
1.59	0.65
1.6	0.589
1.61	0.679
1.62	0.895
1.64	1.53
1.66	2.319
1.68	3.22
1.7	4.218

Table 4-13 Shows the axial ratio for each frequency inside the impedance bandwidth

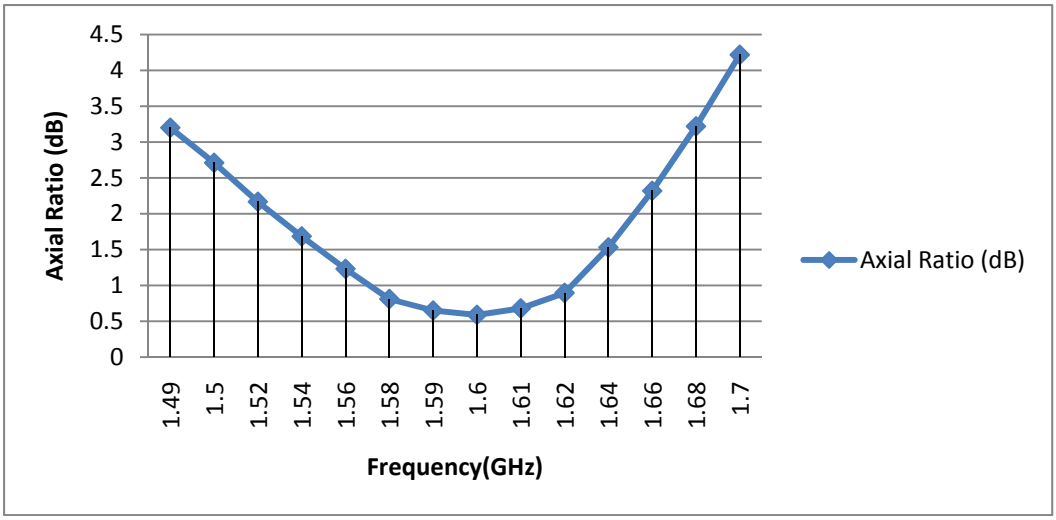

Figure 4.23 Shows the Axial Ratio for each frequency inside the impedance bandwidth

Now, another important target it is the gain of the antenna. Table 4.14 shows the gain vs. frequency for this antenna design. In this case, for each frequency tested, the gain value it is almost the same value of directivity, so we can say that we have a high efficiency. Figure 4.24 shows the plot of the gain vs. frequency for this antenna design.

Frequency(GHz)	Gain (dB)
1.49	7.501
1.5	7.562
1.52	7.673
1.54	7.772
1.56	7.863
1.58	7.946
1.59	7.985
1.6	8.022
1.61	8.057
1.62	8.09
1.64	8.146
1.66	8.147
1.68	8.207
1.7	8.201
1.72	8.163
1.74	8.093

Table 4-14 Shows the gain for each simulated frequency.

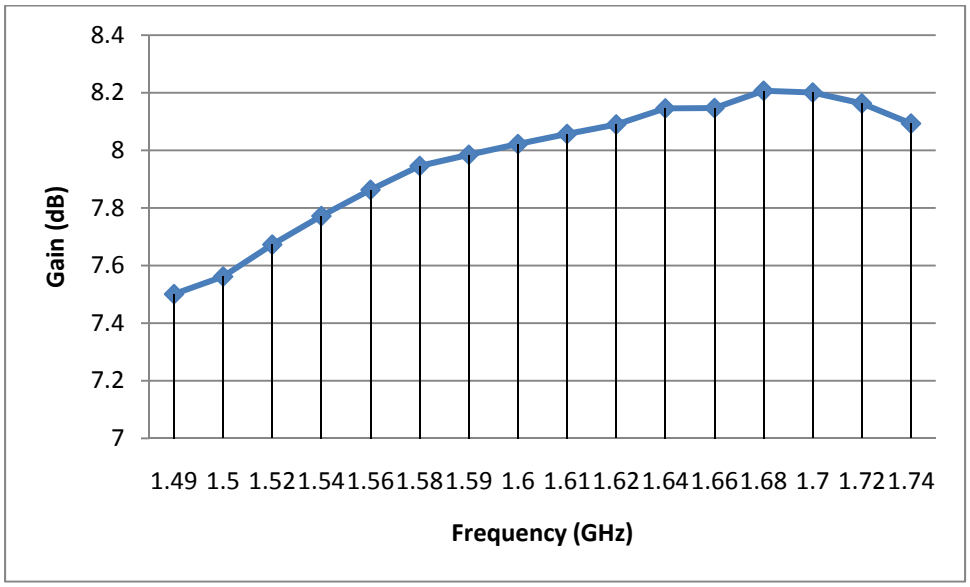

Figure 4.24 Shows the gain values vs frequency.

From these results, we can observe that the highest value of gain (within the target band) it is 8.147dB (measured at 1.66 GHz)

Now, we are going to show the 2D simulated radiation pattern at the central frequency of the target frequency band (1.6GHz), in Figure 4.25 we can see the radiation pattern for a planar cut of 0 degrees and in Figure 4.26, for a planar cut of 90 degrees.

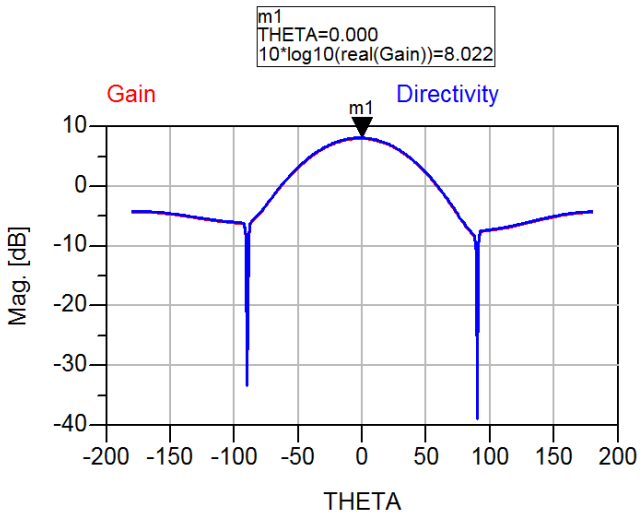

Figure 4.25 Radiation Pattern for a planar cut of 0 degrees at 1.6 GHz.

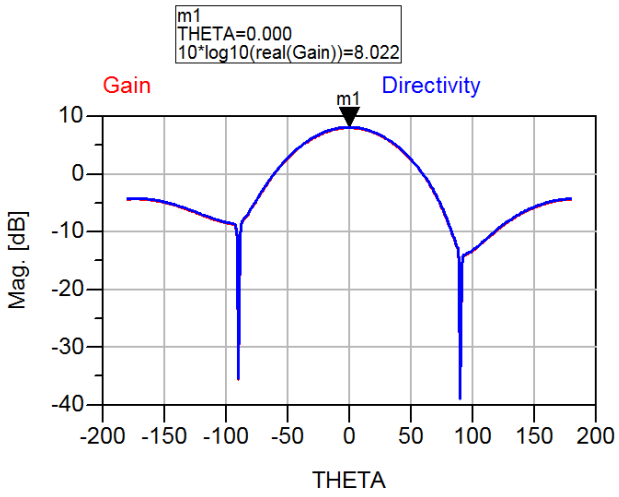

Figure 4.26 Radiation Pattern for a planar cut of 90 degrees at 1.6 GHz**.**

As we can see from the figures 4.25 y 4.26, our antenna has a high value of gain, we can see also that the difference, between the front radiation and back radiation, it is an acceptable value and explains the good efficiency (n= 96.6%).

4.3.1.3.2 Fabrication and Measurements

4.3.1.3.2.1 Fabrication

We have fabricated this antenna design in the CTTC laboratory.
A summary of the process we followed is:

1. We have exported the layouts from Agilent ADS momentum simulation into a Gerber file type. This type of file allows us to work with the LPKF Protolaser-S software. In Figure 4.27 we can see a picture of the machine.

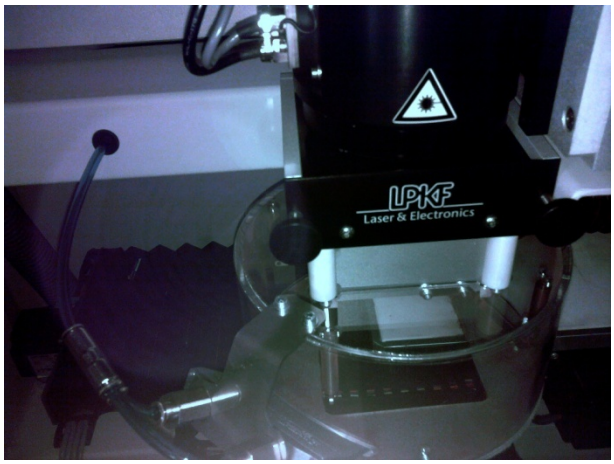

Figure 4.27 Shows the LPKF Protolaser-S machine**.**

2. Depending on the layer in which we work (remember that for each layer we have different substrates), the machine begins to "draw" on the substrate the contours for the feed line, stubs, patch and ground plane.

   In figure 4.28 (a) we show the top view of the bottom substrate and in figure 4.28 (b) we show the bottom view, we can see the contours that are going to be our references to remove the cupper required.

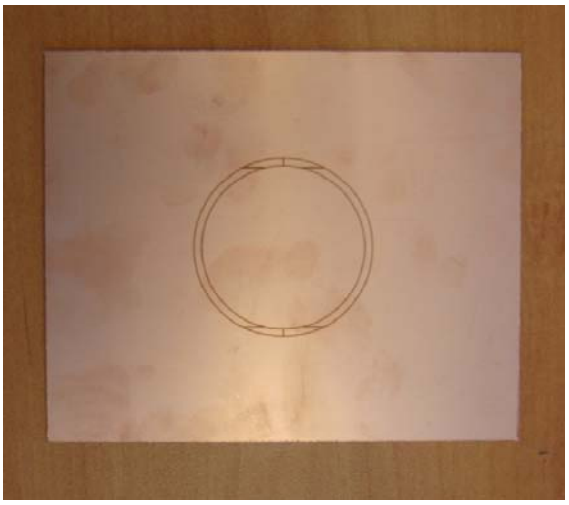

(a)Top view.

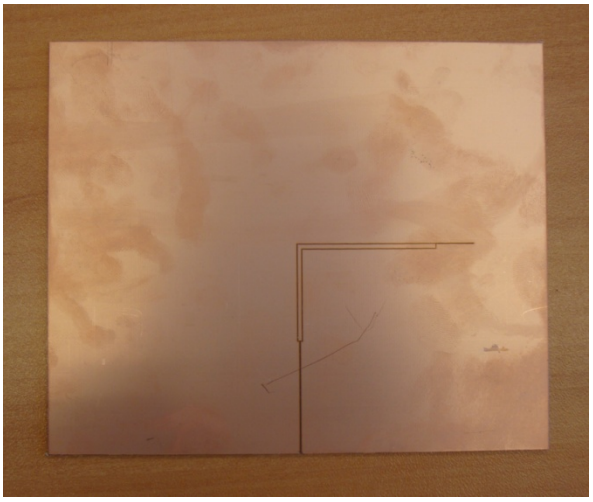

(b) Bottom view.

Figure 4.28 Shows the Bottom substrate with the contours marked by the LPKF Protolaser-S machine

3. All unwanted cooper was removed using a cutter and following the contours made by the LPKF Protolaser-S machine. In figure 4.29 (a) we show the top view of the top substrate (radiating patch) and in figure 4.29 (b) we show the bottom view.

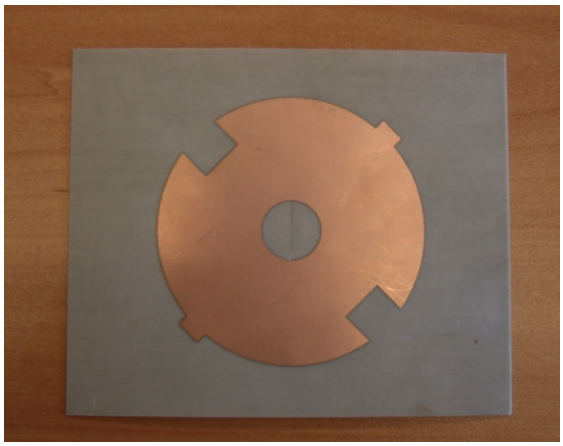

(a) Top view.

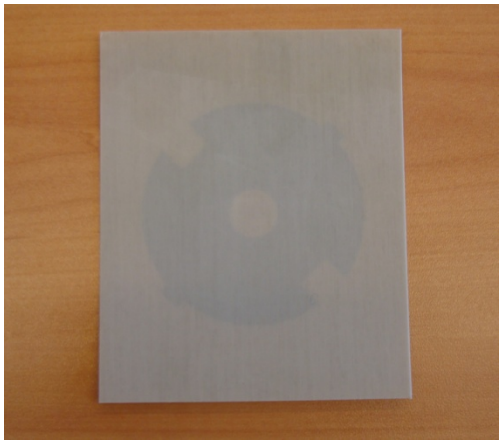

(b) Bottom view.

Figure 4.29 Shows the top substrate with the unwanted cupper removed**.**

4. We have used Rohacell51 for the layer that employs foam, and was easily cut by hand with a cutter, in this design we used 18mm of Rohacel51 (6 foams each one of 3mm).

5. We soldered the connector at the feed point.

6. The six Rohacell51 foams and the A25N substrates were bonded with an uniformly layer of glue spray over each surface. In Figure 4.30 (a) we show the top view of the antenna assembled, in figure 4.30 (b) we show the bottom view and in figure 4.30 (c) we show the side view.

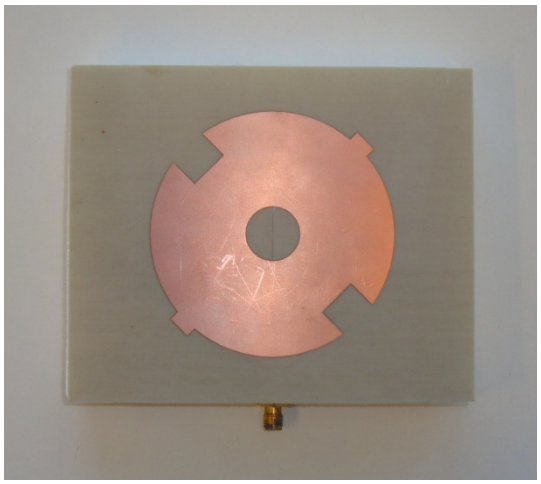

(a) Top view.

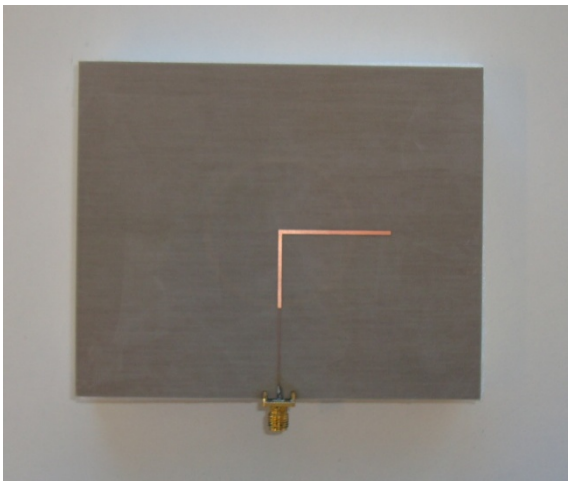

(b) Bottom view.

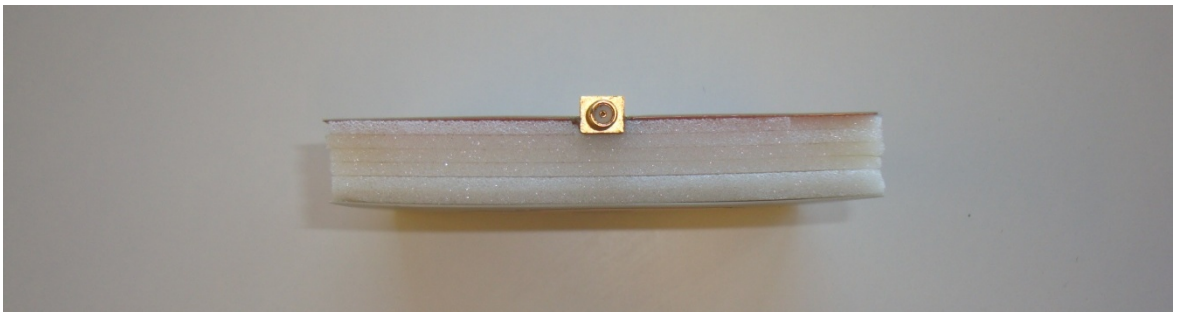

(c) Side view.

Figure 4.30 Shows the antenna assembled

4.3.1.3.2.2 Measurements

For measurements of the antenna we used a ZVA24 Rohde & Schwarz Vector Network Analyzer (VNA), in which we have measured the S11 parameter.

The simulated and measured results are compared in Figure 4.31. And table 4.15 shows a summary of the results.

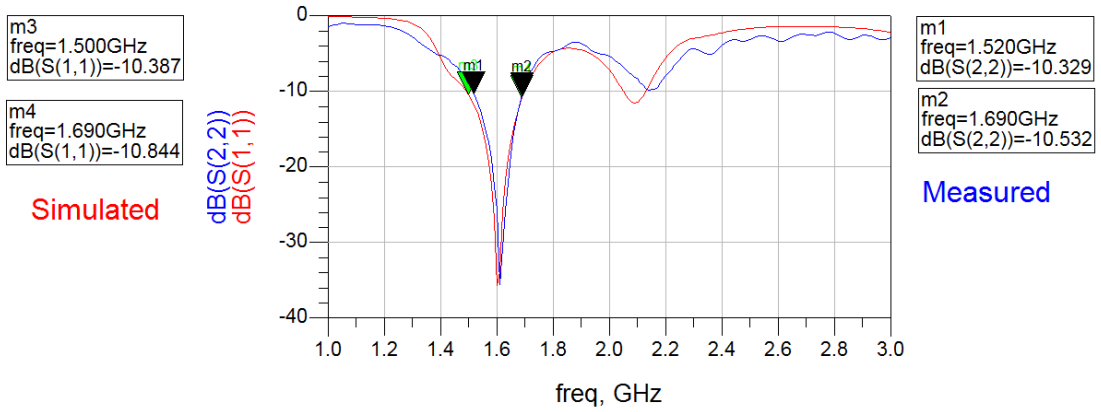

Figure 4.31 Shows the comparison between the simulated and measured results.

	simulated		measured	
Bandwidth	1.5-1.69 GHz	190MHz	1.52-1.69GHz	170 MHz

Table 4-15 Shows a summary of the comparison.

From the Figure 4.31 and the Table 4.15, we can see that there is a good agreement between measurements and simulations, however the measured results (blue graphic) show that have a lower bandwidth (10.59%) than the simulated values(red graphic-12.57%), but both are within the objective bandwidth.

Now we have to measure the antenna axial ratio and for that we are going to use the anechoic chamber.

It is possible to evaluate the performance of our circularly polarized antenna by rotating the test antenna (directed at broadside) relative to the linearly polarized broadband transmit antenna, then we are able to estimate the Axial Ratio at broadside.

In Fig. 4.32 we show how the measurements in the anechoic chamber were done.

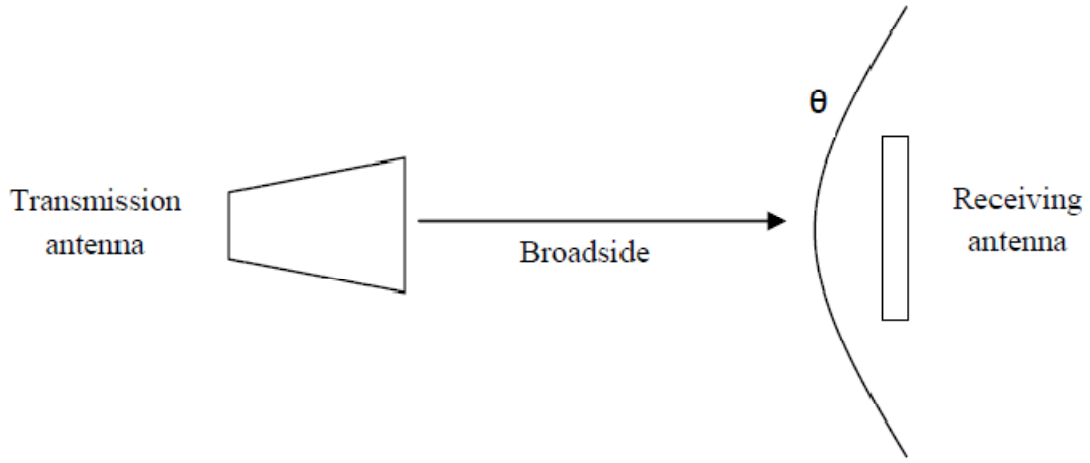

Figure 4.32 Shows the scheme for measuring

Figure 4.33 shows the measured received power at broadside (measured at 1.6 GHz) after rotating our antenna in the anechoic chamber. The observed ripple of approximately 2.48 dB corresponds to the axial ratio at broadside, it is an acceptable value because is below 3dB. This means that our antenna would receive either vertical or horizontal polarization

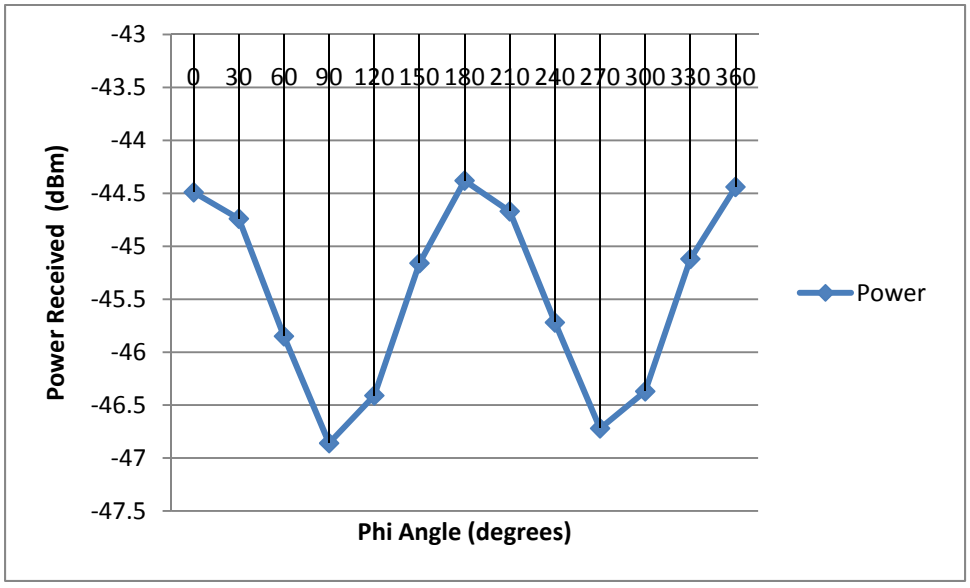

Figure 4.33 Measured Received power at broadside rotating the antenna under test relative to the transmit antenna. The ripple corresponds to the Axial Ratio

In Table 4.16 we can find a comparison between the simulated axial ratio values and the measured axial ratio values. They have been plotted in Figure 4.34.

	Axial Ratio	
Frequency (GHz)	Simulated	Measured
1.44	5.116	4.23594
1.46	4.149	3.46751
1.48	3.359	2.705
1.5	2.711	2.00686
1.52	2.167	1.29327
1.54	1.684	0.490211
1.56	1.231	0.703365
1.58	0.81	1.53618
1.6	0.589	2.25878
1.61	0.679	2.75
1.62	0.895	3.74579
1.64	1.53	5.17502
1.66	2.319	6.72485
1.68	3.22	8.1816
1.7	4.218	9.2654
Percentage	10.12%	8.41%

Table 4-16 Simulated vs Measured axial ratio values.

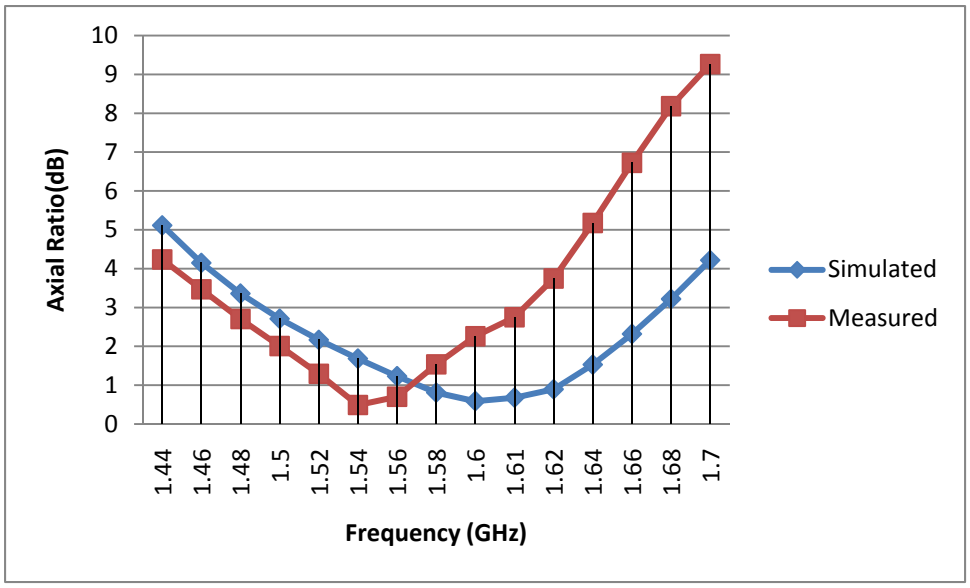

Figure 4.34 Shows the plot comparing simulated vs measured axial ratio values.

As we can see from Table 4.16 and Figure 4.34, in the measured results the axial ratio has shifted to the left and has been reduced compared to the simulated values. This may be due because we were not very accurate at the time of fabricating the antennas, ie patches were not exactly aligned. Another reason may be that the transmitting and receiving antenna at the moment of taking the measurements in the anechoic chamber have not been exactly aligned.

4.3.1.3.2.3 Radiation Pattern

We have measured the radiation pattern at the anechoic chamber using an antenna with linear polarization. The radiation pattern was measured at 1.54 GHz. As we can see at figure 4.35,the polar plot is scaled in degrees and decibels, and its relative (because its peak it is 0 dB). The plot corresponds to the XZ plane.

We can see that has a good main beam and It only has two side lobes, which means that there are not too much waste of energy. In conclusion we have a good radiation pattern.

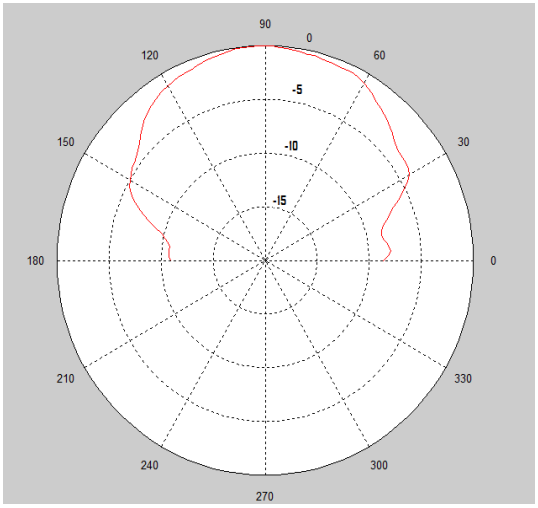

Figure 4.35 Radiation pattern measured for antenna design III

4.3.2 Design of antennas using two feeds.

We have designed one antenna with this feature, and we will demonstrate that the most common and direct way to generate a circular polarization is through the use of a dual-feed technique.

4.3.2.1 Design IV

This design is based in the second design (Design II); the main features that we have taken are the annular shape for the radiating patch and the ring slot. The feed network is going to be composed of a hybrid (see Appendix 3 for more information about dimensions of hybrid). We can see the top view of the antenna at Figure 4.36.

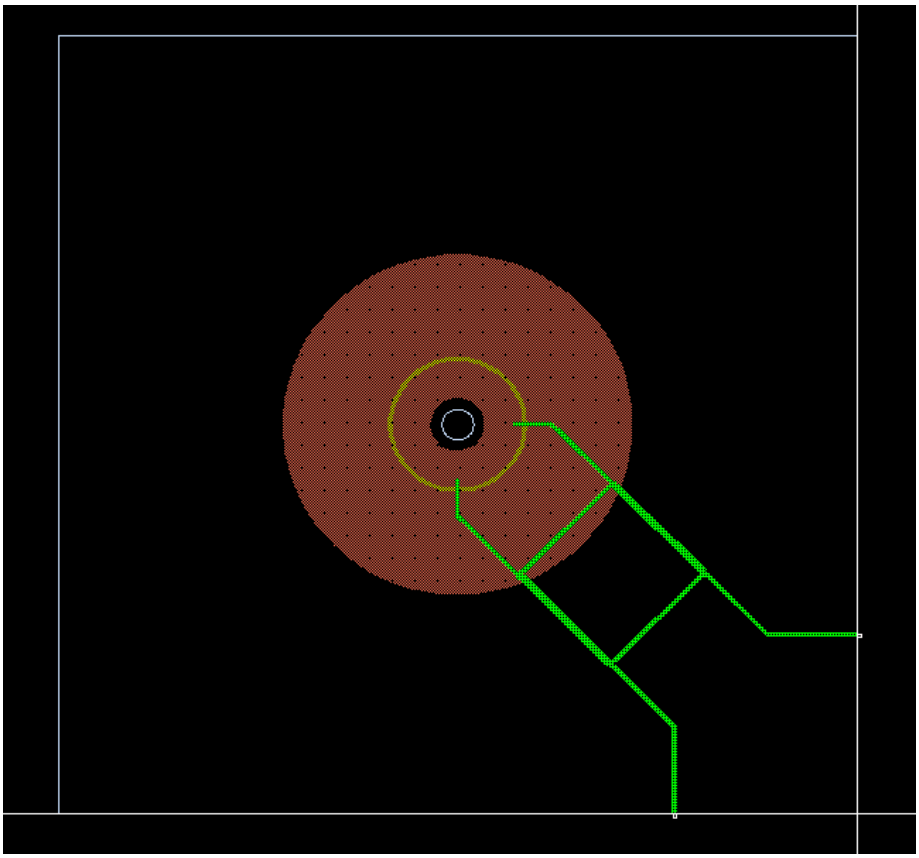

Figure 4.36 Shows the top view of the antenna.

The top substrate (in red color) it is an annular-ring patch.

The middle substrate (foam layer) it is a dielectric material of thickness (h) and relative permittivity (Er) and it is used it for easily adjusting the substrate thickness of antenna.

The bottom substrate it is composed by the feed network (hybrid-in green color), and the ring slot (in yellow color). They are respectively fabricated on the two faces of this substrate.
Following these features, our objective is to design an antenna with an axial ratio bandwidth from 1.52 to 1.66 GHz.

Parametric analysis.

To make the parametric analysis, the Figure 4.37 shows the labels of every part of the antenna that will be employed. (see Appendix 6.2 for more information)

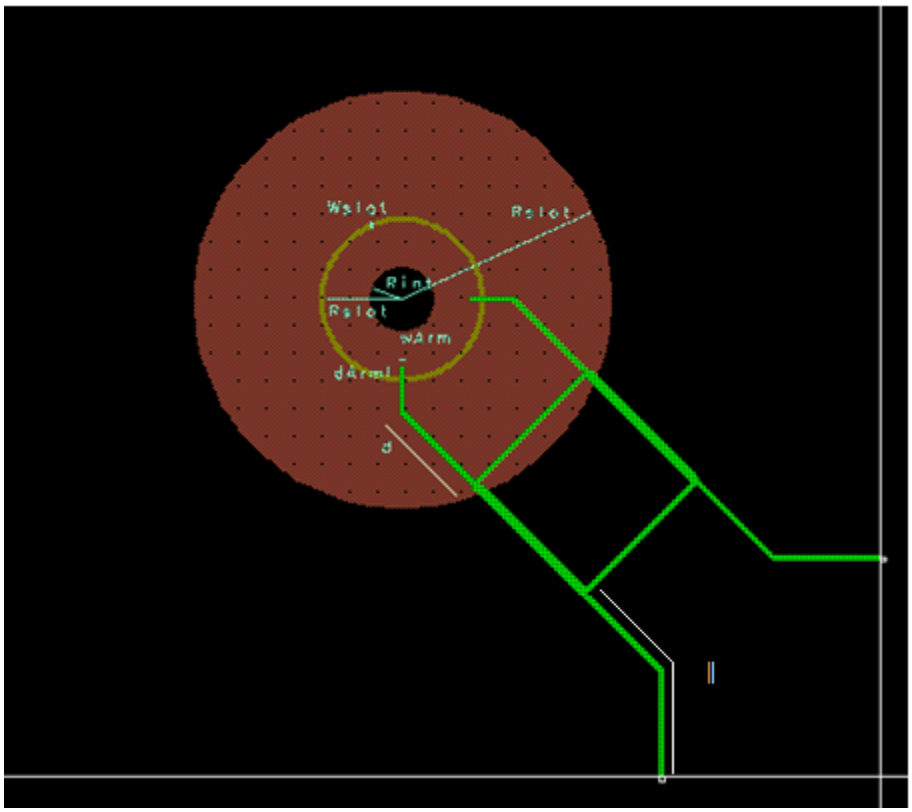

Figure 4.37 Shows the labels of the parts art of the antenna.

When we adjust “Rext”, “dArms” and “wArms” affect the axial ratio; but not too much the input impedance.

When we adjust “Rint” and when its value is different than zero, it has a little effect on the axial ratio and in the input impedance.

When we adjust “Rslot” it affects the axial ratio and we can almost place the minimum value of axial radio in a given frequency. It has a little effect in the input impedance.

When we adjust “d” it affects the axial ratio; and has a noticeable effect on the input impedance.

When we adjust “l” it affects the axial ratio; and also affects to the input impedance.

Having an approximate knowledge of the parameters of the antenna and after having made several simulations, we obtained the dimensions of every part of the antenna to operate in the frequency band of 1.52-1.66 GHz. Table 4.17 shows these values

Part of the antenna	Tag	dimensions(mm)
Outer radius	Rext	39
Inner radius	Rint	6
Mean radius of the ring slot	Rslot	15
Width of the ring slot	Wslot	1
Arms length	dArm	2
Arms width	wArm	1.07
distance	d	18.5
length	l	40
foam	h	3
Permitivity	Er	3.38

Table 4-17 Shows the dimensions of the antenna.

4.3.2.1.1 Simulation results

Now we are going to see the simulation results for this design of antenna, Figure 4.38 shows the simulated return loss of the antenna, which is extended from 1.39 GHz to 1.80 GHz (25.70% with central frequency 1.59 GHz). The Smith chart plot it is shown at Figure 4.39.

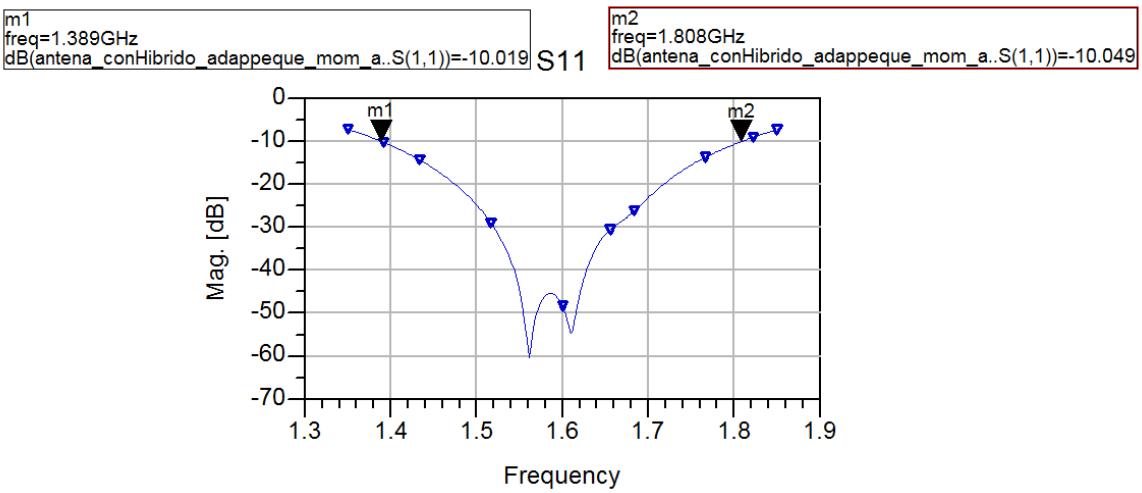

Figure 4.38 Simulated return loss.

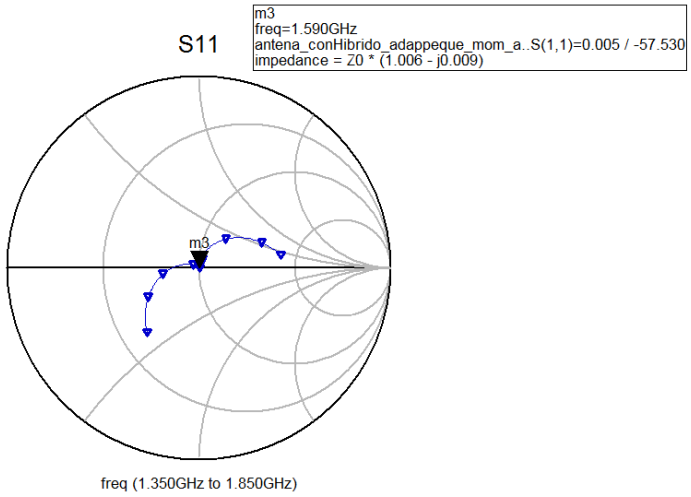

Figure 4.39 Simulated Smith Chart plot.

Table 4.18 shows the axial ratio for this antenna design. Frequencies on green are those which meet the requirement of be minor than 3dB, these frequencies correspond to the axial ratio bandwidth which it is extended from 1.45 GHz to 1.72 GHz (270MHz, 17.03 % with central frequency 1.58GHz).Figure 4.40 shows the plot of the axial ratio vs frequency in all the simulated bandwidth.

Frequency	Axial Ratio
1.39	4.093
1.41	3.696
1.43	3.294
1.45	2.89
1.47	2.485
1.49	2.081
1.51	1.676
1.52	1.478
1.54	1.094
1.56	0.746
1.58	0.504
1.6	0.521
1.62	0.757
1.64	1.073
1.66	1.52
1.68	2.064
1.7	2.539
1.72	2.966
1.74	3.379
1.76	3.788
1.78	4.194
1.8	4.599

Table 4-18 Shows the axial ratio for each frequency inside the impedance bandwidth

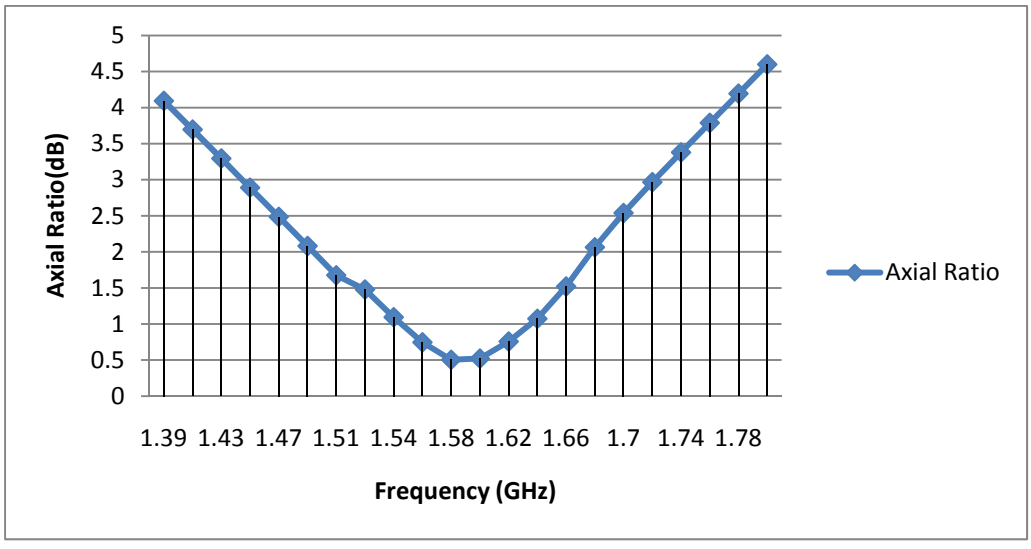

Figure 4.40 Shows the Axial Ratio for each frequency inside the simulated bandwidth

Now, we have to evaluate the gain of the antenna. Table 4.19 shows the gain and the directivity vs frequency for this antenna design. In this case, for each frequency tested, the gain value does not match with the value of directivity, so we do not have a good efficiency. Figure 4.41 shows the plot of the gain and directivity vs frequency for this antenna design.

Frequency (GHz)	Gain	Directivity (dB)
1.39	-7.26	2.649
1.41	-6.336	3.174
1.43	-5.381	3.695
1.45	-4.391	4.209
1.47	-3.356	4.711
1.49	-2.271	5.197
1.51	-1.082	5.679
1.52	0.485	5.903
1.54	0.764	6.331
1.56	2.073	6.729
1.58	3.423	7.095
1.6	4.758	7.427
1.62	5.97	7.723
1.64	6.897	7.982
1.66	7.372	8.207
1.68	7.344	8.396
1.7	6.915	8.552
1.72	6.261	8.674
1.74	5.523	8.765
1.76	4.786	8.824
1.78	4.09	8.851
1.8	3.449	8.848

Table 4-19 Shows the gain and directivity for each simulated frequency.

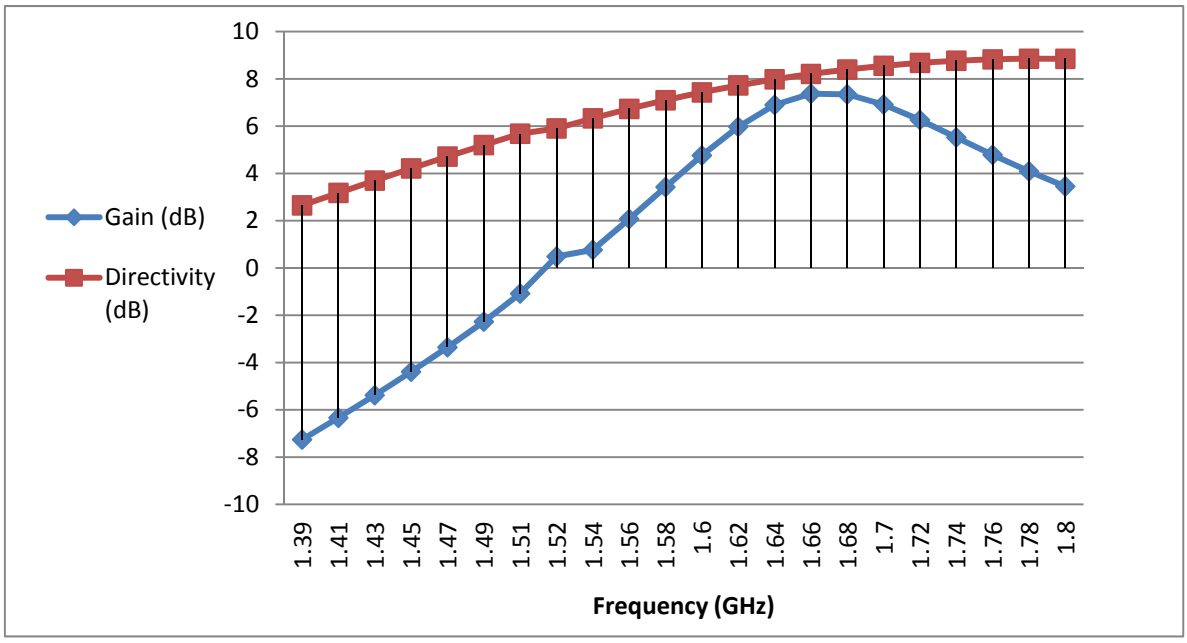

Figure 4.41 Shows the gain and directivity values vs frequency

From these results, we can observe that the highest value of gain (within the target band) it is 7.372 dB, and the highest value of directivity is 8.207 dB (both measured at 1.66 GHz)

Now, we show the 2D simulated radiation pattern at the central frequency of the target range (1.6GHz), in Figure 4.42 we can see the radiation pattern for a planar cut of 0 degrees and in Figure 4.43, for a planar cut of 90 degrees.

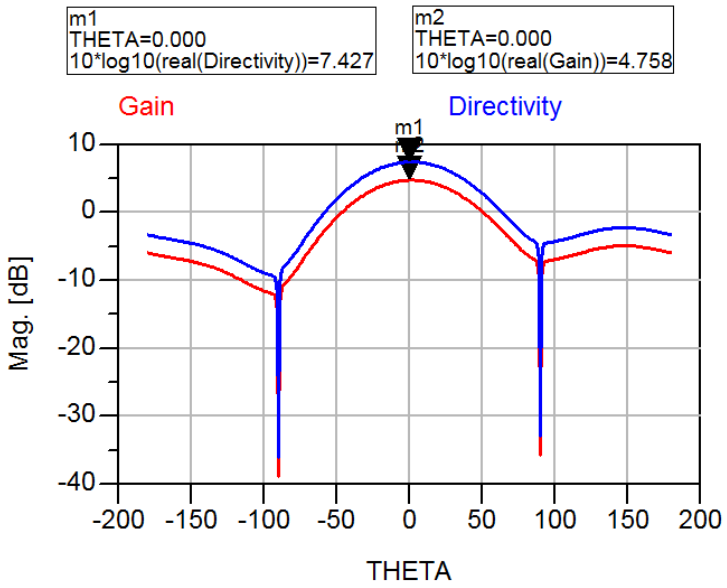

Figure 4.42 Radiation Pattern for a planar cut of 0 degrees at 1.6 GHz.

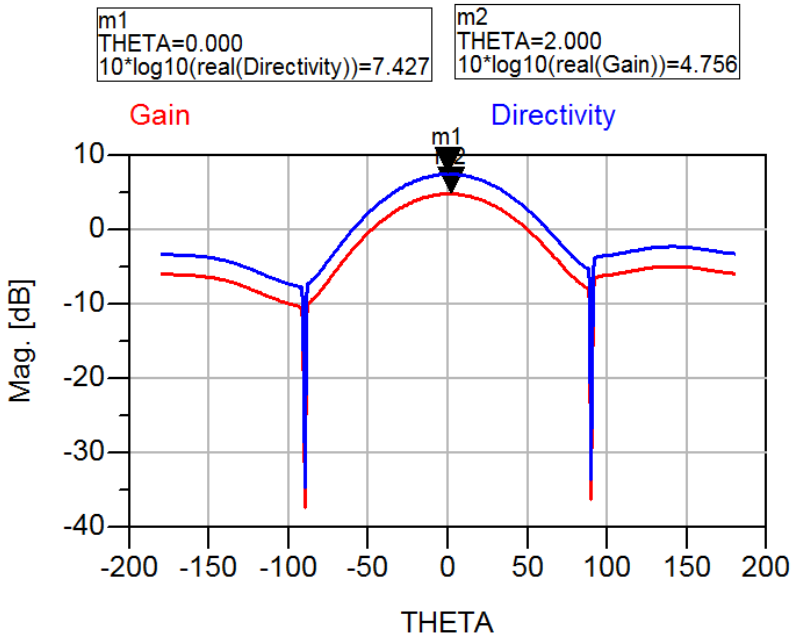

Figure 4.43 Radiation Pattern for a planar cut of 90 degrees at 1.6 GHz

As we can see from the figures 4.42 y 4.43, our antenna does not have a good value of gain. Evaluating the efficiency at 1.6 GHz we have that it is 53.70%.

4.3.2.1.2 Fabrication and Measurements

We followed the same procedure to the fabrication and measurement of Design III.

4.3.2.1.2.1 Fabrication

We also have fabricated this antenna design in the CTTC laboratory.

In figure 4.44 (a) we show the top view of the bottom substrate and in figure 4.44(b) we show the bottom view, we can see the contours that are going to be our references to remove the cupper required.

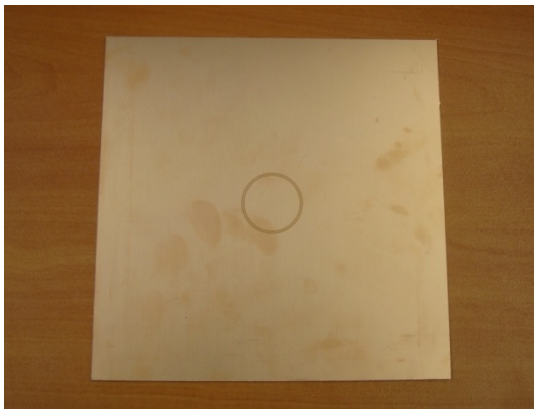

(a)Top view.

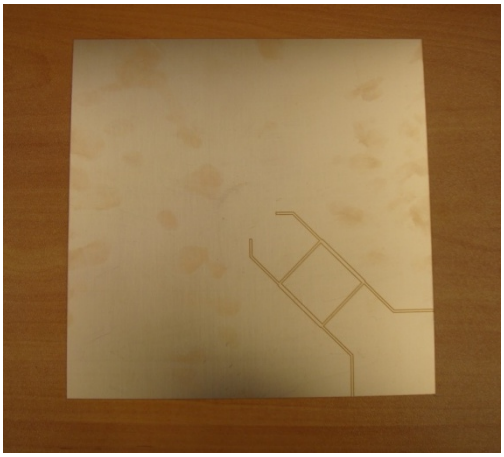

(b) Bottom view.

Figure 4.44 Shows the lower substrate with the contours marked by the LPKF Protolaser-S machine

Figure 4.45 shows the top view (radiating patch) of the upper substrate and does not show the bottom view, because we will remove all the copper in this side.

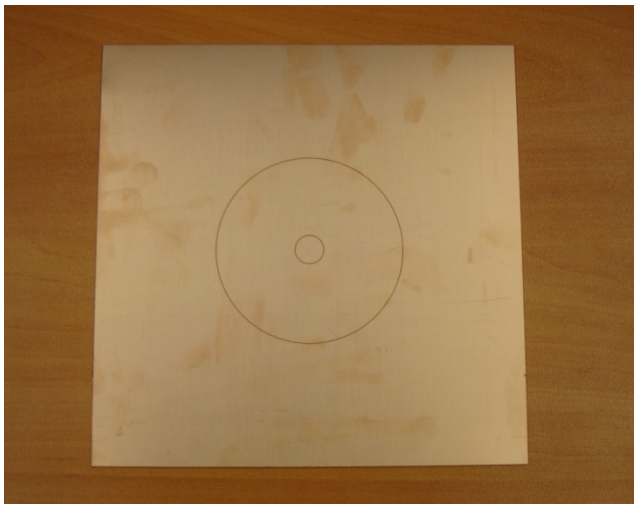

Figure 4.45 Shows the Top view of the upper substrate with the contours marked by the LPKF Protolaser-S machine

All unwanted cooper was removed using a cutter and following the contours made by the LPKF milling LPKF Protolaser-S machine.

For the upper substrate, in figure 4.46 (a) we show the top view(radiating patch) and in figure 4.46 (b) we show the bottom view.

For the lower substrate In figure 4.46 (c) we show the top view and in figure 4.46 (d) we show the bottom view.

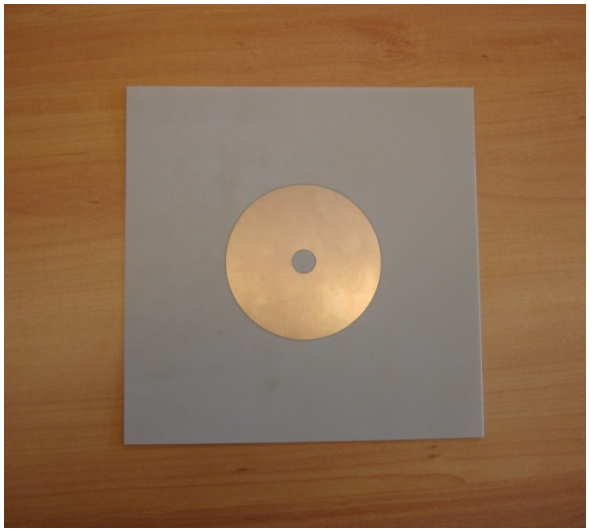

(a) Top view upper substrate

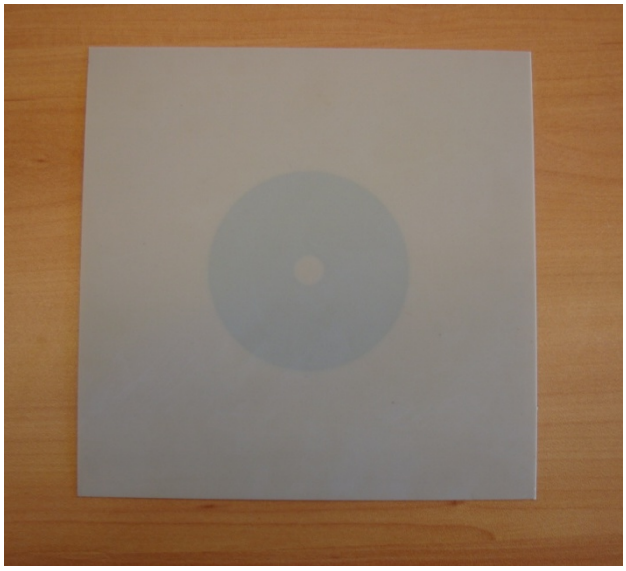

(b) Bottom view upper substrate

(c) Top view lower substrate

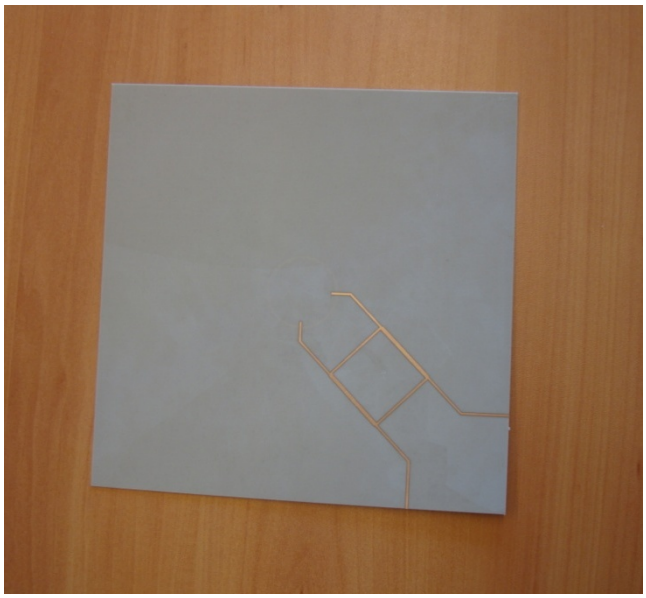

(d) Bottom view lower substrate

Figure 4.46 Shows the upper and lower substrates with the unwanted cupper removed**.**

We also have used Rohacell51 for the layer that employs foam, and was easily cut by hand with a cutter, in this design we used 3mm of Rohacel51 (one foam of 3mm).

We have to soldered the connectors, one at each feed point, then the Rohacell51 foam and the A25N substrates were bonded with an uniformly layer of glue spray over each surface. In Figure 4.47(a) we show the top view of the antenna assembled, we can see at this view that the right feed point is ended with a load of 50Ω (to prevent potential power division degradation of the hybrid which can affect axial ratio performance); in figure 4.47(b) we show the bottom view and in figure 4.47 (c) we show the side view.

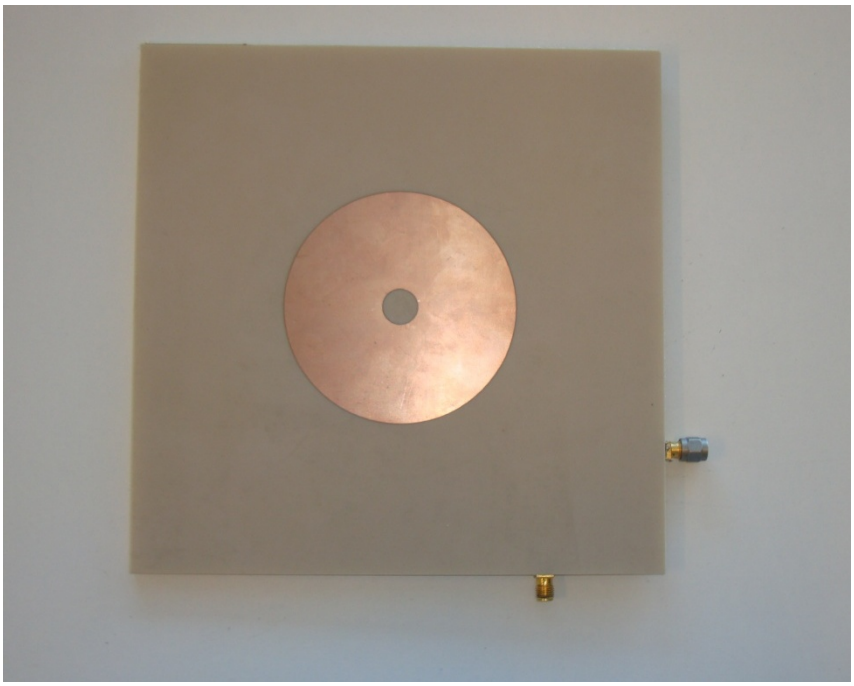

(a) Top view.

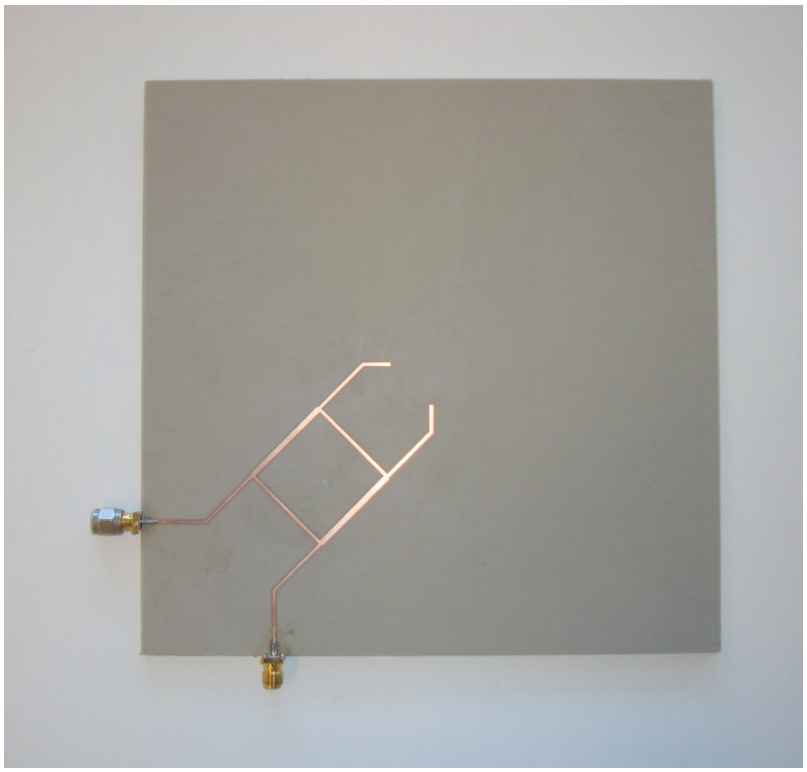

(b) Bottom view.

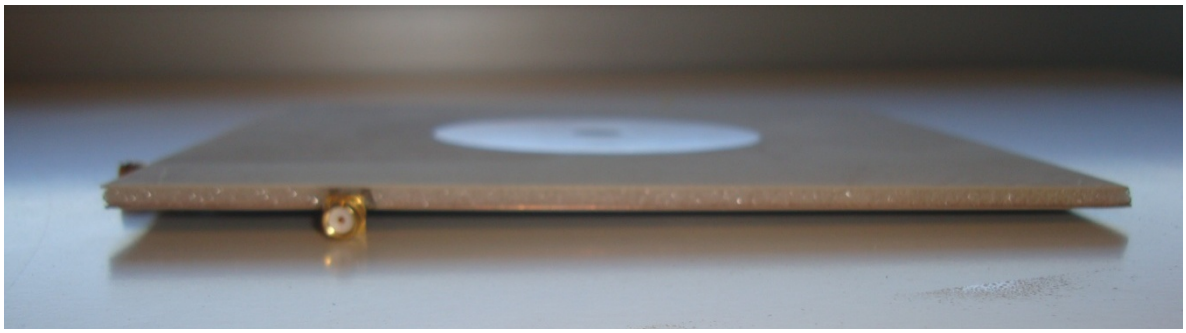

(c) Side view.

Figure 4.47 Shows the antenna assembled

4.3.2.1.2.2 Measurements

For measurements of the antenna we used a ZVA24 Rohde & Schwarz Vector Network Analyzer (VNA), in which we have measured the S11 parameter.

The simulated and measured results are compared in Figure 4.48. And table 4.20 shows a summary of the results.

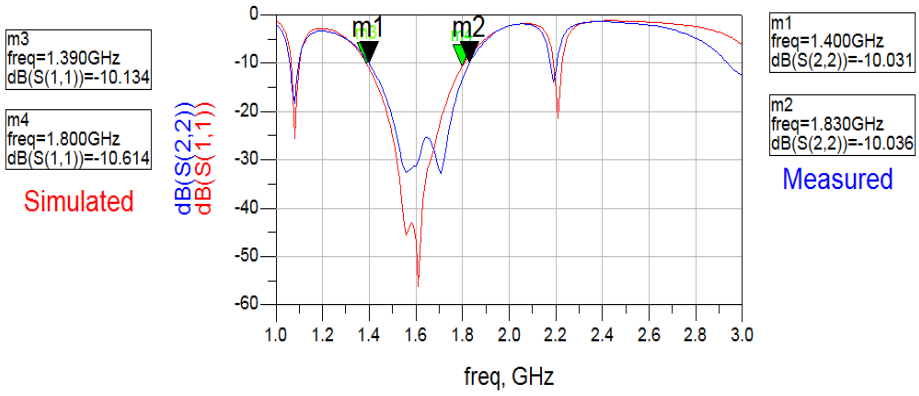

Figure 4.48 Shows the comparison between the simulated and measured results.

	simulated		measured	
Bandwidth	1.39-1.80 GHz	410MHz	1.40-1.83 GHz	430 MHz

Table 4-20 Shows a summary of the comparison.

From the Figure 4.48 and the Table 4.20, we can see that there is a good agreement between measurements and simulations. The measured results (blue graphic) show that have a longer bandwidth (26.62%) than the simulated values (red graphic-25.7 %), both are within the objective bandwidth.

Now we have to measure the antenna axial ratio and for that we are going to use again the anechoic chamber.

We are going to use the same method employed in Design III.

Figure 4.49 shows the measured received power at broadside (measured at 1.6 GHz) after rotating our antenna in the anechoic chamber. The observed ripple of approximately 0.48 dB corresponds to the axial ratio at broadside, it is an acceptable value because is below 3dB.

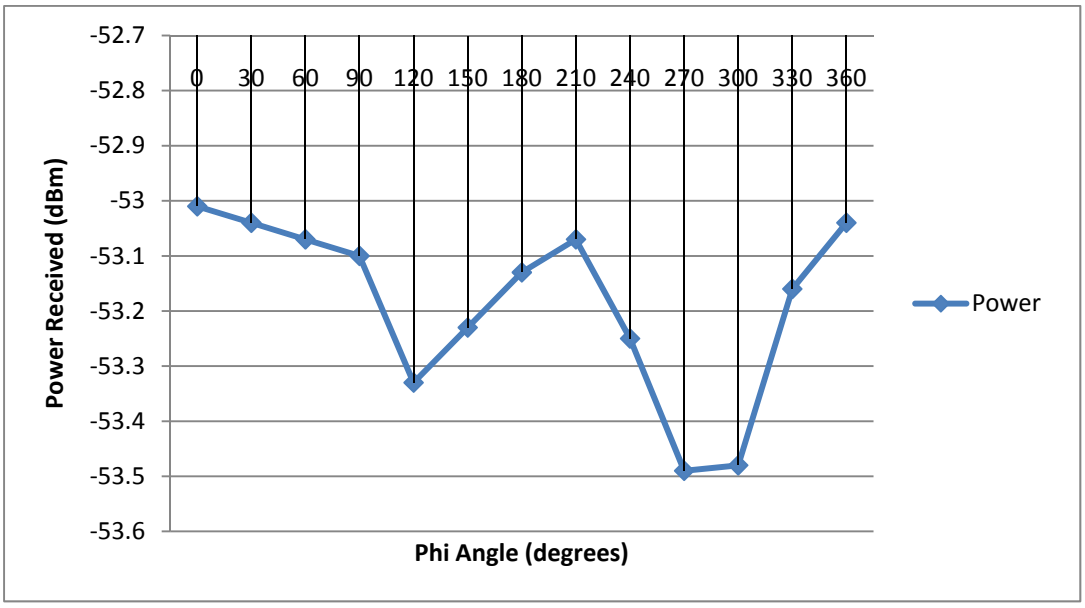

Figure 4.49 Measured Received power at broadside rotating the antenna under test relative to the transmit antenna. The ripple corresponds to the Axial Ratio

In Table 4.21 we can find a comparison between the simulated axial ratio values and the measured axial ratio values. They have been plotted in Figure 4.50.

	Axial Ratio	
Frequency	Simulated	Measured
1.39	4.093	5.27526
1.41	3.696	4.85683
1.43	3.294	4.38421
1.45	2.89	3.73906
1.47	2.485	3.20713
1.49	2.081	2.59582
1.51	1.676	2.16622
1.52	1.478	1.7187
1.54	1.094	1.25524
1.56	0.746	0.75275
1.58	0.504	0.414108
1.6	0.521	0.650242
1.62	0.757	1.06062
1.64	1.073	1.87653
1.66	1.52	2.88025
1.68	2.064	3.68302
1.7	2.539	4.03253
1.72	2.966	4.66843
1.74	3.379	5.07884
1.76	3.788	5.53964
1.78	4.194	5.99962
1.8	4.599	6.3757
Percentage	17.03%	10.79%

Table 4-21 Simulated vs Measured axial ratio values.

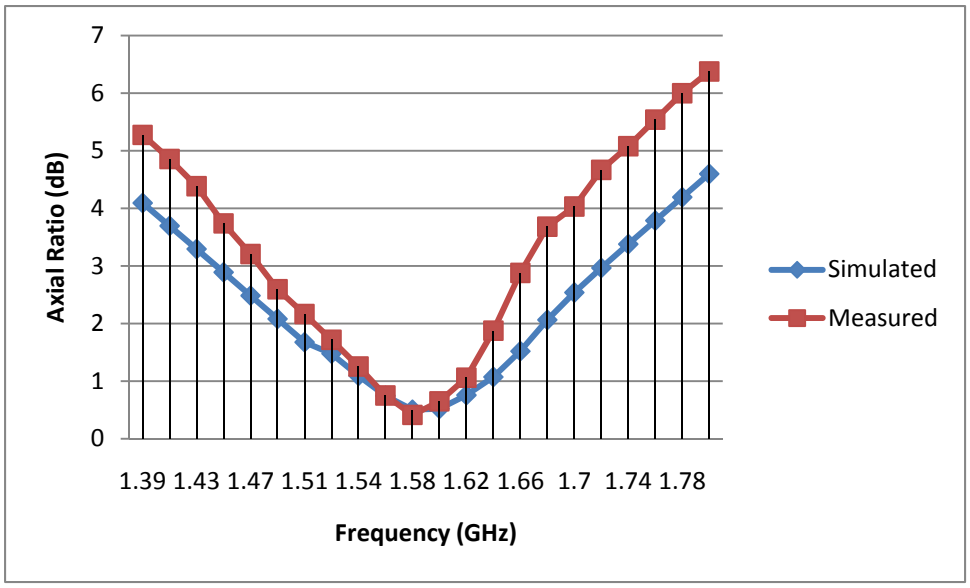

Figure 4.50 Shows the plot comparing simulated vs measured axial ratio values.

As we can see from Table 4.21 and Figure 4.50, in the measured results, the axial ratio has been reduced; but there is still a good approximation.

Despite being a simple and easier design to build, maybe we were not accurate enough at the time of fabricating the antennas, ie patches were not exactly aligned.

Another reason may be that when we were making measurements in the anechoic chamber the transmitting and receiving antenna have not been exactly aligned.

4.4 References.

[4-1] W. Chunlei, C. Kai, “A novel CP Patch Antenna with a simple feed structure”, IEEE Antennas and Prop. Society Inter. Symposium, 2000.

[4-2] J. S. Row, “Design of aperture-coupled annular-ring microstrip antennas for circular polarization,” *IEEE Trans. Antennas Propag.*, vol. 53, no. 5, pp. 1779–1784, May 2005.

5 CONCLUSIONS AND FUTURE WORK

To conclude the project, Table 5-1 shows us a summary of the main features of the antenna that have been simulated and built in this project.

	Impedance Bandwidth		Axial Ratio Bandwidth		Gain		
	GHz	%	GHz	%	value	units	measured in (GHz)
Design I-1	1.48 -1.76	17.28	1.61 - 1.67	3.65	8.907	dB	1.64
Design I-2	1.42- 1.68	16.77	1.52- 1.57	3.24	8.951	dB	1.54
Design II-1	1.47 -1.75	17.37	1.60 - 1.67	4.28	7.862	dB	1.64
Design II-2	1.45 - 1.66	13.5	1.51- 1.55	2.61	8.005	dB	1.53
Design III-simulated	1.49-1.69	12.57	1.5-1.66	10.12	8.147	dB	1.66
Design III-measured	1.52-1.69	10.59	1.48-1.61	8.41	-43.81	dBi	1.54 (*)
Design IV-simulated	1.39-1.80	25.7	1.45-1.72	17.03	7.372	dB	1.66
Design IV-measured	1.40-1.83	26.62	1.49-1.66	10.79	-64.04	dBi	1.61(*)

(*)according to measured of radiation pattern

Table 5-1 Main features of the antennas simulated and built.

The objective of this project was to design an antenna that meets the following specifications:

FREQUENCY BAND	1525-1660 (MHz)
AXIAL RATIO	< 3dB in all the bandwidth
POLARIZATION	RHCP
INPUT IMPEDANCE	50 Ω
GAIN	> 10dBi [1-6]

Table 5-2 Specifications of the antenna design

For the project development we decided to use microstrip antenna technology, because of the advantages that offers and its fast increase in these kinds of applications. Besides we count with the necessary material and equipment which were provided by CTTC.

In all our designs we use the feed technique of aperture-coupled because it allows us to get larger bandwidth.

From the results we can mention that:

All designs reach the specification of right hand circular polarization.

Throughout the design and development process, we concluded that the main limiting factor is the axial ratio bandwidth.

From Table 5.2 shows that the last two antenna designs meet the specification of bandwidth; however when we built the Design III, the axial radio measurements are not the same as those simulated. This may be due different factors like feeding difficulties, ohmic losses of glue used to stick the foam and the substrate or the montage is not exact.

It has been shown that the dual-feed technique (in this case employing a Quadrature Hybrid), is a direct way to generate circular polarization and facilitates the design of the antenna, making it a low profile design and lighter; but the use of the Hybrid increase the size of the antenna.

We can see that the antenna that offers better results, related to axial ratio bandwidth, is the one which uses double feed (Design IV), but we can also see that it has a low gain. This could be due the reflections at the output of the hybrid which result in signal that travels to the isolated port. Other point is that we know that gain and the directivity are related by the efficiency. As we mentioned in paragraph 2.8 total antenna efficiency takes into account the ohmic losses of the antenna through the dielectric material, the reflective losses at the input terminals and losses within the structure of the antenna. In this project we have worked with the dielectric losses; however we have not taken into account the conductor losses, because we were assuming a perfect conductor which it is not true in reality.

We are working to improve the efficiency of the antenna with the hybrid (Design IV), we must investigate and correct the reduction of the value of gain, maybe improving the design of the hybrid, trying to reduce the reflections at the isolated port, or instead of using the hybrid, it can be used any other power divider circuit (referred to paragraph 3.6.1).

In future work, we can use another kind of substrate which has a lower dielectric constant, or we can add more foam; but always remembering that there is a trade-off between the antenna performance and its size.

The most important future work that we can mention is that we can use any of the designed and built antenna to develop an antenna array, employing the sequential rotation

of the feeders and thus able to achieve and far exceed the required specifications

The following paper using the results obtained in this thesis was submitted to the PIERS conference 2011 in Morocco.

[5-1] O. A. Campana Escala, G.A. Sotelo Bazán, A. Georgiadis, and A. Collado, 'A 2.45 GHz Rectenna with Optimized RF-to-DC Conversion Efficiency,' submitted to Progress in Electromagnetics Research Symposium (PIERS), 20-23 March 2011, Marrakesh

6 APPENDIX

6.1 Parametric Analysis of Design III

After many simulations, we have been able to establish an approximate idea about how affects to the axial radio and input impedance, the variation of the most important elements in the antenna. In the following lines we are going to show tables and graphs to explain it.

In the case of axial ratio, the values shaded in green are those that meet the requirement of being less than 3dB.

The design of antenna and the labels used to describe its parts are shown in Figure 6.1.

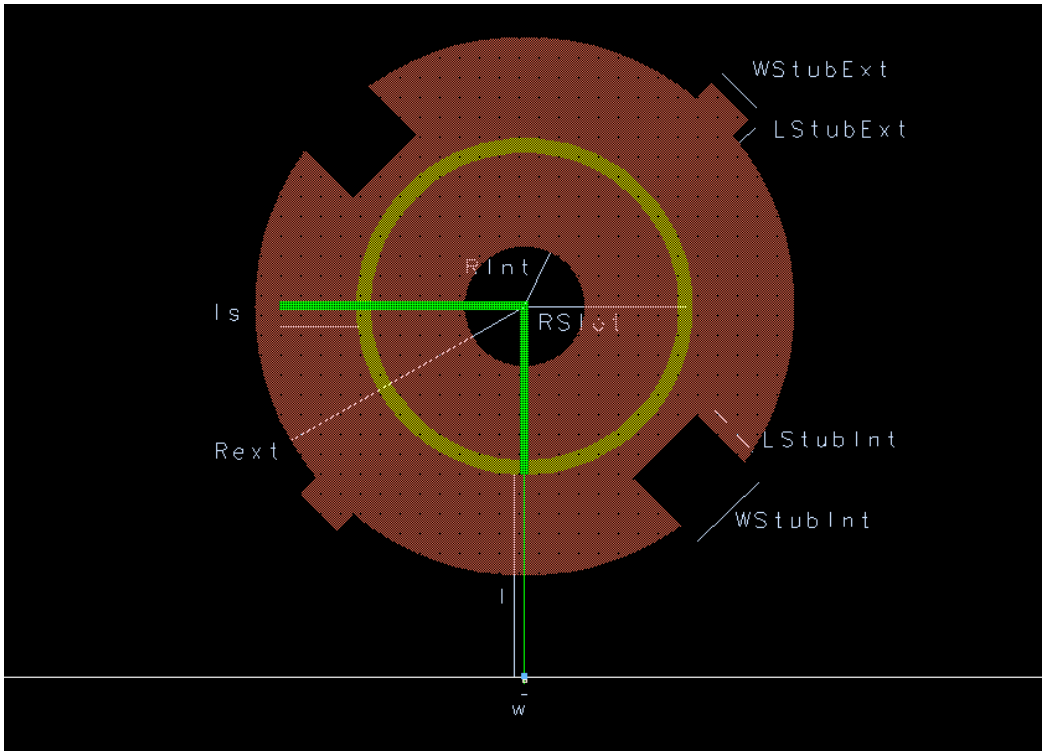

Figure 6.1 Design IV of antenna with its labels

6.1.1 Length of the impedance transformer (l)

In the table 6.1 we can see the different values of axial ratio for each frequency when we adjust the length of the impedance transformer; Figure 6.2 shows them in a graph.

In Figure 6.3 we can see the effect in the input impedance.

	l=32	l=28	l=24	l=20
1.5	3.139	3.138	3.096	3.089
1.52	2.659	2.657	2.625	2.618
1.54	2.265	2.262	2.243	2.237
1.56	1.925	1.921	1.919	1.915
1.58	1.633	1.629	1.646	1.645
1.6	1.432	1.429	1.464	1.467
1.62	1.426	1.425	1.469	1.476
1.64	1.704	1.706	1.744	1.753
1.66	2.245	2.249	2.274	2.283
1.68	2.981	2.986	2.998	3.006
1.7	3.862	3.867	3.869	3.865

Table 6-1 Axial ratio for each frequency and with different values of "l".

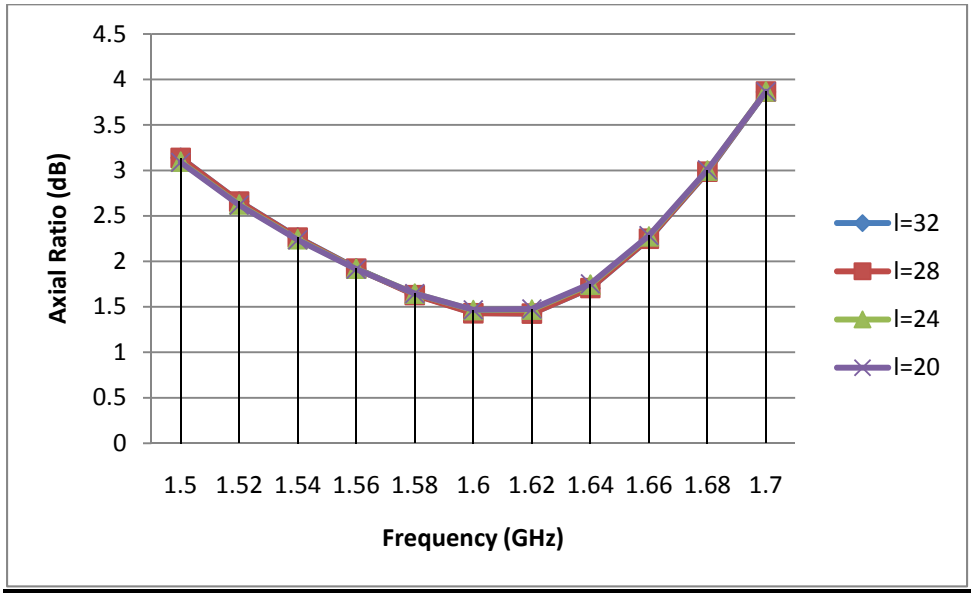

Figure 6.2 Axial Ratio values for each frequency.

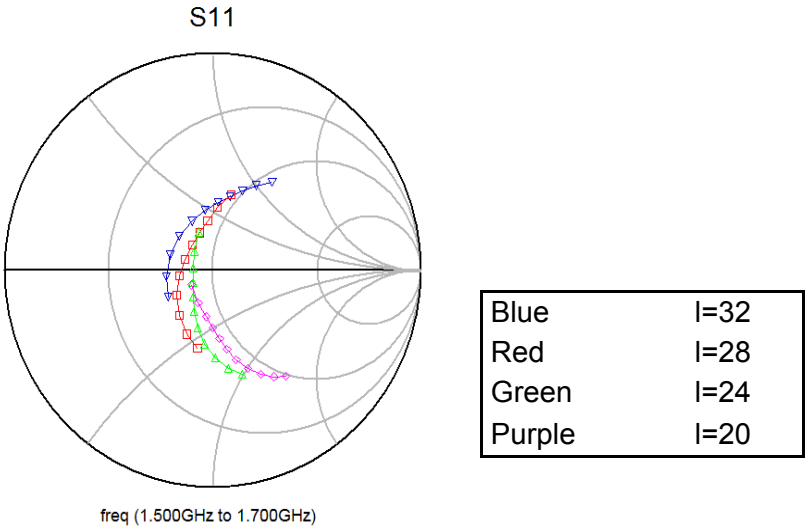

Figure 6.3 Shows the variation of the input impedance in the Smith Chart.

From Figure 6.2 and 6.3, we can see that when we adjust “l” the only parameter that is affected is the input impedance, because there is no variation in axial ratio.

6.1.2 Width of the impedance transformer (w)

In the table 6.2 we can see the different values of axial ratio for each frequency when we adjust the width of the impedance transformer.

Figure 6.4 shows them in a graph. In Figure 6.5 we can see the effect in the input impedance.

	w =0.1939	w=0.2	w=0.22	w=0.25
1.5	2.755	2.982	2.674	3.138
1.52	2.254	2.471	2.194	2.657
1.54	1.899	2.074	1.867	2.262
1.56	1.66	1.769	1.658	1.921
1.58	1.531	1.56	1.55	1.629
1.6	1.536	1.493	1.561	1.429
1.62	1.712	1.634	1.729	1.425
1.64	2.076	2.004	2.077	1.706
1.66	2.617	2.572	2.601	2.249
1.68	3.309	3.298	3.282	2.986
1.7	4.132	4.151	4.1	3.867

Table 6-2 Axial ratio for each frequency and with different values of "w".

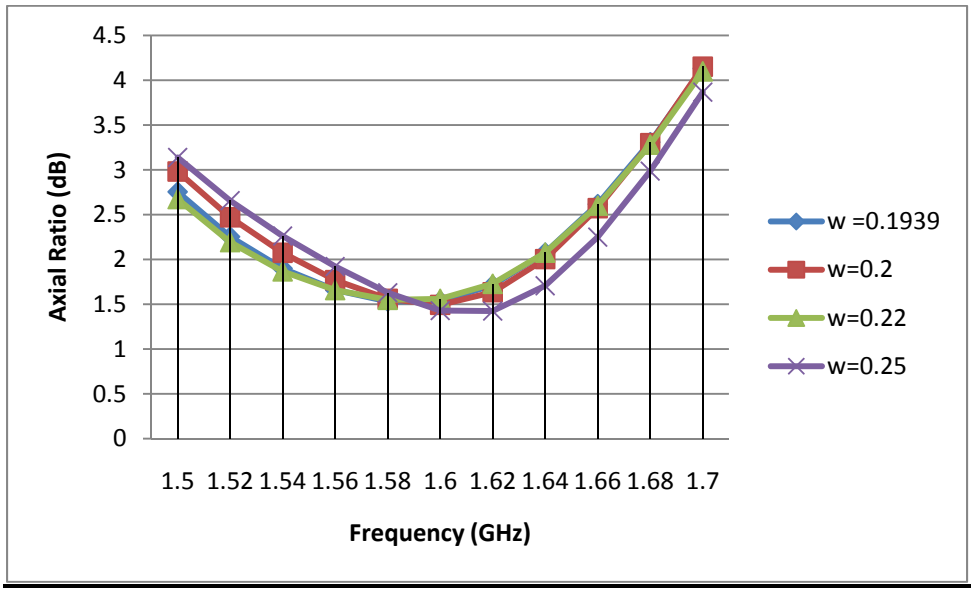

Figure 6.4 Axial Ratio values for each frequency.

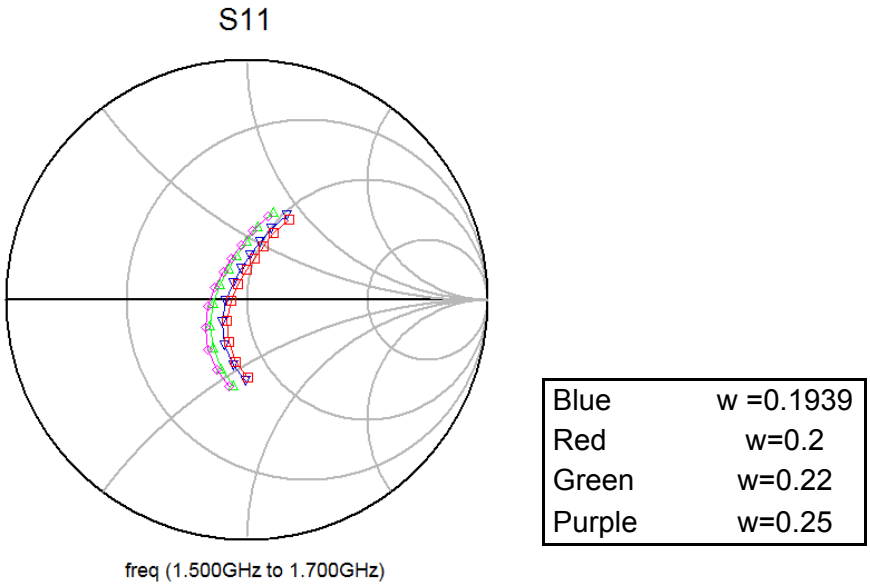

Figure 6.5 Shows the variation of the input impedance in the Smith Chart.

From Figure 6.4 and 6.5, we can see that when we adjust “w”, the effect in axial ratio is not very large; but in input impedance it is an important parameter, because even little the variations in “w” affect to the input impedance.

6.1.3 Outer Radius (Rext)

In the table 6.3 we can see the different values of axial ratio for each frequency when we adjust the outer radius of the radiating patch; Figure 6.6 shows them in a graph.

In Figure 6.7 we can see the effect in the input impedance.

	Rext=36	Rext=37	Rext=37.25	Rext=37.5
1.5	2.711	2.787	2.66	3.617
1.52	2.167	2.234	1.971	2.621
1.54	1.684	1.8	1.463	1.716
1.56	1.231	1.462	1.157	0.875
1.58	0.81	1.238	1.102	0.111
1.6	0.589	1.208	1.304	0.757
1.62	0.895	1.453	1.698	1.58
1.64	1.53	1.95	2.233	2.44
1.66	2.319	2.632	2.884	3.349
1.68	3.22	3.458	3.643	4.311
1.7	4.218	4.401	4.501	5.328

Table 6-3 Axial ratio for each frequency and with different values of “Rext”.

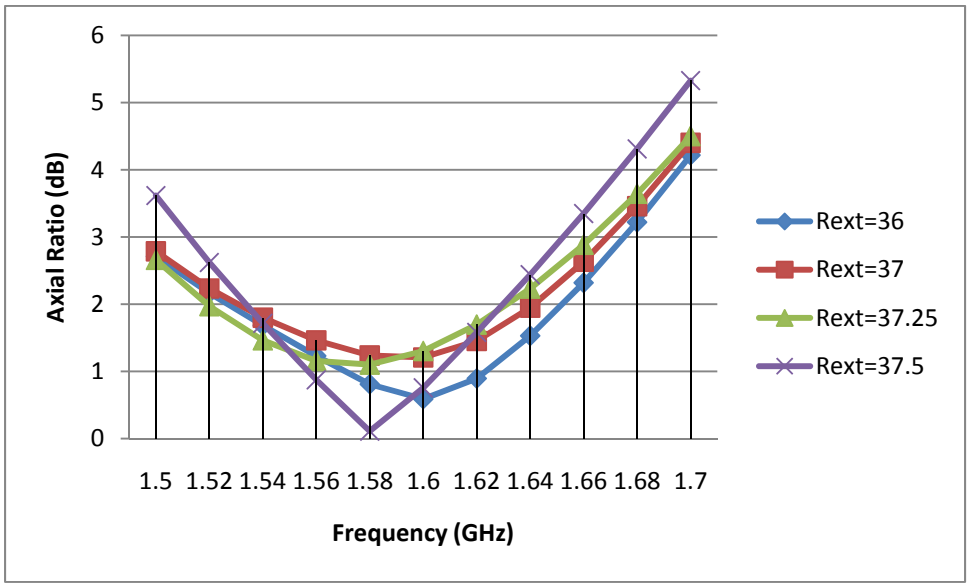

Figure 6.6 Axial Ratio values for each frequency.

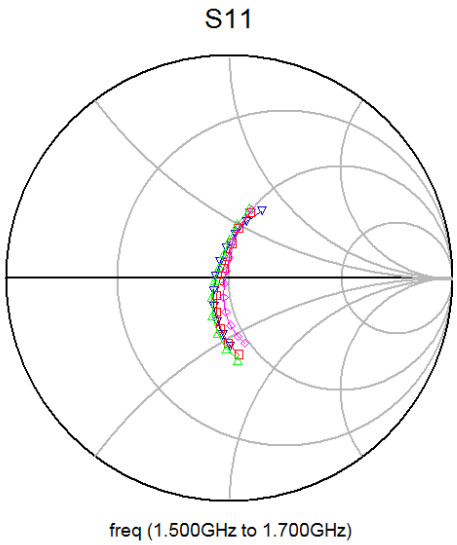

Blue	Rext=36
Red	Rext=37
Green	Rext=37.25
Purple	Rext=37.5

Figure 6.7 Shows the variation of the input impedance in the Smith Chart.

From Figure 6.6 and 6.7, we can see that when we adjust “Rext”, it affects the axial ratio and also affects the input impedance.

6.1.4 Inner Radius (Rint)

In the table 6.4 we can see the different values of axial ratio for each frequency when we adjust the inner radius of the radiating patch, Figure 6.8 shows them in a graph.

In Figure 6.9 we can see the effect in the input impedance.

	Rint=0	Rint=4	Rint=8	Rint=10
1.5	3.249	3.242	3.124	3.03
1.52	3.076	3.062	2.996	2.969
1.54	2.924	2.903	2.883	2.911
1.56	2.752	2.726	2.737	2.825
1.58	2.544	2.514	2.577	2.702
1.6	2.306	2.274	2.384	2.563
1.62	2.074	2.043	2.212	2.457
1.64	1.929	1.903	2.144	2.458
1.66	1.988	1.973	2.279	2.653
1.68	2.332	2.334	2.677	3.086
1.7	2.947	2.963	3.323	3.751

Table 6-4 Axial ratio for each frequency and with different values of “Rint”.

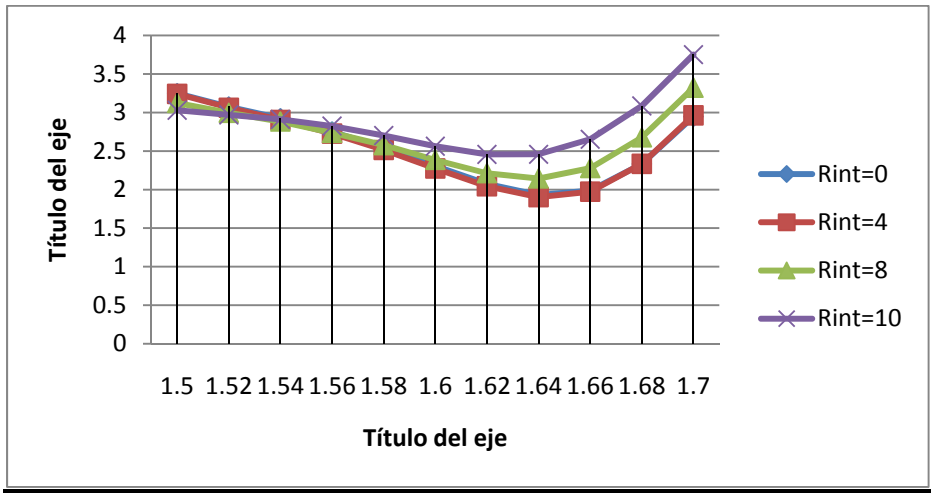

Figure 6.8 Axial Ratio values for each frequency.

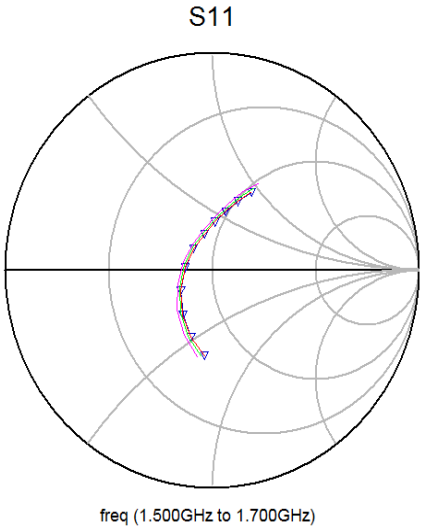

Blue	Rint=0
Red	Rint=4
Green	Rint=8
Purple	Rint=10

Figure 6.9 Shows the variation of the input impedance in the Smith Chart.

From Figure 6.8 and 6.9, we can see that when we adjust “Rint”, it affects the axial ratio; but not to the input impedance.

6.1.5 Stub Length(ls)

In the table 6.5 we can see the different values of axial ratio for each frequency when we adjust the Stub length of 50Ω coupling strip, Figure 6.10 shows them in a graph.

In Figure 6.11 we can see the effect in the input impedance.

	ls=10	ls=12	ls=14	ls=16	ls=18
1.5	2.425	3.124	4.73	6.205	7.515
1.52	3.147	2.996	4.201	5.532	6.783
1.54	3.699	2.883	3.649	4.827	6.024
1.56	4.096	2.737	3.05	4.082	5.245
1.58	4.361	2.577	2.388	3.3	4.472
1.6	4.518	2.384	1.65	2.512	3.77
1.62	4.592	2.212	0.828	1.839	3.281
1.64	4.615	2.144	0.154	1.635	3.221
1.66	4.624	2.279	1.12	2.199	3.724
1.68	4.662	2.677	2.227	3.252	4.701
1.7	4.777	3.323	3.429	4.539	5.992

Table 6-5 Axial ratio for each frequency and with different values of “ls”.

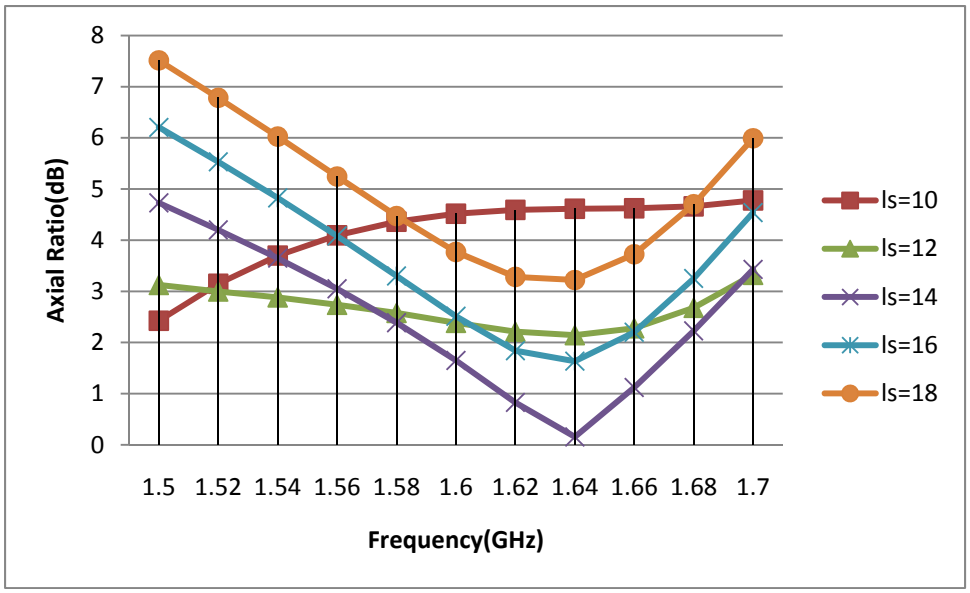

Figure 6.10 Axial Ratio values for each frequency**.**

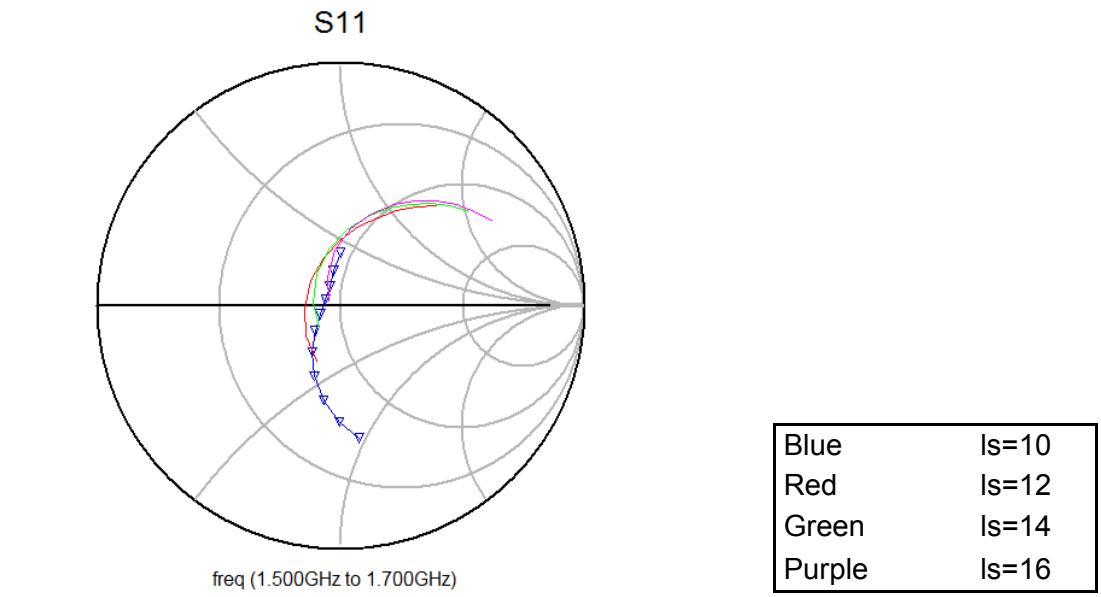

Figure 6.11 Shows the variation of the input impedance in the Smith Chart.

From Figure 6.10 and 6.11, we can see that when we adjust “ls”, it affects the axial ratio and the input impedance.

6.1.6 Inner Stub

For the inner stub, we have studied the behavior of its width and its length.

6.1.6.1 Width of the inner Stub (WStubInt)

In the table 6.6 we can see the different values of axial ratio for each frequency when we adjust the width of the inner stub; Figure 6.12 shows them in a graph.

In Figure 6.13 we can see the effect in the input impedance.

	Wint=0	Wint=4	Wint=8	Wint=14
1.5	9.278	5.763	4.702	4.273
1.52	7.917	4.508	3.568	3.58
1.54	6.746	3.426	2.543	2.982
1.56	5.843	2.601	1.631	2.443
1.58	5.305	2.209	0.93	1.931
1.6	5.209	2.398	0.921	1.43
1.62	5.546	3.033	1.597	0.973
1.64	6.22	3.897	2.461	0.776
1.66	7.111	4.873	3.397	1.131
1.68	8.125	5.912	4.386	1.827
1.7	9.199	6.989	5.423	2.682

Table 6-6 Axial ratio for each frequency and with different values of “WStubInt”.

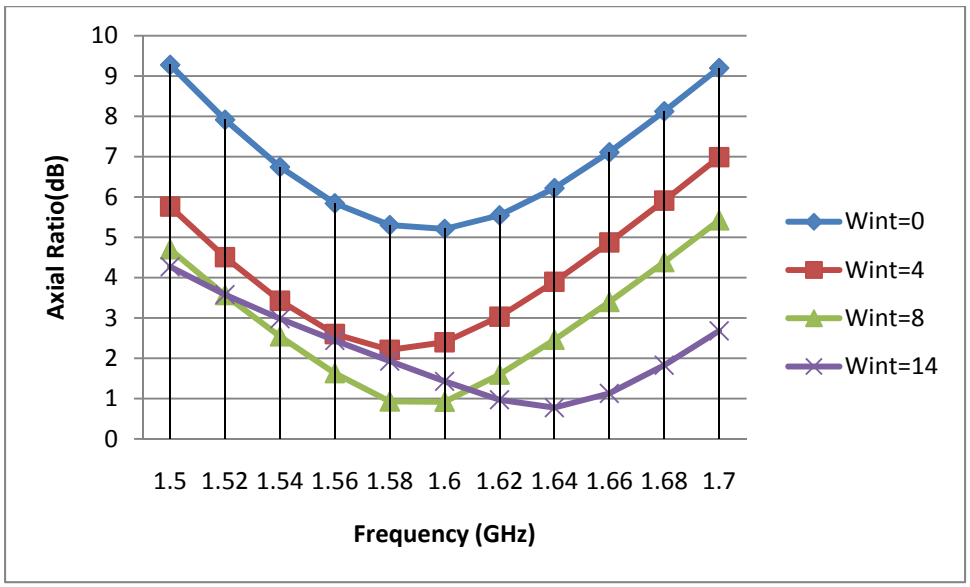

Figure 6.12 Axial Ratio values for each frequency.

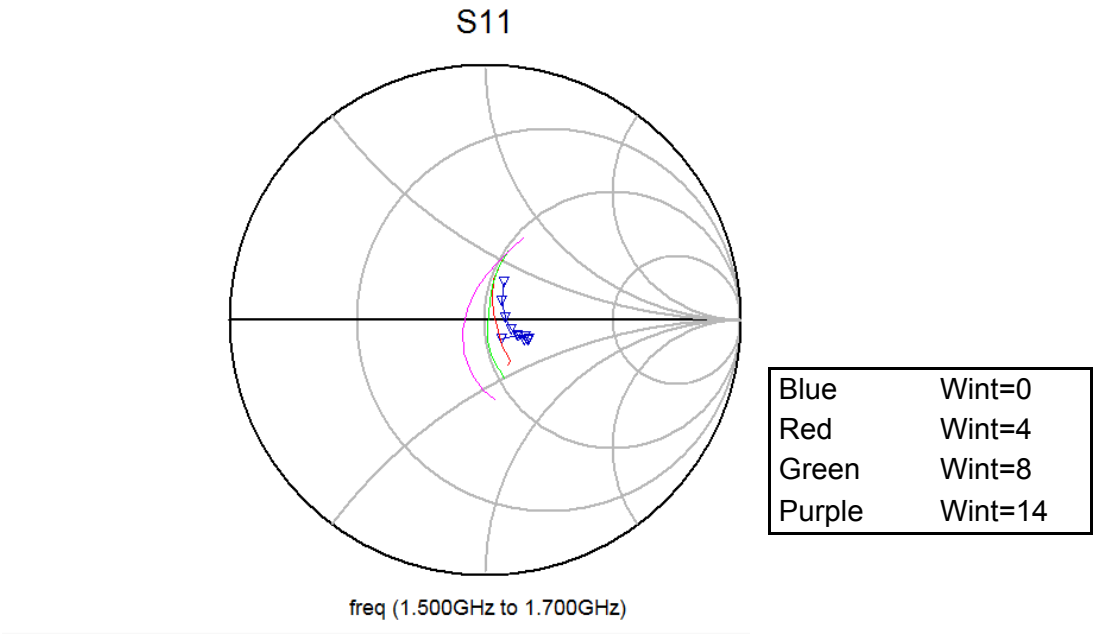

Figure 6.13 Shows the variation of the input impedance in the Smith Chart.

From Figure 6.12 and 6.13, we can see that when we adjust “WStubInt”, it affects the axial ratio and the input impedance.

6.1.6.2 Length of the inner Stub (LStubInt)

In the table 6.7 we can see the different values of axial ratio for each frequency when we adjust the length of the inner stub, Figure 6.14 shows them in a graph.

In Figure 6.15 we can see the effect in the input impedance.

	LStubInt=0	LStubInt=4	LStubInt=8	LStubInt=10
1.5	9.137	7.496	5.598	4.6
1.52	7.801	6.244	4.478	3.613
1.54	6.645	5.121	3.459	2.714
1.56	5.742	4.164	2.54	1.877
1.58	5.191	3.446	1.76	1.077
1.6	5.074	3.094	1.298	0.345
1.62	5.393	3.207	1.469	0.639
1.64	6.058	3.74	2.147	1.475
1.66	6.95	4.553	3.037	2.381
1.68	7.975	5.53	4.029	3.348
1.7	9.065	6.6	5.09	4.374

Table 6-7 Axial ratio for each frequency and with different values of “LStubInt”.

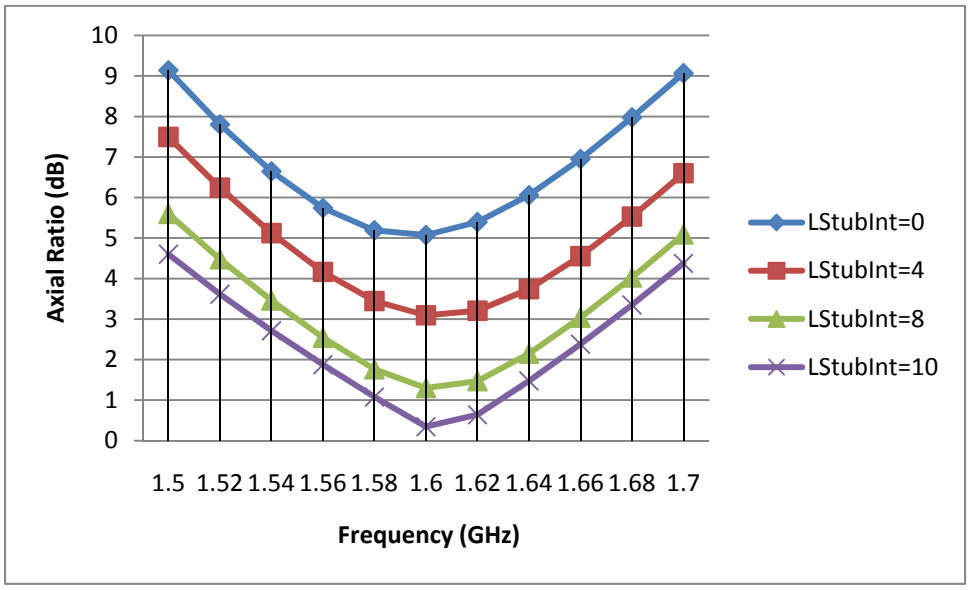

Figure 6.14 Axial Ratio values for each frequency.

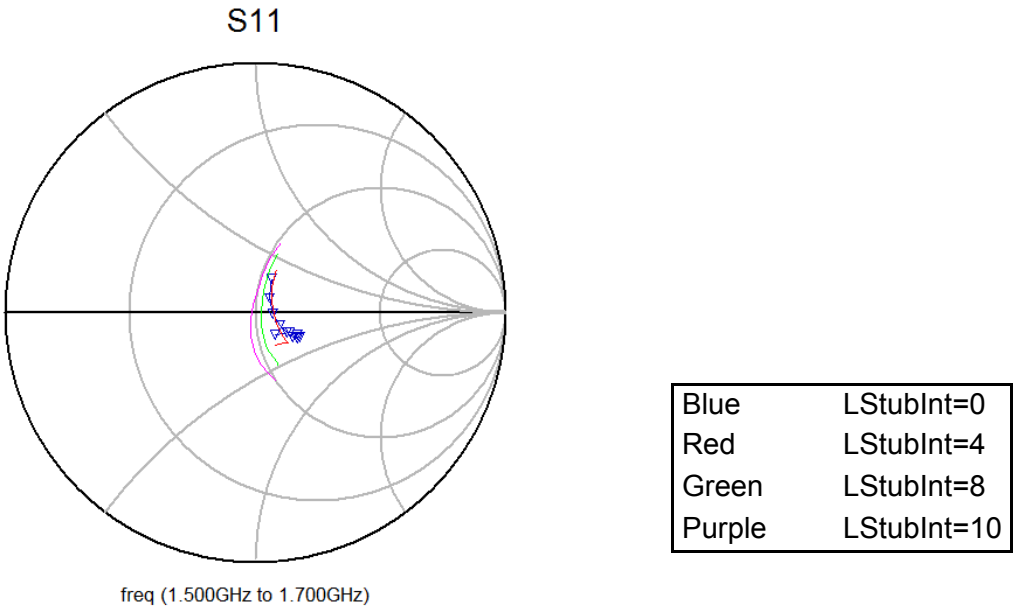

Figure 6.15 Shows the variation of the input impedance in the Smith Chart.

From Figure 6.14 and 6.15, we can see that when we adjust “LStubInt”, it affects the axial ratio and the input impedance.

6.1.7 Outer Stub

For the outer stub, we also have studied the behavior of its width and its length.

6.1.7.1 Width of the outer Stub (WStubExt)

In the table 6.8 we can see the different values of axial ratio for each frequency when we adjust the width of the outer stub, Figure 6.16 shows them in a graph.

In Figure 6.17 we can see the effect in the input impedance.

	WStubExt=1	WStubExt=3	WStubExt=5	WStubExt=7
1.5	2.755	2.652	3.121	3.246
1.52	2.254	2.47	3.074	3.305
1.54	1.899	2.37	3.016	3.327
1.56	1.66	2.3	2.915	3.288
1.58	1.531	2.24	2.768	3.187
1.6	1.536	2.202	2.591	3.038
1.62	1.712	2.231	2.431	2.877
1.64	2.076	2.387	2.369	2.763
1.66	2.617	2.719	2.5	2.78
1.68	3.309	3.243	2.89	3.009
1.7	4.132	3.945	3.531	3.487

Table 6-8 Axial ratio for each frequency and with different values of “WStubExt”.

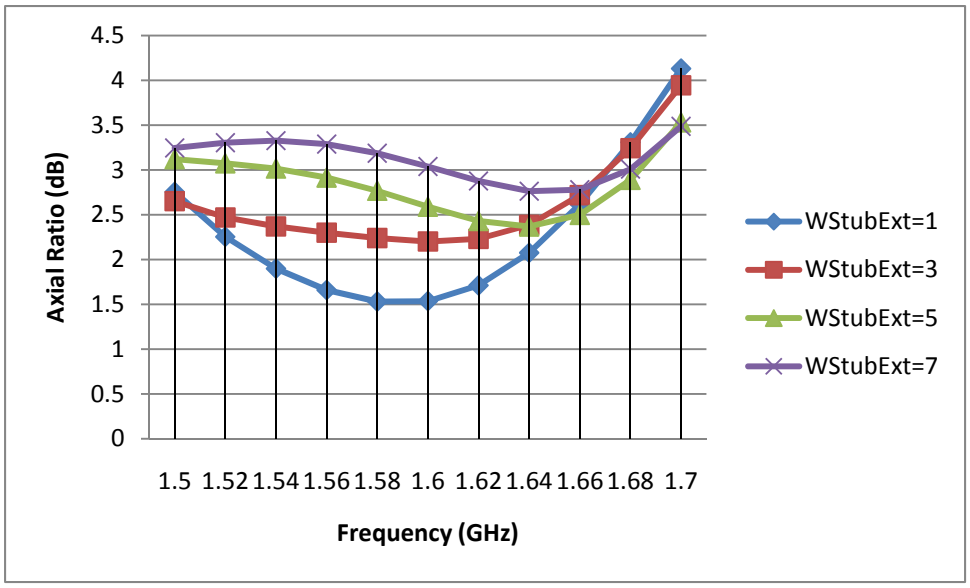

Figure 6.16 Axial Ratio values for each frequency.

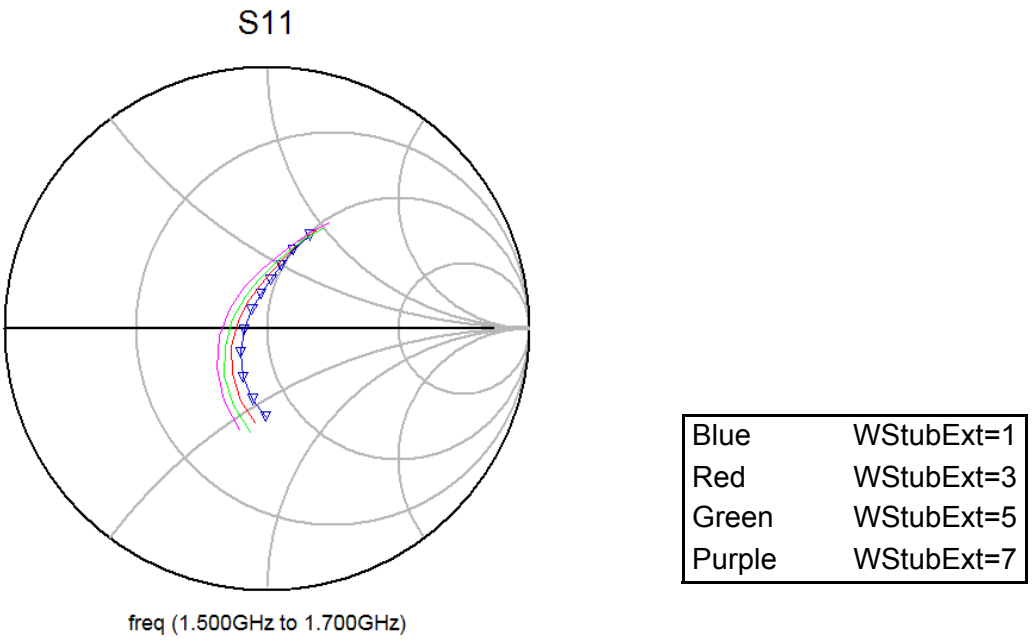

Figure 6.17 Shows the variation of the input impedance in the Smith Chart.

From Figure 6.16 and 6.17, we can see that when we adjust “WStubExt”, it affects the axial ratio and the input impedance; but not in large scale

6.1.7.2 Length of the outer Stub (LStubExt)

In the table 6.9 we can see the different values of axial ratio for each frequency when we adjust the length of the outer stub, Figure 6.18 shows them in a graph.

In Figure 6.19 we can see the effect in the input impedance.

	LStubExt=0	LStubExt=2	LStubExt=4	LStubExt=8
1.5	4.605	4.069	3.515	3.044
1.52	3.533	3.168	2.844	3.026
1.54	2.559	2.363	2.266	3.004
1.56	1.664	1.621	1.751	2.944
1.58	0.84	0.911	1.289	2.838
1.6	0.374	0.249	0.937	2.699
1.62	1.012	0.602	0.909	2.566
1.64	1.858	1.382	1.319	2.505
1.66	2.762	2.233	1.988	2.6
1.68	3.718	3.154	2.805	2.92
1.7	4.725	4.147	3.731	3.48

Table 6-9 Axial ratio for each frequency and with different values of “LStubExt”.

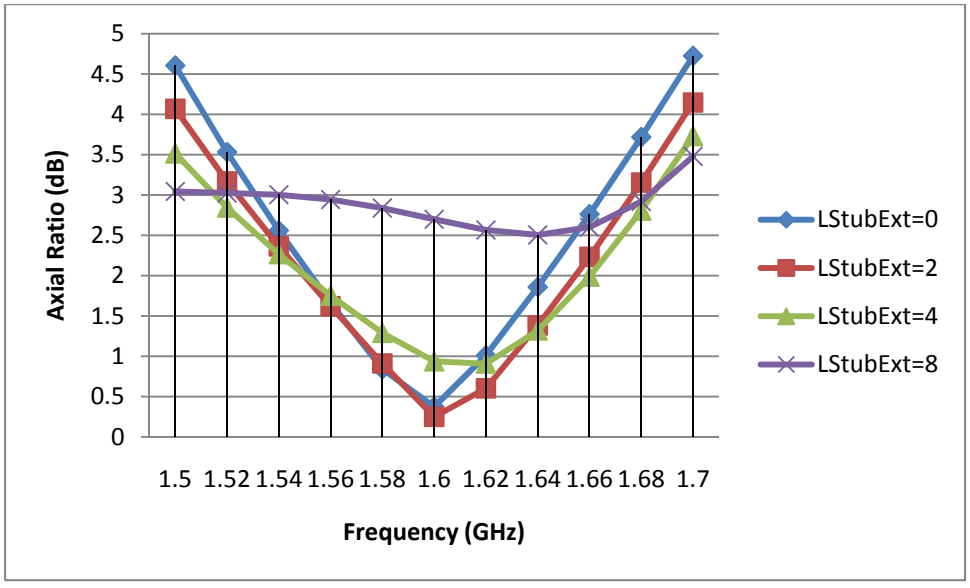

Figure 6.18 Axial Ratio values for each frequency.

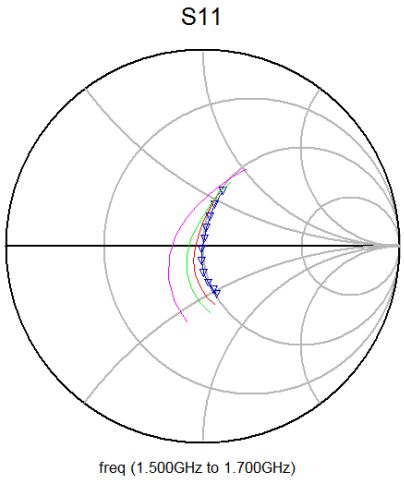

Blue	LStubExt=0
Red	LStubExt=2
Green	LStubExt=4
Purple	LStubExt=8

Figure 6.19 Shows the variation of the input impedance in the Smith Chart.

From Figure 6.18 and 6.19, we can see that when we adjust “LStubExt”, it affects the axial ratio and the input impedance.

6.2 Parametric Analysis of Design IV

After many simulations, we have been able to establish an approximate idea about how affects to the axial radio and input impedance, the variation of the most important elements in the antenna. In the following lines we are going to show tables and graphs to explain it.

The design of antenna and the labels used to describe its parts are shown in Figure 6.20.

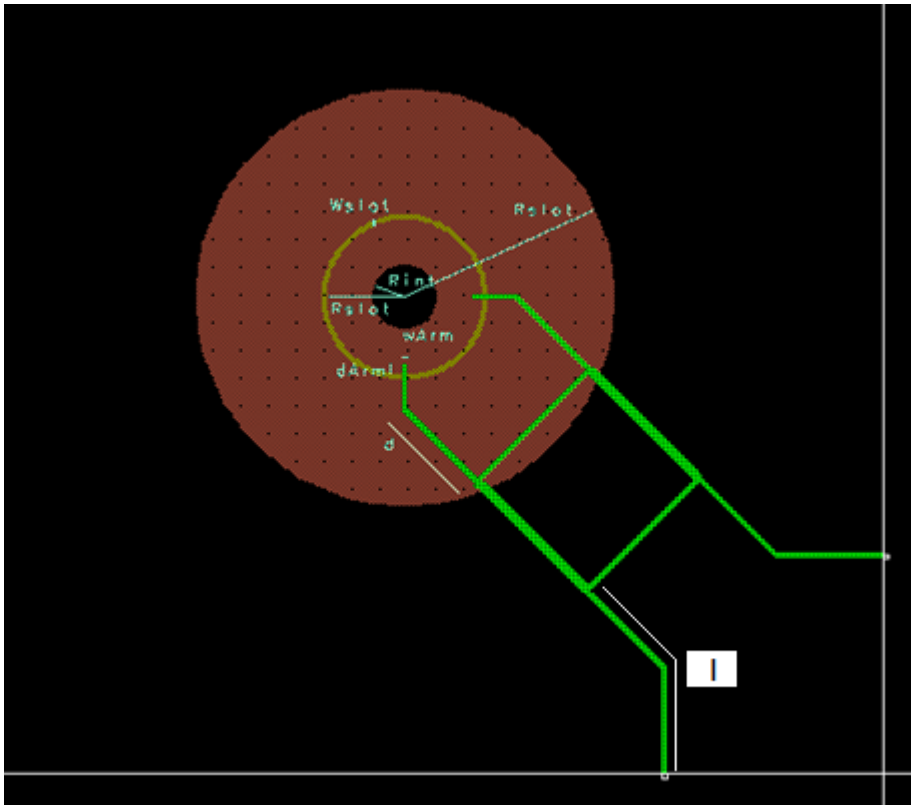

Figure 6.20 Design IV of antenna with its labels

6.2.1 Outer Radius (Rext)

In the table 6.10 we can see the different values of axial ratio for each frequency when we adjust the outer radius of the radiating patch; Figure 6.21 shows them in a graph.

In Figure 6.22 we can see the effect in the input impedance.

	Rext=35	Rext=37	Rext=39	Rext=41.5
1.52	1.787	1.806	1.834	1.888
1.54	1.402	1.424	1.467	1.56
1.56	1.03	1.056	1.122	1.26
1.58	0.698	0.724	0.823	0.955
1.6	0.494	0.494	0.634	0.797
1.62	0.571	0.509	0.661	0.908
1.64	0.849	0.725	0.982	1.178
1.66	1.186	0.985	1.483	1.517

Table 6-10 Axial ratio for each frequency and with different values of “Rext”.

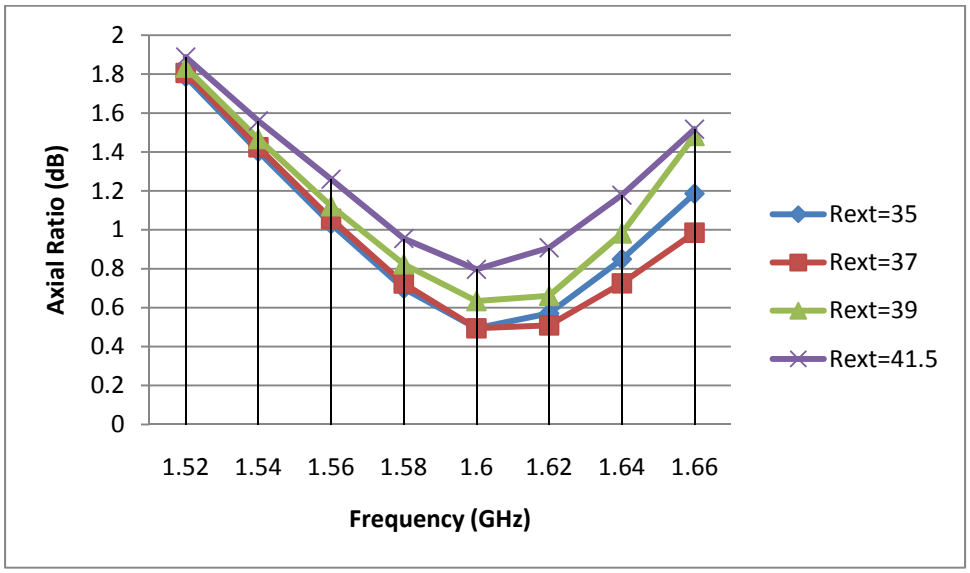

Figure 6.21 Axial Ratio values for each frequency.

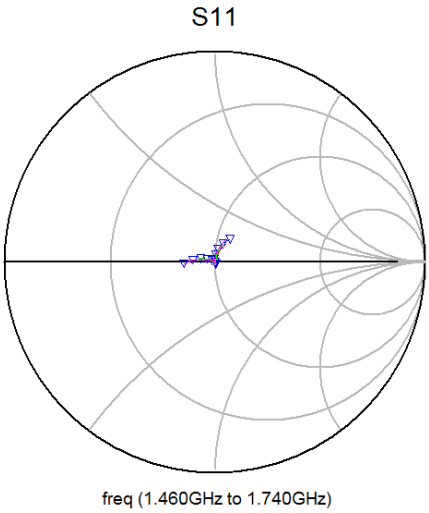

Blue	Rext=35
Red	Rext=37
Green	Rext=39
Purple	Rext=41.5

Figure 6.22 Shows the variation of the input impedance in the Smith Chart**.**

From Figure 6.21 and 6.22, we can see that when we adjust “Rext”, it affects the axial ratio; but not too much the input impedance.

6.2.2 Inner Radius (Rint)

In the table 6.11 we can see the different values of axial ratio for each frequency when we adjust the inner radius of the radiating patch; Figure 6.23 shows them in a graph.

In Figure 6.24 we can see the effect in the input impedance.

	Rint=0	Rint=3	Rint=8	Rint=10
1.52	1.592	1.846	1.821	1.785
1.54	1.337	1.482	1.452	1.413
1.56	1.146	1.138	1.103	1.062
1.58	1.054	0.838	0.8	0.76
1.6	1.081	0.635	0.605	0.575
1.62	1.196	0.629	0.636	0.654
1.64	1.348	0.913	0.984	1.07
1.66	1.601	1.419	1.487	1.526

Table 6-11 Axial ratio for each frequency and with different values of “Rint”.

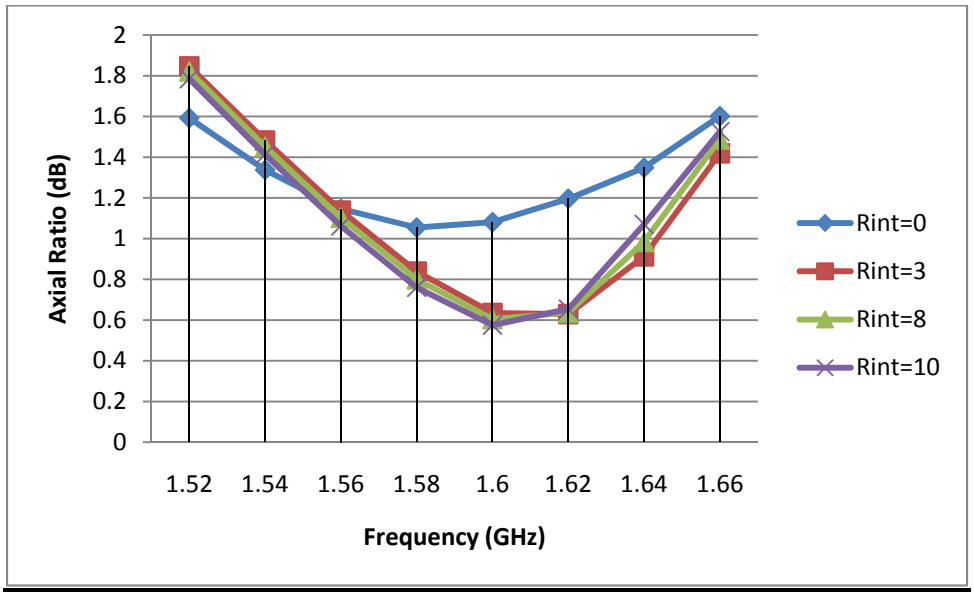

Figure 6.23 Axial Ratio values for each frequency.

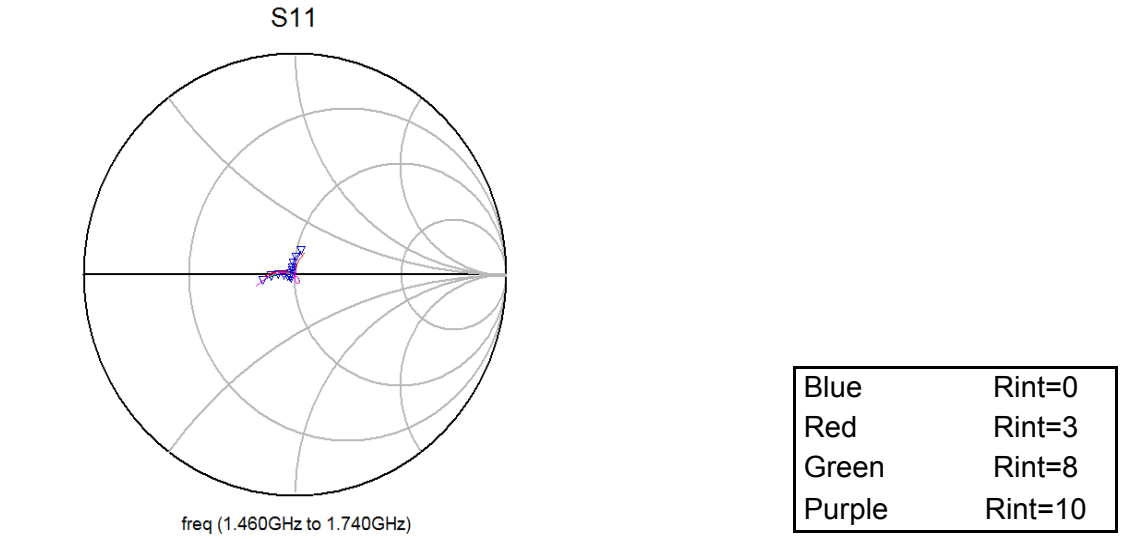

Figure 6.24 Shows the variation of the input impedance in the Smith Chart.

From Figure 6.23 and 6.24, we can see that when we adjust “Rint” and when its value is different than zero, it has a little effect on the axial ratio and input impedance.

6.2.3 Length of arms (dArm)

In the table 6.12 we can see the different values of axial ratio for each frequency when we adjust the length of the arms; Figure 6.25 shows them in a graph.

In Figure 6.26 we can see the effect in the input impedance.

	dArm=0	dArm=1	dArm=1.5	dArm=2
1.52	3.784	2.276	1.817	1.399
1.54	3.472	1.93	1.45	1.013
1.56	3.159	1.598	1.105	0.666
1.58	2.857	1.296	0.8	0.444
1.6	2.587	1.057	0.624	0.509
1.62	2.38	0.947	0.659	0.786
1.64	2.231	1.069	0.986	1.221
1.66	1.94	1.36	1.491	1.781

Table 6-12 Axial ratio for each frequency and with different values of “dArm”.

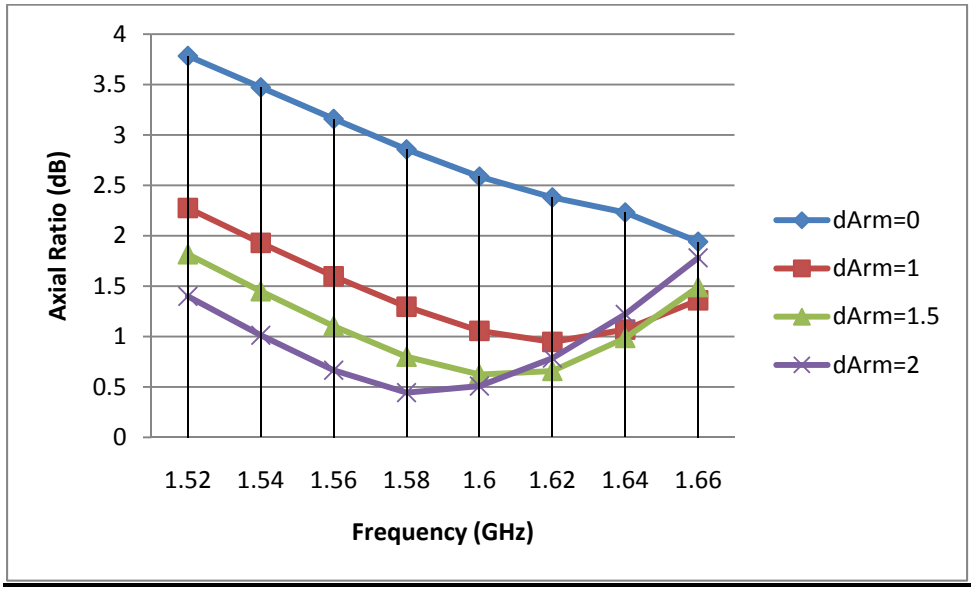

Figure 6.25 Axial Ratio values for each frequency.

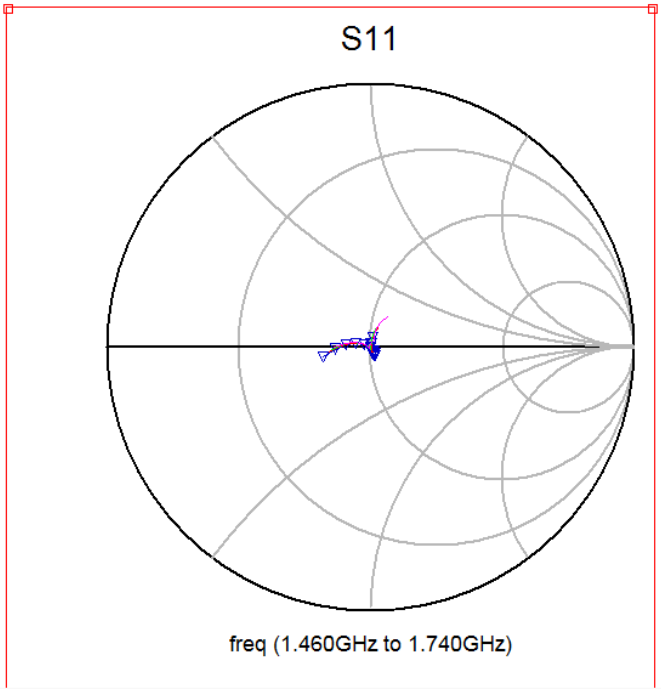

Blue	l=32
Red	l=28
Green	l=24
Purple	l=20

Figure 6.26 Shows the variation of the input impedance in the Smith Chart.

From Figure 6.25 and 6.26, we can see that when we adjust “dArms”, it affects the axial ratio; but not to the input impedance.

6.2.4 Width of arms (wArm)

In the table 6.13 we can see the different values of axial ratio for each frequency when we adjust the width of the arms; Figure 6.27 shows them in a graph.

In Figure 6.28 we can see the effect in the input impedance.

	wArm=0.5	wArm=1.25	wArm=2	wArm=2.5
1.52	1.818	1.686	1.28	1.174
1.54	1.487	1.335	1.155	0.913
1.56	1.166	1.016	1.187	0.811
1.58	0.878	0.769	1.376	0.926
1.6	0.667	0.664	1.687	1.212
1.62	0.608	0.768	2.077	1.62
1.64	0.74	1.118	2.408	2.122
1.66	1.081	1.63	2.568	2.55

Table 6-13 Axial ratio for each frequency and with different values of “wArm”.

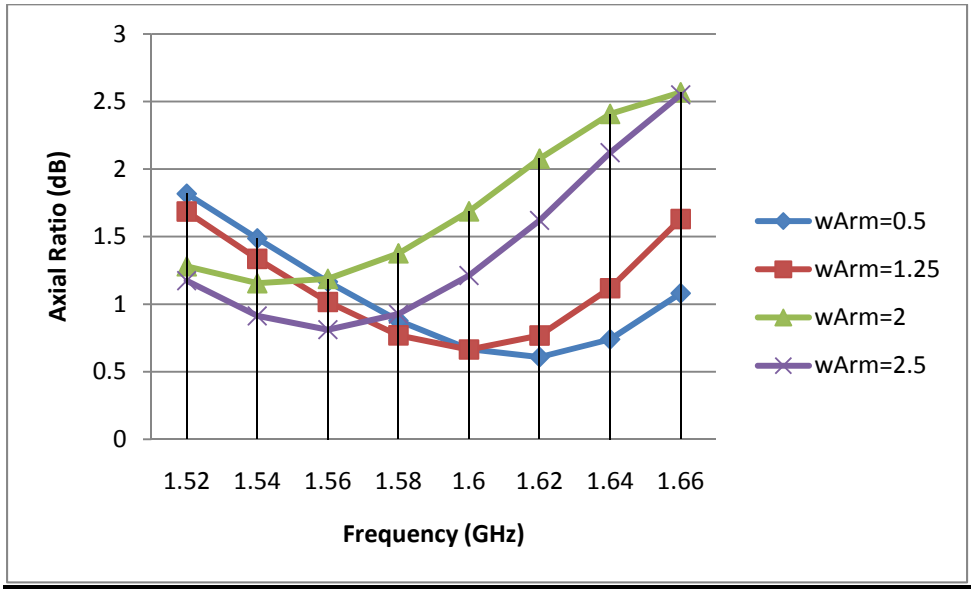

Figure 6.27 Axial Ratio values for each frequency.

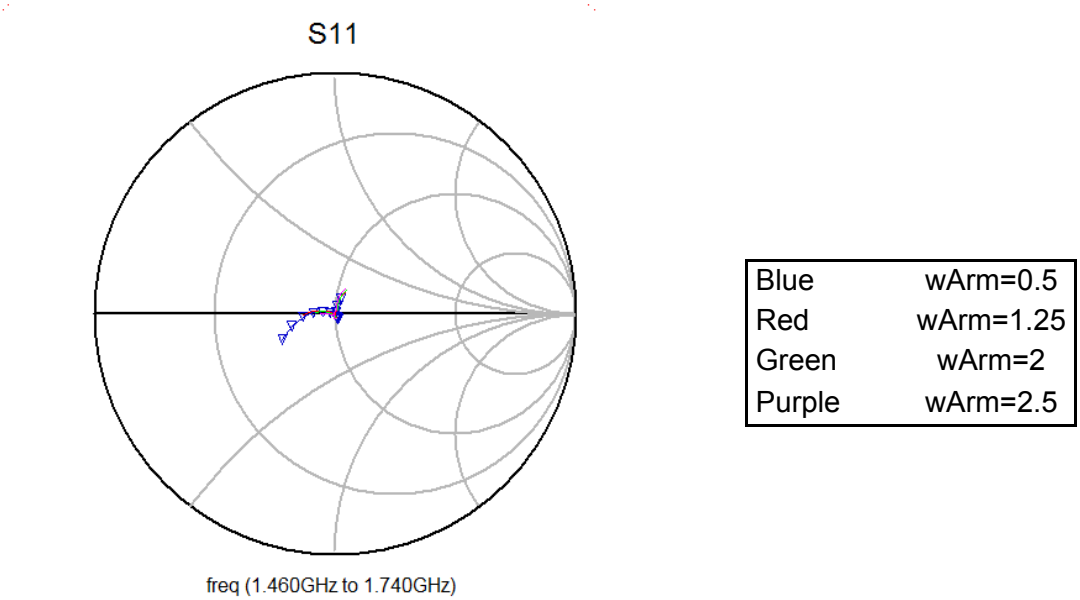

Figure 6.28 Shows the variation of the input impedance in the Smith Chart.

From Figure 6.27 and 6.28, we can see that when we adjust “wArms” it affects the axial ratio; but not to the input impedance.

6.2.5 Radius of Slot (Rslot)

In the table 6.14 we can see the different values of axial ratio for each frequency when we adjust the radius of the slot; Figure 6.29 shows them in a graph.

In Figure 6.30 we can see the effect in the input impedance.

	Rslot=13	Rslot=14	Rslot=15	Rslot=16
1.52	3.5	2.089	1.456	1.062
1.54	3.157	1.713	1.1	0.688
1.56	2.811	1.348	0.791	0.535
1.58	2.467	1.006	0.593	0.582
1.6	2.13	0.727	0.616	0.518
1.62	1.813	0.595	0.911	0.85
1.64	1.535	0.679	1.423	1.43
1.66	1.336	0.93	1.901	1.988

Table 6-14 Axial ratio for each frequency and with different values of “Rslot”.

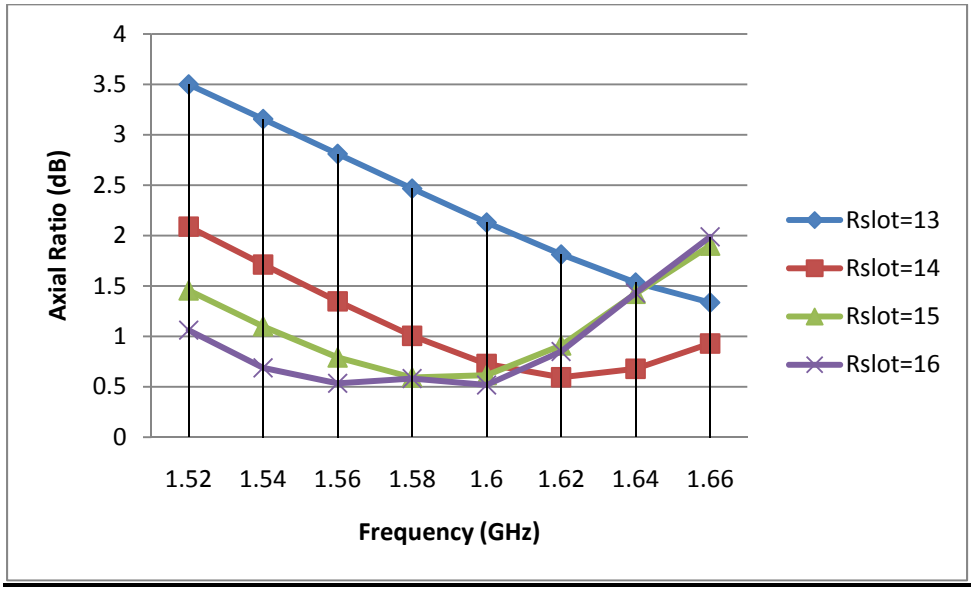

Figure 6.29 Axial Ratio values for each frequency.

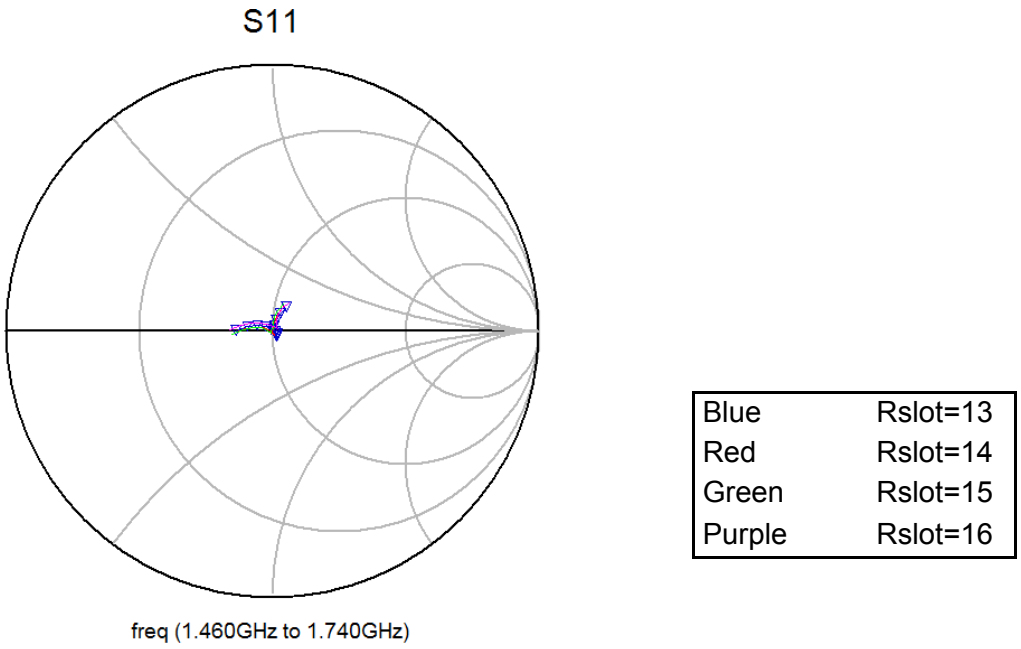

Figure 6.30 Shows the variation of the input impedance in the Smith Chart.

From Figure 6.29 and 6.30, we can see that when we adjust “Rslot” it affects the axial ratio and we can almost place the minimum value of axial radio in a given frequency. It has a little effect in the input impedance.

6.2.6 Width of Slot (Wslot)

In the table 6.15 we can see the different values of axial ratio for each frequency when we adjust the width of the slot; Figure 6.31 shows them in a graph.

In Figure 6.32 we can see the effect in the input impedance.

	Wslot=0.5	Wslot=1	Wslot=2	Wslot=2.5
1.52	2.144	1.87	1.735	1.816
1.54	1.786	1.491	1.389	1.453
1.56	1.443	1.128	1.078	1.125
1.58	1.133	0.807	0.84	0.874
1.6	0.901	0.593	0.758	0.807
1.62	0.821	0.601	0.965	1.023
1.64	0.942	0.819	1.424	1.356
1.66	1.212	1.191	1.837	1.698

Table 6-15 Axial ratio for each frequency and with different values of "Wslot".

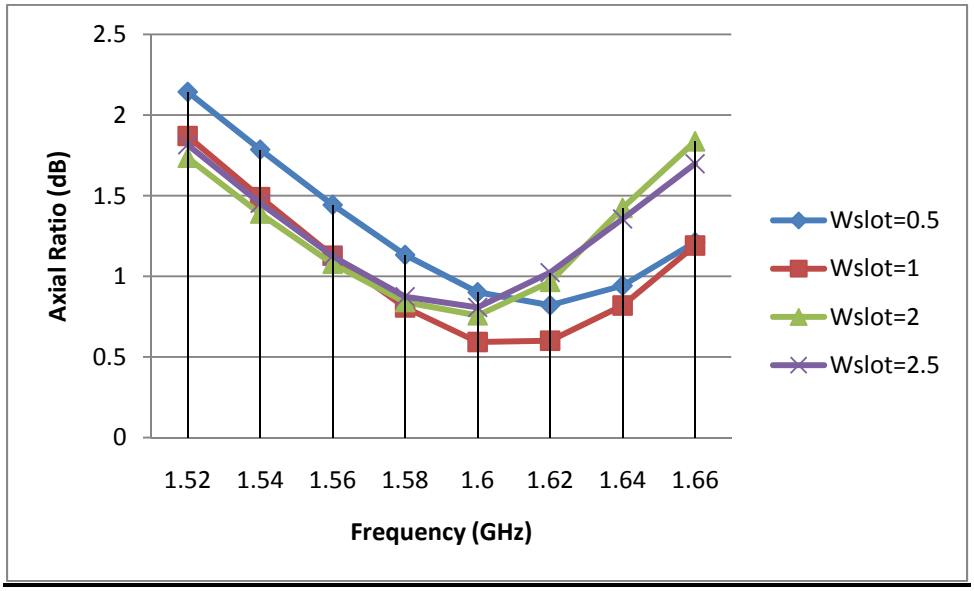

Figure 6.31 Axial Ratio values for each frequency.

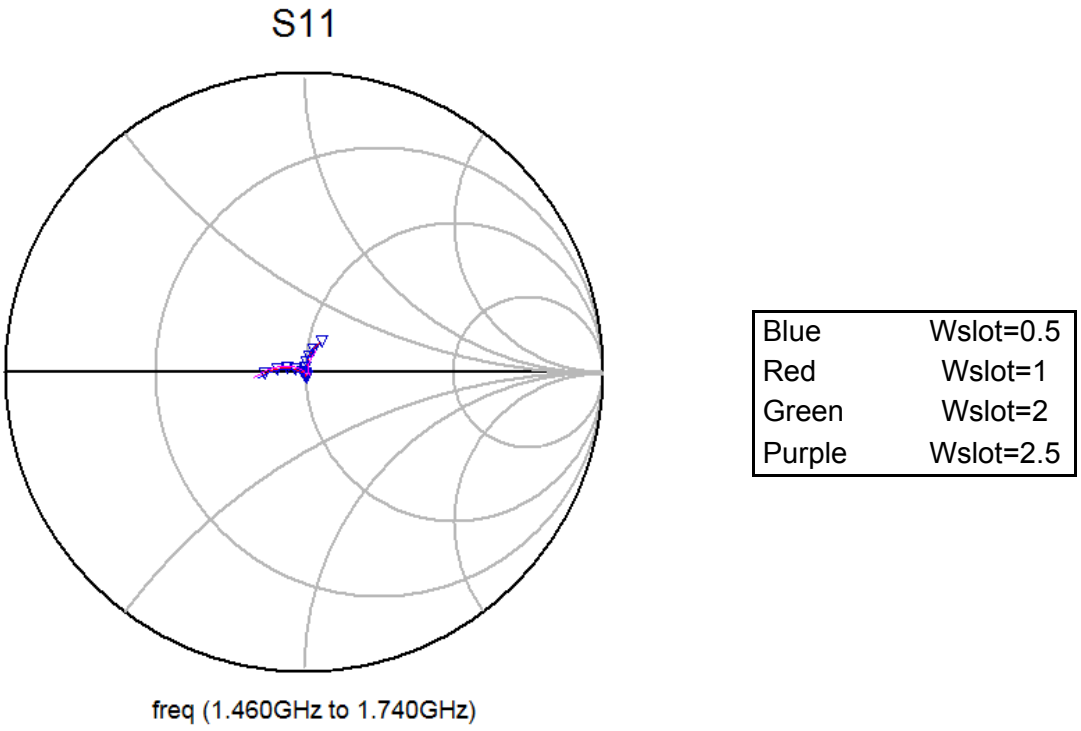

Figure 6.32 Shows the variation of the input impedance in the Smith Chart.

From Figure 6.31 and 6.32, we can see that when we adjust “Rslot” it affects the axial ratio; but not to the input impedance.

6.2.7 Distance (d)

In the table 6.16 we can see the different values of axial ratio for each frequency when we adjust the length of the impedance transformer; Figure 6.33 shows them in a graph.

In Figure 6.34 we can see the effect in the input impedance.

	d=10	d=17	d=18.5	d=22
1.52	1.722	1.796	1.743	1.745
1.54	1.578	1.448	1.379	1.343
1.56	1.477	1.129	1.038	0.956
1.58	1.44	0.869	0.749	0.605
1.6	1.487	0.735	0.578	0.355
1.62	1.656	0.813	0.622	0.377
1.64	1.969	1.15	0.955	0.708
1.66	2.252	1.616	1.488	1.289

Table 6-16 Axial ratio for each frequency and with different values of “d”.

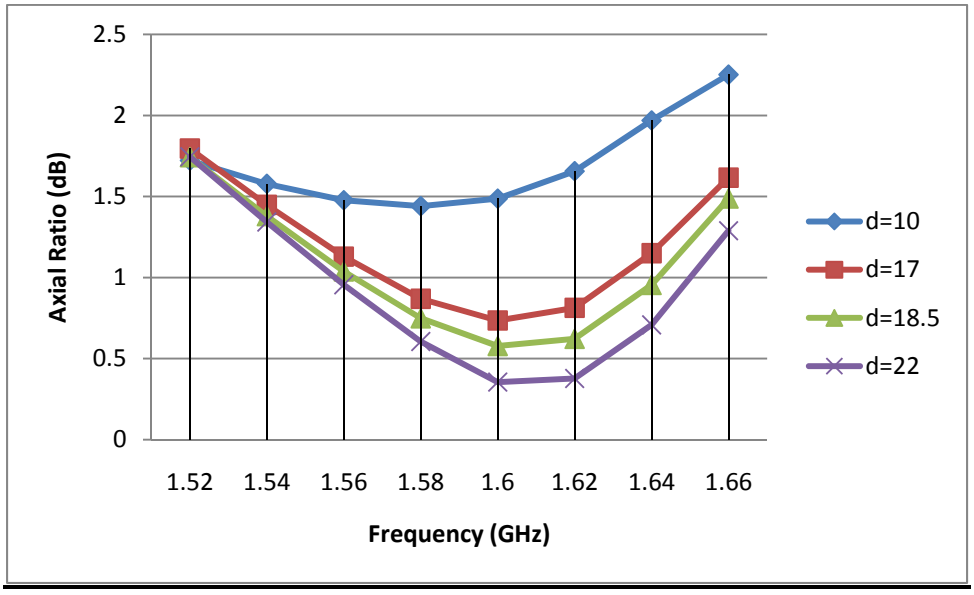

Figure 6.33 Axial Ratio values for each frequency.

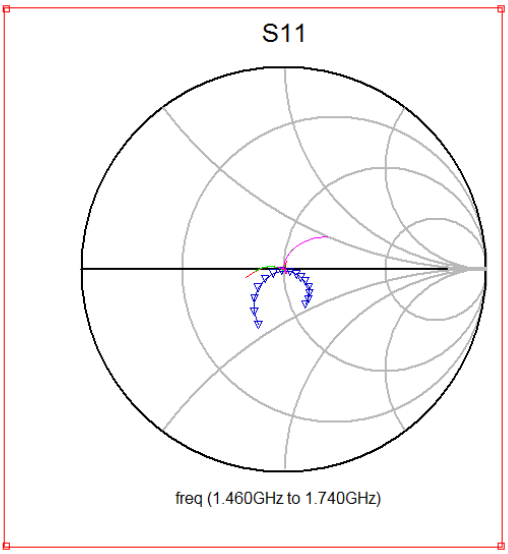

Blue	d=10
Red	d=17
Green	d=18.5
Purple	d=22

Figure 6.34 Shows the variation of the input impedance in the Smith Chart.

From Figure 6.33 and 6.34, we can see that when we adjust “d” it affects the axial ratio; and has a noticeable effect on the input impedance.

6.2.8 Lenght (l)

In the table 6.17 we can see the different values of axial ratio for each frequency when we adjust the length of the impedance transformer; Figure 6.35 shows them in a graph.

In Figure 6.36 we can see the effect in the input impedance.

	l=20	l=28	l=35	l=40
1.52	2.736	2.531	2.142	1.832
1.54	2.385	2.174	1.779	1.465
1.56	2.043	1.834	1.44	1.119
1.58	1.721	1.529	1.148	0.821
1.6	1.442	1.292	0.951	0.633
1.62	1.252	1.191	0.931	0.662
1.64	1.202	1.309	1.181	0.985
1.66	1.254	1.565	1.599	1.492

Table 6-17 Axial ratio for each frequency and with different values of "l".

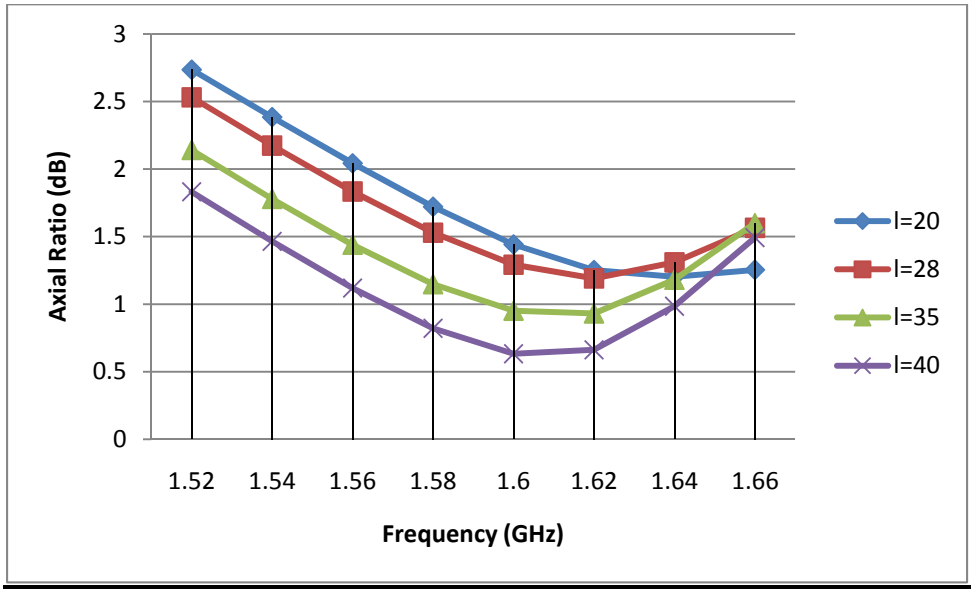

Figure 6.35 Axial Ratio values for each frequency.

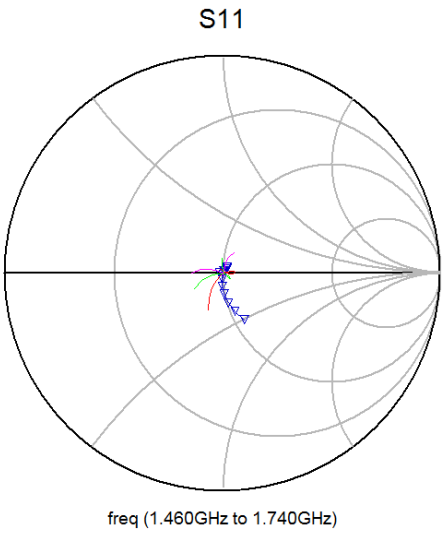

Blue	l=20
Red	l=28
Green	l=35
Purple	l=40

Figure 6.36 Shows the variation of the input impedance in the Smith Chart.

From Figure 6.35 and 6.36, we can see that when we adjust “l” it affects the axial ratio; and also affects to the input impedance.

6.3 Design of the Quadrature (90 º) Hybrid

Now we will explain the procedure followed for the design of a quadrature hybrid in microstrip technology, whose layout is shown in Figure 6.37.

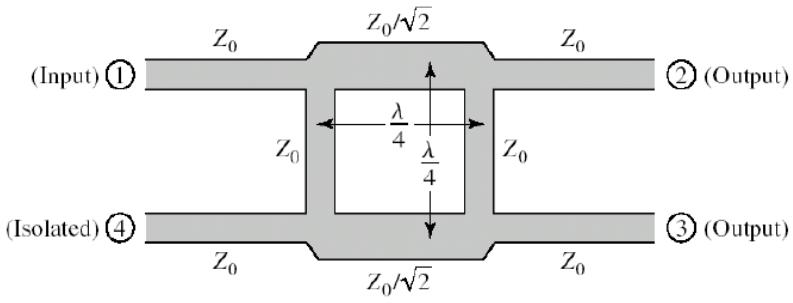

Figure 6.37 Layout of a Quadrature Hybrid in microstrip technology [6-1]

We have to mention that the parameters of the hybrid as the adaptation of the ports (S11 = S22 = S33 = S44), the isolation between ports not coupled (S14 = S41 = S23 = S32), the phase difference at the output and the balance of magnitude at the output won't be ideal when the operating frequency gets away from the design frequency.

This fact is very important and we must take into account, because it affects the design of the hybrid and we have to remember that we are going to work in a wide frequency band (1.52 to 1.66 GHz which is our bandwidth objective).

For the hybrid design we are going to use again the ADS program; but in this case we are not going to work on the Layout window, but in Schematic window.

The substrate we are going to use is A25N, so we have to set its features on the ADS simulator.

Height (H) : 20mm
Permitivity(Er) : 3.38
Relative permeability(Mur) : 1
Conductor conductivity in Siemens/meter (Cond) :1.0E+50
Cover height(Hu) : 1.0e+033
Conductor thickness (T) : 0
Dielectric loss tangent (TanD) : 0.0025
Conductor surface roughness (Rough):0

From Figure 34, we can see that in the model there are two types of line, one has impedance of 50 Ω (Z0 = 50 Ω) and the other has impedance of 35.35 Ω (Z1 = Z0/1.414 = 35.35 Ω).

The length of the lines has to be λ_{ef} / 4 from the center frequency of the hybrid.

The length of the lines of the ports is arbitrary; we are going to evaluate them in the parametric analysis of the antenna.

The model used in the ADS program for the design is shown in Figure 6.38.

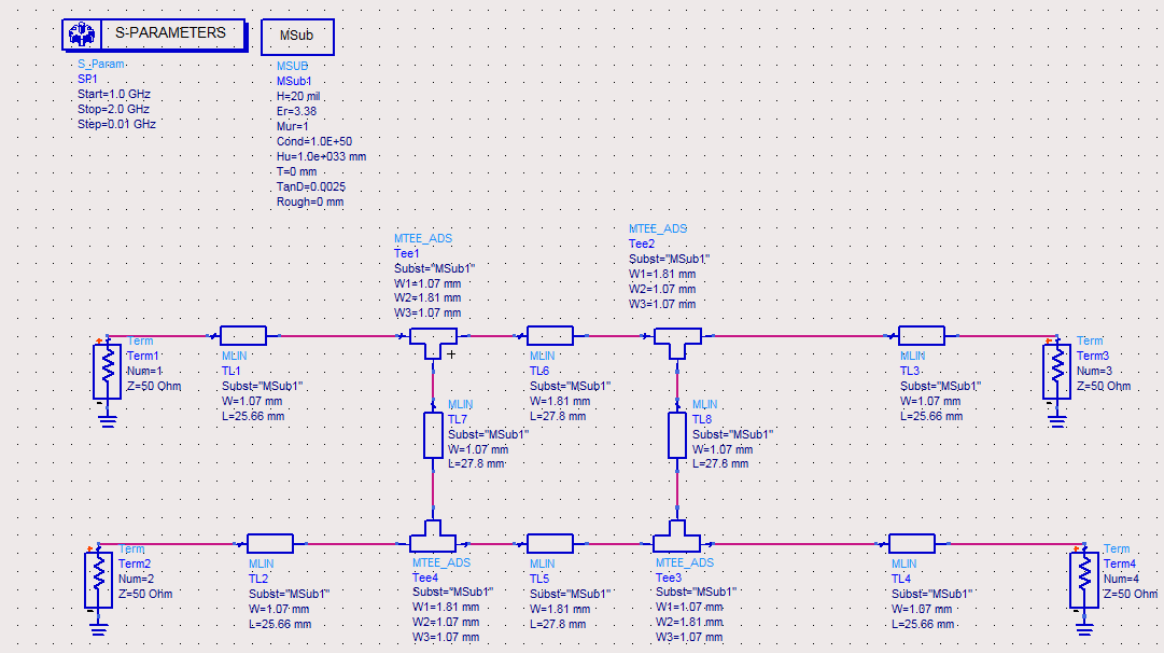

Figure 6.38 Model of the Hybrid used in ADS

Now we have to calculate λ_{ef} / 4, for the frequency of 1.59 GHz (central frequency of the bandwidth).

$$\lambda_{ef} = \frac{C}{f * \sqrt{Er}}$$

Eq (6.1)

Now replacing values, we obtained:

$$\lambda_{ef} = 102.628$$

$$\frac{\lambda_{ef}}{4} = 25.657$$

To obtain the values of Z_0 and Z1, we are going to use the Line calc tool.

For Z_0 we have: In Figure 6.39 we can see the parameters that have been set it and the results of the simulation.

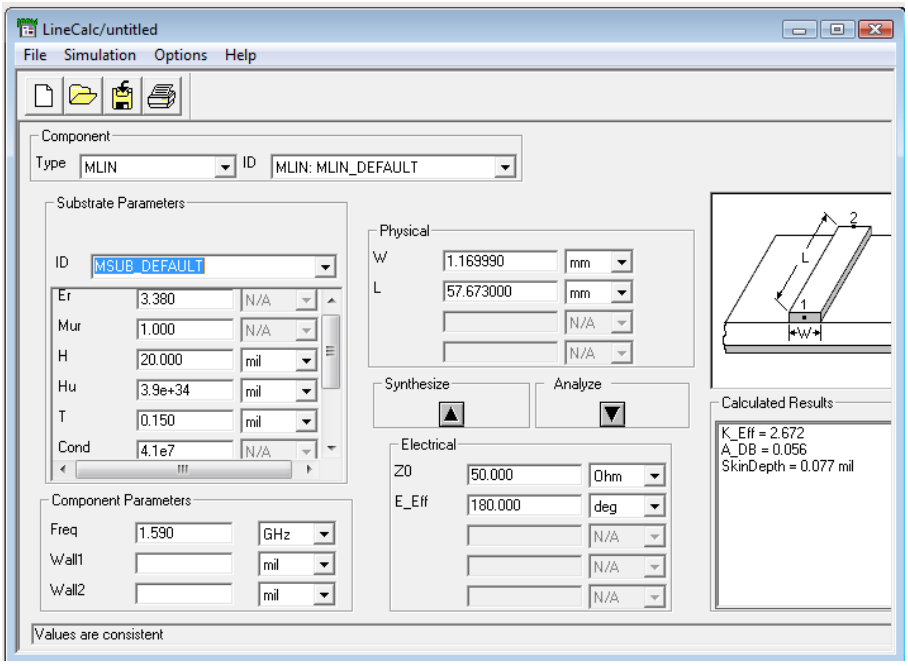

Figure 6.39 Line Calc analysis to obtain the parameters of Z0

We obtained:

Width : 1.16 mm
Length =25.657

For Z_1 we have: In Figure 6.40 we can see the parameters that have been set it and the results of the simulation.

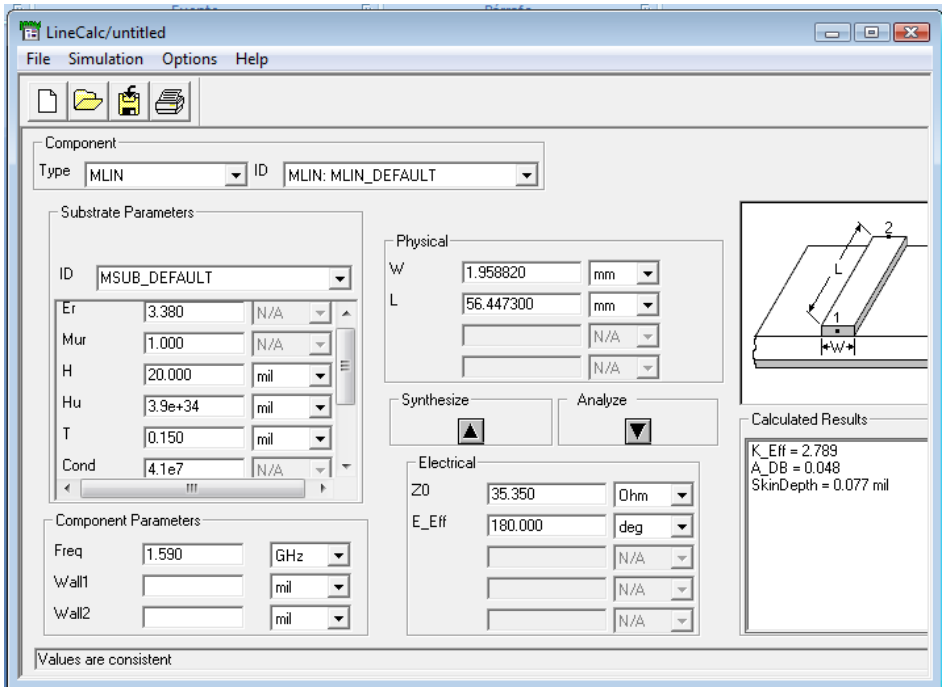

Figure 6.40 Line Calc analysis to obtain the parameters of Z_1

We obtained:

Width : 1.95mm
Length =25.657

We proceed to simulate the hybrid using these values; but we do not get good results.

After a process of optimization of the parameters that define the model, we have finally obtained the right values for our hybrid.

For Z_0 we have:

Width : 1.07mm
Length =27.8

For Z_1 we have:

Width : 1.81mm
Length =27.8

We have to make an observation, because in our project we used another numbering for the ports in the hybrid. In Figure 6.41 we can see the numbering employed.

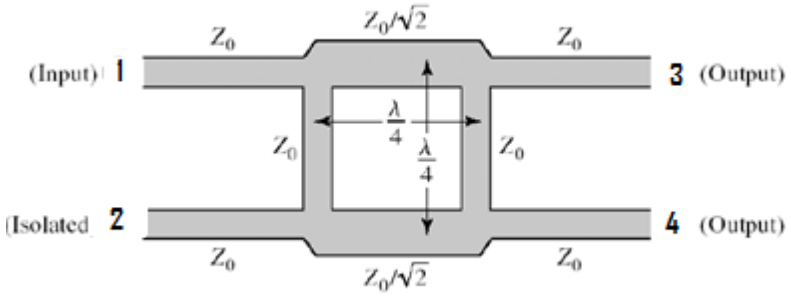

Figure 6.41 Shows the numbering employed for the ports**.**

The results of the simulation, using the values described above, can be seen in figure 6.42 and Figure 6.43.

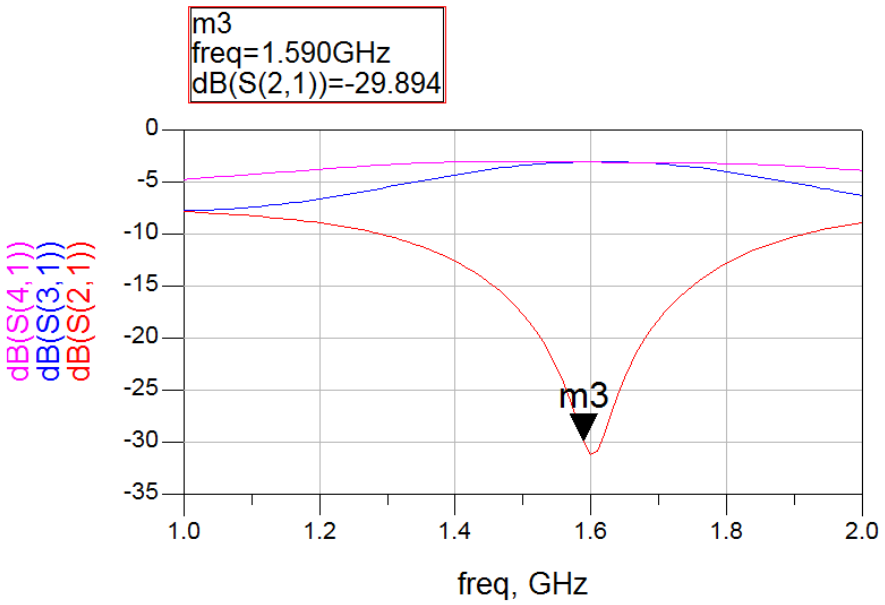

Figure 6.42 S parameter magnitudes versus frequency for the hybrid

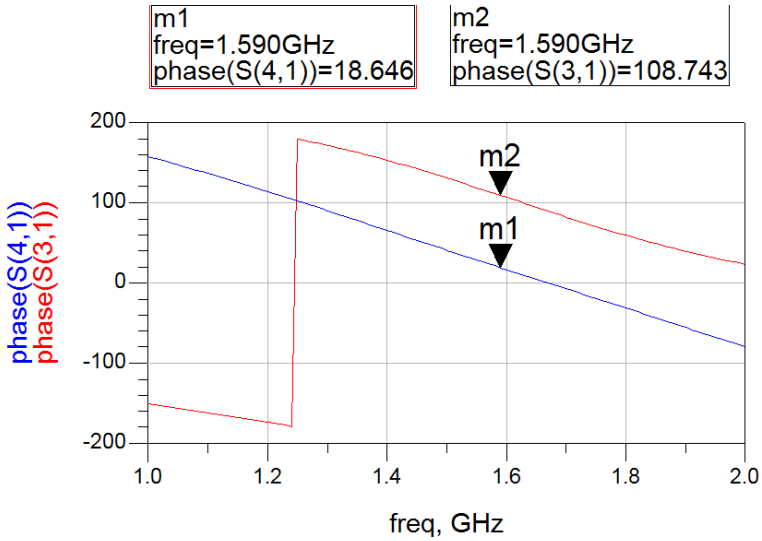

Figure 6.43 Shows the phase for port 4 and 3 at the frequency of 1.59GHz

We can see at Figure 6.43 that the phase difference between the port 3 (108.743 degrees) and port 4 (18.646) is a little bit more than 90 degrees (90.097).

Finally we obtained our quadrature that will be used at Design IV.

References

[6-1] D. M. Pozar **"Microwave Engineering**", 2nd Ed, Wiley, 1998.